

Featuring work led by Professor Tomás Torres and Doctor Andrés de la Escosura, from Universidad Autónoma de Madrid, Spain. This artwork has been designed and developed by Doctor Eduardo Anaya-Plaza.

Porphyrinoid biohybrid materials as an emerging toolbox for biomedical light management

The review examines the most important developing strategies in light-induced nanomedicine, based on the combination of porphyrinoid photosensitizers with a wide variety of biomolecules and biomolecular assemblies.

### As featured in:



See Tomás Torres,  
Andrés de la Escosura et al.,  
*Chem. Soc. Rev.*, 2018, **47**, 7369.



Cite this: *Chem. Soc. Rev.*, 2018, 47, 7369

Received 28th June 2018

DOI: 10.1039/c7cs00554g

[rsc.li/chem-soc-rev](http://rsc.li/chem-soc-rev)

## Porphyrinoid biohybrid materials as an emerging toolbox for biomedical light management

Verónica Almeida-Marrero, <sup>a</sup> Eveline van de Winckel, <sup>a</sup> Eduardo Anaya-Plaza, <sup>a</sup> Tomás Torres <sup>abc</sup> and Andrés de la Escosura <sup>ab</sup>

The development of photoactive and biocompatible nanomaterials is a current major challenge of materials science and nanotechnology, as they will contribute to promoting current and future biomedical applications. A growing strategy in this direction consists of using biologically inspired hybrid materials to maintain or even enhance the optical properties of chromophores and fluorophores in biological media. Within this area, porphyrinoids constitute the most important family of organic photosensitizers. The following extensive review will cover their incorporation into different kinds of photosensitizing biohybrid materials, as a fundamental research effort toward the management of light for biomedical use, including technologies such as photochemical internalization (PCI), photoimmunotherapy (PIT), and theranostic combinations of fluorescence imaging and photodynamic therapy (PDT) or photodynamic inactivation (PDI) of microorganisms.

### 1. Introduction

#### 1.1. Light-induced nanomedicine

The use of nanotechnology for medical purposes (*i.e.*, nanomedicine) has grown exponentially over the past few decades, as it is expected to enable more site-specific, efficient and personalized healthcare.<sup>1,2</sup> Nanostructured materials present numerous advantages for application in different areas of biomedicine, including the design and development of nanodrugs, multimodal imaging agents, and efficient and selective drug delivery systems.<sup>3,4</sup> A straightforward approach towards these

<sup>a</sup> Departamento de Química Orgánica, Universidad Autónoma de Madrid, Cantoblanco 28049, Madrid, Spain. E-mail: andres.delaescosura@uam.es, tomas.torres@uam.es; Web: <http://www.phthalocyanines.es>

<sup>b</sup> Institute for Advanced Research in Chemistry (IAdChem), Cantoblanco 28049, Madrid, Spain

<sup>c</sup> IMDEA Nanociencia, Cantoblanco 28049, Madrid, Spain

† These authors contributed equally to this work.



**Verónica Almeida-Marrero**

and biological studies of phthalocyanine-carbohydrate biohybrid materials.



**Eveline van de Winckel**

Eveline van de Winckel graduated from the University of Ghent (Belgium) as an MSc in Chemistry in 2013. Afterwards, she continued her postgraduate research in the field of photodynamic therapy at the Universidad Autónoma de Madrid (Spain), funded by a Marie Curie scholarship. After completing her PhD in 2017, Eveline's current interests focus on the transfer of her expertise in light-induced therapies for cancer treatment into clinical research, holding a Clinical Research Associate position in the pharmaceutical industry and actively participating in the organization of Phase I to Phase III clinical trials in different oncological areas.



global goals involves the use of theranostics, which comprise the inclusion of therapeutic and diagnostic functions within a single nanostructure. Optical methods for imaging and therapy are becoming indispensable in this respect, because they allow tuning both kinds of functions through designed interactions of the theranostic agent with light.<sup>5</sup> Achieving an optimal management of light therefore represents a great challenge in biomedicine, which will pave the way to new promising medical technologies in the near-future.

The human knowledge about how light can be employed with a therapeutic objective actually deepens its routes in ancient civilizations, yet the scientific fundaments of phototherapy were



**Eduardo Anaya-Plaza**

*Eduardo Anaya-Plaza received his PhD in 2016 from the Universidad Autónoma de Madrid (Spain), under the supervision of Prof. Torres and Dr de la Escosura, focusing on the synthesis and characterization of water-soluble phthalocyanines. He conducted two postdoctoral periods at the University of Birmingham (UK) and Aalto University (Finland), where he is currently a recipient of a MSCA Individual Fellowship.*

*His research interests lie at the*

*interface of chemistry, biology and physics. He is currently working on the synthesis and conjugation of organic chromophores with biological scaffolds such as proteins, DNA origami, and cellulose derivatives, in order to develop biohybrids with optoelectronic properties.*



**Tomás Torres**

*which presently consists of twenty-five researchers, is currently exploring several areas of basic research and applications of phthalocyanines, porphyrins and carbon nanostructures (fullerenes, carbon nanotubes, graphene), including organic and hybrid solar cells, and photodynamic therapy, with a focus on nanotechnology.*

only recognized at the beginning of the twentieth century, when the Danish physician Niels Finsen received the Nobel Prize in this field.<sup>6</sup> The concept of photodynamic action was introduced by Oscar Raab, a medical student of Hermann von Tappeiner at the University of Munich, also in the early 1900s.<sup>7</sup> For a historical perspective on photodynamic therapy see ref. 8, where further information about the following milestones can be found. The modern explosion of interest in photosensitizing molecules (*i.e.*, photosensitizers, PS) for cancer treatment began around the 1960s, when Lipson and coworkers described the tumor accumulation of a haematoporphyrin derivative (HpD, a mix of monomers, dimers and oligomers, developed by S. Swartz) and its use in the photodetection of tumors. A significant breakthrough happened in 1975, when T. Dougherty and colleagues reported that the administration of HpD, together with a local irradiation with red light, completely eradicates mammary tumor growth in mice. In 1976, Kelly and co-workers initiated the first successful clinical trial of HpD in patients with bladder cancer. Further research into partially purified HpD for tumor therapy resulted in the first clinically approved PS, Photofrin. In 1993 Photofrin received regulatory approval in Canada and subsequent endorsement for specific clinical uses in the USA, various European countries and Japan. Since then, many other photosensitizing molecules have been approved and commercialized,<sup>9,10</sup> including, among others, 5-aminolevulinic acid (ALA) for topical diseases such as basal cell carcinoma, verteporfin (Visudyne) for the treatment of age-related macular degeneration, and *meta*-tetrahydroxyphenylchlorin (Foscan) or sulfonated aluminum phthalocyanines (Photosens) for different cancer types. An overview of PS can be found in ref. 9 and 10.

Regarding biomedical light management through the use of PS, there are currently a number of possible applications, which present different degrees of development. The most common



**Andrés de la Escosura**

*Andrés de la Escosura (PhD 2005) carried out postdoctoral studies at Radboud University Nijmegen (The Netherlands). He joined the Universidad Autónoma de Madrid (UAM) in 2009, first as Assistant Professor and, since February 2012, as a Ramón y Cajal Fellow. Currently, he belongs to the recently created Institute for Advanced Research in Chemical Sciences (IAdChem) and the Organic Chemistry Department at UAM, where he leads a small research subgroup concerned with the study of biohybrid materials and systems chemistry. After finding the useful properties of protein capsids as nanoreactors and nanocontainers to incorporate different kinds of materials, he is currently working in areas that include biomedical applications and prebiotic systems chemistry.*



one is photodynamic therapy (PDT),<sup>11</sup> a clinically approved form of phototherapy in which PS become toxic to targeted malignant and other diseased cells, through photoinduced generation of singlet oxygen ( $^1\text{O}_2$ ) and other reactive oxygen species (ROS).<sup>12</sup> When this kind of therapy is used to kill microbial cells, including bacteria, yeasts, fungi and viruses, researchers also refer to this treatment as photodynamic inactivation (PDI), anti-microbial PDT (aPDT) or photodynamic antimicrobial chemotherapy (PACT).<sup>13</sup> Herein we will use the acronym PDI. A very promising, more specific form of PDT involves the combination of standard PDT with immunotherapy of tumours.<sup>14</sup> This treatment option is referred to as photoimmunotherapy (PIT). Besides these therapies, PS can also assist in the administration of other drugs, *e.g.*, in gene therapy, through the so-called photochemical internalization (PCI) technique.<sup>15,16</sup> PCI is an intracellular delivery method that increases the endosomal release of the drug by co-administration of PS agents, which help in disrupting the membranes of endocytic vesicles upon activation by light. On the other hand, if PS convert the absorbed light into a fluorescence emission, they can also be used for optical imaging. Compared to other imaging modalities, fluorescence imaging presents various advantages such as its non-invasive character, subcellular spatial resolution, high temporal resolution, and high sensitivity in the detection of biological structures at low concentration levels.<sup>17</sup> Importantly, in the way to theranostic applications, all these optical methods are susceptible to be combined with other, non-optical therapeutic and imaging modalities.<sup>9,18</sup>

PS are generally classified as either porphyrinoids or non-porphyrinoids.<sup>19,20</sup> Due to the limited potency and various side effects associated with most non-porphyrinoid PS, their application in medicine has lagged considerably behind. Porphyrinoids, in turn, are further classified as first-, second- and third-generation PS.<sup>21</sup> First-generation PS include hematoporphyrin derivatives (HpD) and porfimer sodium (Photofrin). A number of second-generation PS, including porphyrin (Por), phthalocyanine (Pc), naphthalocyanine (Nc), chlorin and boron dipyrromethene (BODIPY) derivatives, have been developed to alleviate certain problems associated with the first-generation ones, such as prolonged skin photosensitization and suboptimal tissue penetration. Finally, third-generation PS consist of second-generation PS covalently conjugated to site-specific delivery agents and/or formulated with nanocarriers, in order to obtain improved characteristics, such as less aggregation, better solubility in physiological media and selective accumulation within the targeted tissue.

Apart from the above-mentioned classification into three generations, which does not always imply that third-generation PS perform better than first- or second-generation PS, PS have also been categorized according to their chemical structure (Fig. 1). In particular, three broad categories are distinguished: (i) Por, (ii) chlorins and (iii) synthetic dyes.<sup>22</sup> The first category consists of Por (Fig. 1a), such as the naturally prevalent HpD and its derivatives, while the second one includes chlorophyll-like substances that were discovered in photosynthetic systems of plants (chlorins, Fig. 1b) or of bacteria and algae (bacteriochlorins, Fig. 1c). The latter are in fact reduced forms of Por, and were found to possess equally great photosensitizing

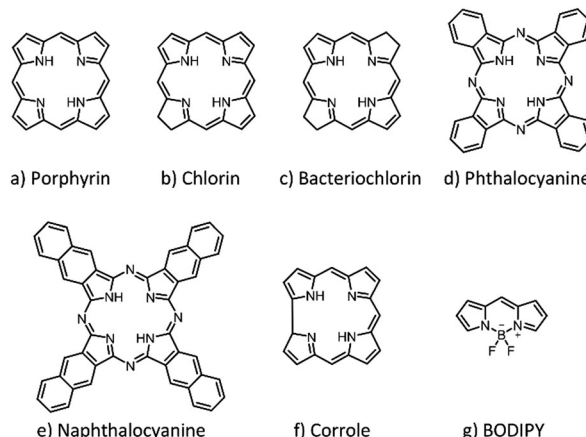


Fig. 1 Basic structures of the main porphyrinoid PS that have been used to build up photoactive biohybrid materials, including (a) porphyrin, (b) chlorin, (c) bacteriochlorin, (d) phthalocyanine, (e) naphthalocyanine, (f) corrole, and (g) BODIPY derivatives.

properties. Among the category of synthetic dyes, in turn, Pc (Fig. 1d) and its derivatives with extended conjugation, *e.g.*, Nc (Fig. 1e), represent the most prominent family, and have been widely used in PDT.<sup>23–25</sup> Corroles (Fig. 1f) are synthetic tetrapyrrolic macrocycles with chemical and photophysical properties that are very similar to those of Por, yet only have three NH groups in the inner core, which makes them stabilize high-valent transition metal ions.<sup>26</sup> Finally, BODIPY derivatives<sup>27</sup> (Fig. 1g), whose structure resembles half of a Por ring, are well-recognized by their excellent fluorescence properties, which are commonly employed in the context of bioimaging. All of the biohybrid materials shown in this review involve the use of PS from any of the above-mentioned families. As Por and Pc are the most commonly used PS families in biomedical applications, they will be normally discussed first in the different sections, in that order, followed by the remaining possible PS families. For a more detailed description of the chemical, photochemical and photophysical properties of these organic pigments, there are various excellent reviews in the literature, some of them focused on PDT and optical imaging.<sup>9,13,18</sup> Besides, there exist other synthetic porphyrinoid PS families that have not been included in the present review, either because their use in biomedicine has been scarce, such as for subporphyrins, subphthalocyanines, porphyrazines and subporphyrazines,<sup>28</sup> or because their incorporation into biohybrid materials is very rare, such as for texaphyrins and other isomeric/expanded porphyrin analogues. The chemistry<sup>29</sup> and biomedical applications<sup>30</sup> of the latter families have actually been reviewed recently.

## 1.2. Photosensitizing biohybrid materials

An important drawback of most organic PS systems, including third-generation ones, is their low biocompatibility and unspecific tissue accumulation, especially when they are not adequately decorated with immunosuppressing moieties and targeting labels, respectively. A recent strategy to tackle such important issues consists of mimicking Nature, using biologically inspired hybrid materials to maintain or even enhance the optical properties of PS



in physiological media. The notion of photosensitizing biohybrid materials, which is new, will help in embracing many previous experimental approaches regarding PS that could actually be considered within the same conceptual framework. Research efforts towards combining the aqueous solubility, biocompatibility and drug delivery properties of certain biomolecules and their non-covalent assemblies with the biomedical functions of organic PS comprise an emerging field with high growing potential, nourished by intricate interactions between various scientific disciplines such as physics, chemistry, biology and medical technology. The results coming from such fields have never been put together under a single perspective, as we do herein. Embracing all those approaches from the same perspective is also important to push forward the capacity of biomedicine for light management, which will lead to crucial advances in the form of fundamental knowledge and technological developments. Concerning the chemistry and physics of biohybrid materials, for example, endowing them with genuine optical and photochemical features represents a successful approach toward novel optoelectronic systems where the biological component induces unprecedented behaviours. On the other hand, biomedicine can certainly benefit from incorporating functional dyes into different biological architectures.

On these bases, herein we have reviewed the existing literature about photosensitizing biohybrids, which could be classified into different groups depending on the nature of the biological component in the biohybrid (Fig. 2). In particular, we have distinguished between five categories of PS biohybrids, including peptides, proteins (e.g., serum proteins, antibodies, protein cages),

nucleic acids, carbohydrates or liposome entities as biological components in their structure. These categories actually constitute the different sections into which this review has been structured (Sections 3–7). There are other kinds of biomolecules, such as hormones and folic acid, which have been combined with PS to a lesser extent, yet their impact in biomedicine may also be substantial and, thus, they have also been covered in the present review (Section 8). The purpose of this review is, in any case, not to cover all the work that has been published so far, but to review the most important work that has been carried out in such an extensive field. In particular, we focus on hybrids that present demonstrated potential for biomedical use, leaving aside approaches that combine porphyrinoids with biomolecular species and assemblies for other kinds of applications (e.g., optoelectronics, sensors, *etc.*), which follow clearly different research trends, and would make the present review just intractable.

Although from a wide perspective all the discussed biohybrids serve to enhance the PS photochemical use in biological contexts, the type of biomolecule that is employed somewhat biases the application aimed in each case. Peptides, either natural or synthetic, are for instance normally used to increase the PS selectivity and affinity for specific biological targets, which makes them ideal PS delivery vehicles. Serum proteins facilitate the transportation of PS through the body, improving the photodynamic action and enhancing the intracellular accumulation *via* receptor-mediated endocytosis. Antibodies are key to the promising technology of PCI, while viral capsids and other protein cages have a wide applicability in different (bio-)nanotechnology applications. The merging of PS with oligonucleotides has been utilized to perform photocatalytic oxidative modifications of DNA, to build up fluorescence-based diagnostic systems, and for the onset of light-induced gene transfer. Concerning sugars, it is difficult to establish a clear association of each type of carbohydrate with a specific type of application, as they are all being commonly studied for PDT, PDI and theranostic applications. Finally, liposomal drug formulations have been intensively employed in clinical applications since the 1970s, and they are considered the traditional way to formulate PS. In recent years, more challenging goals have been pursued, like the development of PS–liposome–antibody and PS–liposome–protein biohybrids, as targeted drug delivery systems. All these concepts will be reviewed in the following sections, where the reader will also encounter appropriate references.

## 2. Biohybrid conjugation strategies

The term ‘bioconjugation’ refers to the chemical linkage of two biomolecules, or of a biomolecule to one or more synthetic functional labels.<sup>31</sup> It actually represents a research field with tremendous activity, mainly because methods for mild and site-specific modification of proteins, nucleic acids, carbohydrates, liposomes, *etc.*, have an increasing impact on various aspects of biotechnology, including the discovery of new biological interactions, biochemical assays, and diagnostic and therapeutic

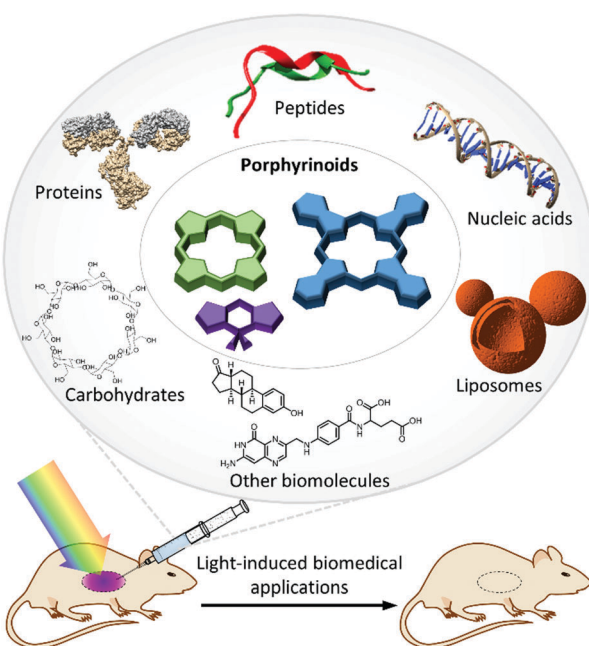


Fig. 2 Schematic representation of the photoactive biohybrids reviewed in this review article. Porphyrinoids serve as photosensitizers, in combination with six main types of biomolecules acting as nanocarriers. On these bases, photosensitizing biohybrid materials are increasingly being employed in a wide variety of light-induced biomedical applications.



applications, among others. Such a perspective also applies, of course, to the case of photosensitizing biohybrids and, as will be shown along this review, the methods available to this end are mostly the same as those utilized for other kinds of bioconjugates. The references to such methods will be cited when discussing specific examples in the subsequent sections, yet a few guidelines concluded from the elaboration of this review are shortly sketched in the next three paragraphs.

Photoactive biohybrids can be obtained by either covalent or non-covalent association of PS with different biomolecules. The advantages of covalent approaches, as compared to supramolecular strategies, are the stability and the possibility of achieving a well-defined localization of the PS in the biomolecule structure, thanks to the use of modern biorthogonal and site-specific reactions. The covalent approach also has disadvantages, however, such as the requirement of having complementary functional groups in both the biomolecule and the PS, which demands in many occasions more complex designs and synthetic routes. Supramolecular strategies, on the other hand, offer a wider choice in terms of the nature of the conjugation partner, and so they grant the possibility of interaction with a diversity of biological components. They also simplify, normally, the design and synthesis of the hybrids. As drawbacks, non-covalent biohybrids are usually less specific regarding the localization of the PS on the biomolecule, and are not always stable under physiological conditions, sometimes resulting in the leakage of the PS before addressing the biological target.

The vast majority of publications concerning photoactive biohybrids refer to species where the PS is linked to the biomolecule *via* a covalent bond. In this way, PS have been conjugated to tumour antigens, sugars, oligonucleotides, hormones, metabolites, cellular signalling species, and, to a great extent, peptides and proteins. Regarding the functional groups involved in the conjugation reaction, the methodologies adopted so far can be divided into two classes. The first class of methods are very straightforward, involving the targeting of the amino or carboxylic groups naturally present in most biomolecules (e.g., amino acids, peptides, proteins, some carbohydrates, folic acid, *etc.*) through amide formation with carboxylic or amino groups, respectively, previously incorporated in the PS structure. Due to the ubiquity of those functional groups in biology, these “traditional” conjugation methods are usually not selective, and their efficiency is limited under certain conditions, which often results in purification problems. The second class of conjugation methods is based on reactions with non-naturally occurring (abiotic) functionalities, which are introduced into the PS and/or the biomolecule especially for this purpose. From a chemical viewpoint, various groups of reactions can be differentiated, such as metal-catalysed coupling reactions, the formation of thioether and imine linkages, and cycloaddition transformations, many of which can be performed as “click” processes. A comprehensive overview of the main covalent conjugation methods that have been utilized to connect PS to different biomolecules is provided in Table 1.

Supramolecular approaches, on the other hand, are less abundant and more specific to the kind of biomolecule. Among the types of existent non-covalent interactions, binding occurs

in many cases by a proper balance between hydrophobicity and hydrophilicity in the PS structure (*e.g.*, for the encapsulation of PS in serum proteins or in the membranes of liposomes). Electrostatic interactions are also commonly used to promote the incorporation of charged PS into certain biomolecular assemblies (*e.g.*, protein cages, DNA or sugar nanostructures). The intercalation of porphyrinoid PS into DNA double helices or quadruplexes is normally driven by a fine combination of hydrogen bonding, electrostatic interactions and  $\pi$ - $\pi$  stacking. Finally, it is common to utilize biological recognition motifs such as the biotin-(strept)avidin interaction, to produce protein biohybrids. Due to the diversity of supramolecular strategies toward PS biohybrids, however, they cannot be discussed in detail in this section, and so they will be discussed when the corresponding examples are mentioned in the text.

### 3. PS–peptide biohybrids

The bioconjugation of peptides to PS has received considerable attention in the last few years, as it is an expedient method to overcome issues generally associated with the use of hydrophobic PS, including their scarce aqueous solubility and a strong tendency to aggregation. Moreover, the utilization of natural peptides, peptide analogues and newly designed synthetic peptides can provide additional promising features such as a better affinity and selectivity for certain biological targets.<sup>32</sup>

#### 3.1. Conjugation of PS to amino acids

The incorporation of amino acids (AA, the basic components of peptides) into the structure of PS molecules is interesting because it increases the aqueous solubility and biocompatibility of the resulting hybrids. Although such hybrids cannot be considered as peptide derivatives, and thus do not have the potential to address specific biological targets, the possibility of choosing between different amino acid units enables tuning their biological properties.

One of the roles that amino acids can play when linked to PS is to promote their supramolecular organization into different kinds of aggregated structures. A lot of research has also been focused on studies about molecular recognition between AA and Por.<sup>33–36</sup> This kind of supramolecular approach constitutes an active research field but lies beyond the scope of the present review, as the resulting ensembles currently lack any biomedical applications.

As a widely explored conjugation strategy, amino acids can be anchored to PS through amide bond formation, making use of their carboxylic acid or amino functionalities to react with PS compounds that bear the complementary functional group.<sup>37,38</sup> Gu *et al.* explored the possibility of obtaining completely water-soluble Zn(II)Pc derivatives with glycine units at the macrocycle periphery.<sup>37</sup> Drechsler *et al.* expanded the collection of Zn(II)Pc-AA conjugates by anchoring two different AA units, phenylalanine and serine, while they also investigated the use of less branched alkyl or alkoxy chains as spacers, aiming at a reduction of the aggregation tendency of these PS systems.<sup>38</sup> The conjugates



Table 1 Main reaction types that have been used to prepare covalently linked PS biohybrid materials

Reaction type	Coupling unit on the PS	Coupling unit on the biomolecule	Resulting conjugate	Examples of biomolecules employed
Amide formation		$\text{H}_2\text{N}-$		Amino acids, short peptide sequences, serum proteins, antibodies, nucleic acids, carbohydrates, folic acid
		$\text{HOOC}-$		
Sulphonamide formation		$\text{H}_2\text{N}-$		Amino acids, short peptide sequences, antibodies
Sonogashira coupling reaction		$\equiv-$		Short peptide sequences, nucleic acids, steroid hormones
Buchwald–Hartwig reaction		$\text{H}_2\text{N}-$		Short peptide sequences
Suzuki–Miyaura coupling reaction		$\text{x}-$		Short peptide sequences
Copper catalysed Huisgen [3+2] cycloaddition		$\equiv-$		Short peptide sequences, carbohydrates, antibodies
Isothiocyanate conjugation		$\text{NH}_2-$		Serum proteins, antibodies, nucleic acids
		$\text{N}_3-$		
O-Alkylation		$\text{Br}-$		Nucleic acids
Ester formation		$\text{HO}-$		Steroid hormones
Nucleophilic substitution		$\text{HO}-$		Carbohydrates
Sulphonate ester formation		$\text{HO}-$		Carbohydrates
		$\text{HO}-$		
Thiol–maleimide “click” chemistry		$\text{HS}-$		Antibodies, proteins, short peptide sequences, liposomes
Axial substitution		$\text{HO}-$		Nucleic acids, steroid hormones, carbohydrates
		$\text{Cl}-\text{Si}(\text{R})_2-$		

showed an excellent solubility and little aggregation in water, but the phototoxicity assays showed poor results, and the serine-containing hybrid was toxic in the dark. More successful results were obtained by Haywood-Small *et al.*, who incorporated glycine,  $\alpha$ -alanine,  $\beta$ -alanine, aminobutyric acid, aminovaleric acid

and aminocaproic acid at the periphery of  $\text{Zn}(\text{II})\text{Pc}$ , in all cases through sulphonamide formation.<sup>39</sup> The phototoxicities shown by these derivatives were very similar to that of tetrasulphonated  $\text{Zn}(\text{II})\text{Pc}$ , when tested in SiHa human cervical carcinoma cells. Importantly, tumour tissues normally have a lower pH (pH 6.5)



compared to blood and normal tissues (pH 7.4).<sup>40</sup> Based on this factor, Wang *et al.* further investigated if there is a positive correlation between the pH-dependent behaviour of *Pc*-AA conjugates and their PDT activity.<sup>41</sup> In particular, they synthesized a series of AA-substituted *Zn(II)Pc* compounds that, depending on the tumour microenvironment, can change their overall charge, from positive to negative. As a consequence of that change, the conjugates showed a higher photodynamic activity and cellular uptake.

AA have also been covalently linked to *Por*-based PS. Ramaiah and co-workers, for example, synthesized a series of conjugates of *H<sub>2</sub>Por* and *Zn(II)Por* with proline and tryptophan, for the study of their photophysical properties, their potential generation of <sup>1</sup>O<sub>2</sub>, and their interaction with biologically relevant metal ions.<sup>42</sup> Meng *et al.*, in turn, worked on the conjugation of aminophenyl-*H<sub>2</sub>Por* with L-lysine, L-arginine and L-histidine for PDI applications.<sup>43</sup> One of the advantages of using these AA residues is that they are cationic under slightly acidic conditions, thus promoting a higher affinity of the PS for microbial cells. Moreover, they make the PS biocompatible while ensuring that it remains resistant to degradation by proteases, which is an important limitation of PS-peptide hybrids. *In vitro* experiments using these PS biohybrids against *MRSA*, *E. coli* and *P. aeruginosa* actually showed that increasing the number of AA residues linked to the *Por* macrocycle increased the observed PDI efficacy, the most effective photoinactivation effect being produced by the *Por* derivative with four lysine moieties, which also exhibited a lower dark toxicity.

Ding and co-workers also studied the antimicrobial efficacy of Lys-*H<sub>2</sub>Por*, in this case against different strains of *Acinetobacter baumannii*, showing good results both *in vitro* and *in vivo*.<sup>44</sup> In a different approach, Serra *et al.* synthesized four *H<sub>2</sub>Por*-AA conjugates with glycine, serine, tyrosine and methionine.<sup>45</sup> Biological assays were performed *in vitro*, against tumoral (HeLa) and non-tumoral (HaCaT) human cell lines. All the PS biohybrids showed good photostability and were able to generate <sup>1</sup>O<sub>2</sub> upon irradiation, while no dark toxicity was observed for an incubation period of one day.

Regarding other PS families, examples of conjugation to amino acids can be found in the literature. Water-soluble conjugates have been synthesized with chlorin p6 as the PS and glutamic acid or aspartic acid as amino acid units.<sup>46</sup> The conjugate with aspartic acid showed a higher phototoxicity against melanoma, compared to, for example, verteporfin, with a lower cytotoxicity and a multiple subcellular localization that favours cell death as a consequence of PDT treatment (Fig. 3). In a similar way, lysine and aspartic acid have been conjugated to chlorin e6 in different positions of the macrocycle, and the PDT efficacy of the resulting biohybrids has been tested in human carcinoma Hep2 cells, showing different results depending on the conjugation site.<sup>47</sup>

### 3.2. Conjugation of PS to short peptide sequences

Due to the small size of peptides (<50 AA residues), linking them to PS represents a potent strategy for providing the resulting hybrids with low immunogenicity and good tissue penetration properties. Peptides can be either natural or synthetic, and they

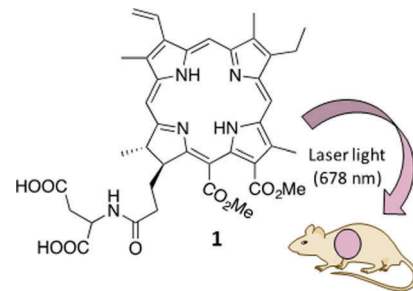


Fig. 3 Structure of the aspartylchlorin p6 dimethyl ester derivative (**1**), which has shown excellent phototoxicity against melanoma in mice.<sup>46</sup>

can be chemically modified, allowing tuning of their interactions with different target molecules. Many functional peptide libraries have actually been described in the literature, with different sequences and functions, offering a versatile platform of delivery agents to localize PS conjugates in different kinds of cells and tissues.<sup>48</sup>

Covalently linked PS-peptide biohybrids can be synthesized, taking advantage of mild synthetic organic methodologies such as amide<sup>49–53,77,78,81,85–87,89,91–93,95,97,104,105</sup> or sulphonamide<sup>54</sup> bond formation, palladium-catalysed cross-coupling reactions,<sup>55,56</sup> click-chemistry reactions<sup>57–59,81,94</sup> and isothiocyanate chemistry,<sup>60,82</sup> among other strategies. Supramolecular approaches have also been used toward self-assembled peptide nanofibers,<sup>61</sup> nanodots,<sup>62</sup> vesicles,<sup>63</sup> light harvesting complexes,<sup>64</sup> arrays<sup>65</sup> or polymeric micelles with a peptide-decorated surface,<sup>66</sup> among others.<sup>67,68</sup> In particular, Yan and co-workers successfully used such supramolecular approaches towards biomedical applications, through peptide-tuned self-assembly of PS,<sup>69</sup> or by use of dipeptide hydrogels with incorporation of PS.<sup>70,71</sup> The resulting supramolecular biohybrids, mostly employing chlorin e6, have been extensively tested both *in vitro* (in MCF-7 cells) and *in vivo* (in mice), confirming their potential use for different anticancer PDT applications. For further reference, this research group has also published some good reviews about the supramolecular complexation of photodynamic and photothermal agents with peptides or proteins, resulting in new platforms for drug delivery purposes.<sup>72,73</sup> However, as the supramolecular approach has not been as commonly directed towards biomedical research as the covalent approach, the next paragraphs will be mostly focused on covalent conjugates.

In general, most of the PS-peptide conjugates have been applied to PDT, with the peptide units being responsible for the targeting of specific receptors, whereas biosensing by fluorescence and that by positron emission tomography (PET) are other potential applications of PS-peptide conjugates. Regarding the different PS that could be employed, a great number of the discussed examples are related to *Pc* and *Por*; however, other PS such as BODIPY and chlorins have also been employed. In the next subsections the different applications of these PS-peptide biohybrids will be discussed in detail, categorized as per specific receptors they target.

**3.2.1. Targeting of the epidermal growth factor receptor (EGFR).** One of the most targeted receptors in PDT is the EGFR.



This receptor is a member of the ErbB family of cell-surface receptors for peptide ligands, and has an important role in different cellular processes related to cancerous disorders.<sup>74</sup>

Among all EGFR-targeting biomolecules reported in the literature, two small peptides with sequences LARLLT<sup>75</sup> (EGFR-L1) and YHWYGYTPQNV<sup>76</sup> (EGFR-L2) are particularly attractive, due to their low immunogenicity, good capacity of conjugation and high EGFR targeting ability (Fig. 4a). Vicente and co-workers were the first to synthesize various Zn(II)Pc-peptide biohybrids using both previously mentioned peptide sequences (Fig. 4b).<sup>52</sup> The studied Zn(II)Pc-peptide conjugates were shown to bind the EGFR, and their photodynamic activity was tested in the human carcinoma cell lines A431 and Hep2, and in the human colorectal cell line HT-29. The Zn(II)Pc-EGFR-L1 conjugates (2a and 2b) efficiently targeted EGFR and were actually internalized. The reason for this positive result could be the presence of cationic charges, whereas the lower aqueous solubility of the uncharged Zn(II)Pc-EGFR-L2 conjugate (3a) lowered its targeting ability. Importantly, the Zn(II)Pc-EGFR-L1 conjugates 2a and 2b could also be used as new imaging agents (Fig. 4c), taking advantage of the low toxicity that they present.

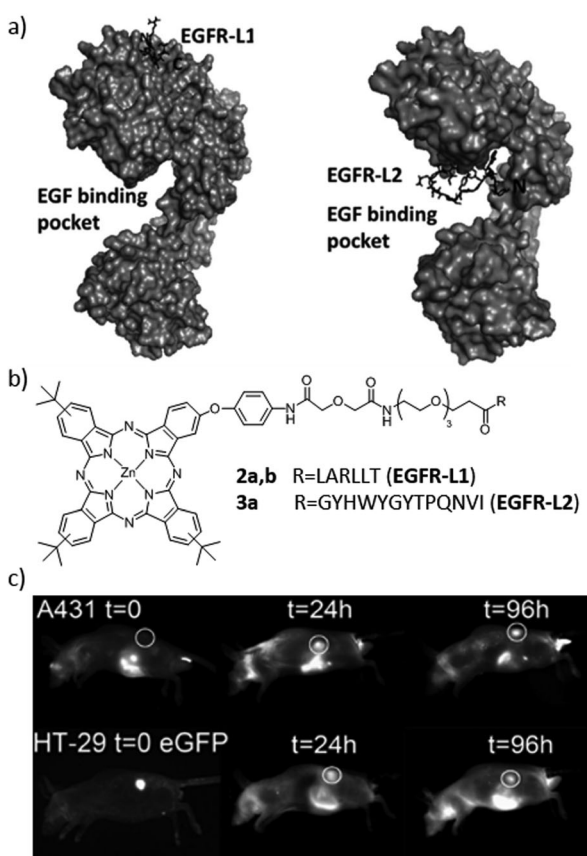


Fig. 4 (a) Low-energy docked structures of EGFR-L1 (left) and EGFR-L2 (right) peptides with the EGFR receptor. (b) Structures of the Zn(II)Pc-peptide conjugates prepared to target the EGFR receptor. (c) Fluorescence images (exc. 630 nm/em. 700 nm) of nude mice bearing subcutaneous tumour implants of A431 (top) or HT-29 (bottom) cancer cells at various times following the administration of biohybrid 2b. Adapted with permission from ref. 52. Copyright 2012 American Chemical Society.

In a different approach, peptides with LARLLT (EGFR-L1) and GYHWYGYTPQNV (EGFR-L3) sequences have been linked to mesoporphyrin IX, using one or two propionic side chains, connected directly or through a triethylene glycol spacer.<sup>77</sup> Cytotoxicity was tested in human Hep2 cells. The authors of this work conclude that the nature of the peptide and the spacer influences the targeting ability and cellular uptake. The conjugate that showed a higher affinity for EGFR was the one bearing two EGFR-L1 sequences, with no triethylene glycol spacers. After that, the synthesis of a BODIPY bearing an isothiocyanate group allowed its conjugation with the same peptides.<sup>60</sup> After studies with human Hep2 cells that overexpress the EGFR, the BODIPY conjugates showed a low toxicity, and their targeting ability was much higher compared to that of the non-conjugated BODIPY. Based on these results, the authors proposed the conjugates as potential near-IR fluorescence imaging agents. Concerning BODIPY compounds, a final example describes the conjugation of these PS to a peptidomimetic capable of binding to HER2, which belongs to the family of EGFR receptors.<sup>78</sup> The cellular uptake of the conjugate was studied by confocal fluorescence microscopy, showing a clear interaction with the receptor and the PS internalization in cells that overexpressed HER2.

**3.2.2. Targeting of the gastrin-releasing peptide (GRP) and integrin receptors.** The GRP receptor and the integrin  $\alpha_v\beta_3$  are other types of biological targets overexpressed in tumours of different natures. In particular, they can be targeted by bombesin (*i.e.*, a 14-AA peptide with the sequence pEQRLGNQWAVGHL-NH<sub>2</sub>) or arginine-glycine-aspartic acid (RGD) derivatives.<sup>79,80</sup> Consequently, in 2008, van Lier and co-workers were the first to synthesize a bombesin-Pc conjugate to target the GRP receptor.<sup>54</sup> To this end, they made use of tetrasulphonated Al(III)Pc (AlPcS<sub>4</sub>), observing that the photodynamic efficacy in PC-3 human prostate cancer cells had improved with conjugation. In 2017, Giuliana *et al.* synthesized two additional conjugates composed of bombesin and an asymmetric Zn(II)Por, linked to a chelator that allows metal coordination, in order to target prostate cancer cells for PDT and imaging applications.<sup>81</sup> The preparation of such PS was carried out by click chemistry and amide coupling reactions, yet the compounds were obtained in very low yields and with a laborious HPLC purification. In order to achieve higher yields, the authors suggested that the choice of the PS might be a critical point. Besides, bombesin has been linked to a BODIPY in experiments carried out by Brizet *et al.*, the resulting hybrid being suitable for bimodal PET/optical imaging.<sup>82</sup>

The  $\alpha_v\beta_3$  integrin, on the other hand, is a protein present in many tumour cells, which is implicated in different tumoural processes such as tumour growth, angiogenesis and metastasis. This protein is expressed in tumour endothelial cells, and it can be recognized by the RGD triad. In this way, RGD peptides have been used as blockers of integrins, in order to avoid tumoural events.<sup>83,84</sup> Chaleix *et al.* designed, for example, a procedure for the synthesis of RGD-substituted Por.<sup>85</sup> This method is based on the linkage of H<sub>2</sub>Por bearing a carboxylic acid function at their meso position and the RGD peptide through a solid phase approach. The phototoxicity of the obtained conjugates was tested in a K562 Human Chronic Myelogenous Leukaemia cell line,



and compared to the activity of Photofrin II, demonstrating its possible use in PDT. Cyclic RGD peptides have also been conjugated to tetraphenylchlorin and protoporphyrin IX using solid phase peptide synthesis (SPPS) as a chemical strategy, showing interesting results of phototoxicity.<sup>86,87</sup>

Finally, in 2013, the synthesis of a series of Zn(II)Pc–bombesin and Zn(II)Pc–RGD peptide conjugates (**4a–4e**) was reported by the van Lier group, targeting both the GRP and integrin receptors (Fig. 5).<sup>56</sup> The resulting conjugates showed a good aqueous solubility, and their photodynamic effects were evaluated in cell lines that express GRP and integrin receptors at different levels. The Zn(II)Pc–bombesin conjugate **4e** showed promising results as a dual fluorescence imaging probe and photodynamic agent. In particular, this biohybrid could be used as a PS for PDT of cancers where the GRP receptor is overexpressed, as such as prostate, breast and lung cancers. In 2014, Lo and co-workers published a different Zn(II)Pc–RGD peptide conjugate.<sup>57</sup> In particular, they covalently linked a Zn(II)Pc with a monomeric cyclic Arg-Gly-Asp-D-Phe-Lys (cRGDFK) moiety, which is an  $\alpha_v\beta_3$  integrin antagonist. The cellular uptake was higher in  $\alpha_v\beta_3^+$  U87-MG human glioblastoma cells, which present a higher expression of  $\alpha_v\beta_3$  integrin, as compared with  $\alpha_v\beta_3^-$  MCF-7 human breast adenocarcinoma cells, with a lower  $\alpha_v\beta_3$  integrin expression.

**3.2.3. Targeting of the gonadotropin releasing hormone (GnRH) receptor.** GnRH is a pituitary hormone, and its receptor appears in different reproductive tissues and tumours associated with them.<sup>88</sup> To target this receptor, in 2002 Koch and co-workers synthesized two conjugates composed of protoporphyrin IX and some GnRH analogues, an agonist and an antagonist, through the reaction between a free amino group from the peptides and a carboxylic group from the PS.<sup>89</sup> The binding ability of the conjugates to the receptor was lower than expected, however, probably due to the steric effects produced by the PS. Using a pituitary gonadotrope cell line, phototoxicity studies were carried out, showing that the binding of GnRH to protoporphyrin IX did not affect the conjugate phototoxicity.

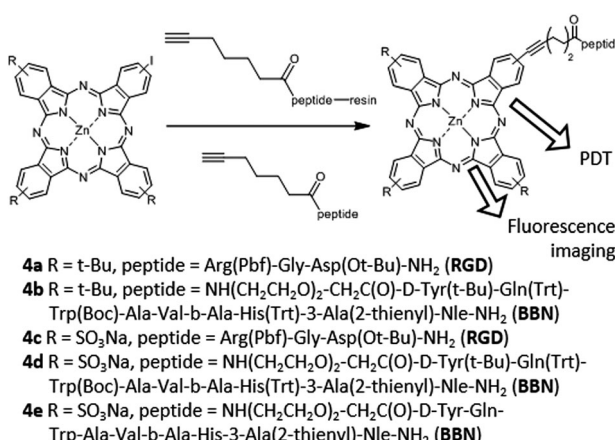


Fig. 5 Structures, synthetic strategies and uses of Pc–peptide conjugates for targeting the GRP and integrin receptors. Adapted with permission from ref. 56. Copyright 2013 American Chemical Society.

About a decade later, in 2012, Huang and co-workers reported a Zn(II)Pc-peptide biohybrid targeting the GnRH receptor.<sup>50</sup> The hybrid was able to photogenerate  $^1\text{O}_2$  as efficiently as the free Zn(II)Pc, while phototoxicity and cellular uptake were more pronounced in cell lines overexpressing GnRH receptors (MDA-MB-231 and MCF-7), *e.g.*, in human breast cancer cells, than in normal ones. Moreover, it was demonstrated, through the use of Cetrorelix (*i.e.*, a GnRH blocker), that the GnRH receptor is responsible for cellular uptake, *e.g.*, in MCF-7 cells. These results prove the covalent conjugation of Zn(II)Pc with GnRH analogues as an excellent strategy to increase the selectivity for GnRH-overexpressing cells or tissues.

**3.2.4. Nuclear targeting.** Nuclear localization signals (NLS) are sequences of amino acids that proteins carry to be imported to the cell nucleus.<sup>90</sup> In 1999, the synthesis of some conjugates composed of covalently linked chlorin e6 and a NLS peptide was described, and confocal fluorescence microscopy confirmed the PS localization in the cell nuclei of CHO and RIF-1 cell lines.<sup>91</sup> In 2012, Lo and co-workers synthesized a novel Zn(II)Pc conjugate with a NLS peptide, through a protocol that combined click chemistry and Fmoc-based SPPS,<sup>53</sup> achieving good results of cellular uptake and ROS generation in HT29 human colorectal carcinoma cells. Sibrian-Vazquez *et al.* synthesized, in turn, multimeric Por-NLS conjugates (**5a–5f**), carrying between two and four NLS peptide moieties, linked to H<sub>2</sub>Por through PEG or 5-carbon spacers, located at the meso positions of the Por macrocycle (Fig. 6).<sup>92</sup> The uptakes of the conjugates were different depending on the configuration of the NLS peptides in the Por structure, and on the number of peptide units. The conjugate carrying a sequence of three consecutive NLS linked by a PEG group to the Por core (**5a**) showed the highest cellular uptake and phototoxicity in human carcinoma HEp2 cells. However, no correlation could be observed between the number of NLS units and the cellular uptake. The phototoxicity observed in most cases was actually low, which can be explained by an inefficient delivery into the cytoplasm. This work was in any case interesting as one of the few studies aiming to establish structure–activity relationships for PS–peptide hybrid systems.

A different example of conjugation of a NLS sequence to H<sub>2</sub>Por was described by Kahl and co-workers.<sup>93</sup> In this case, the conjugate was able to interact *in vitro* with low density lipoproteins (LDL) (see Section 4.1), allowing the delivery of the PS into tumorigenic cells overexpressing LDL receptors. Finally, as another interesting example, the conjugation of NLS peptides to BODIPY derivatives was carried out by De Borggraeve and co-workers,<sup>94</sup> through a copper catalysed azide–alkyne cycloaddition. Unfortunately, no nuclear localization was observed for such hybrids.

**3.2.5. Antimicrobial peptides.** Currently, different strategies are being searched to discover new therapies against microbial agents, in order to tackle the appearance of new forms of resistance to classical antibiotic drugs. PDI offers an excellent alternative in this respect, and the conjugation with antimicrobial peptides could certainly help in directing PS to specific target microorganisms.

In this direction, Dosselli *et al.* developed the conjugation of both a cationic H<sub>2</sub>Por and a neutral porphycene to the N- and



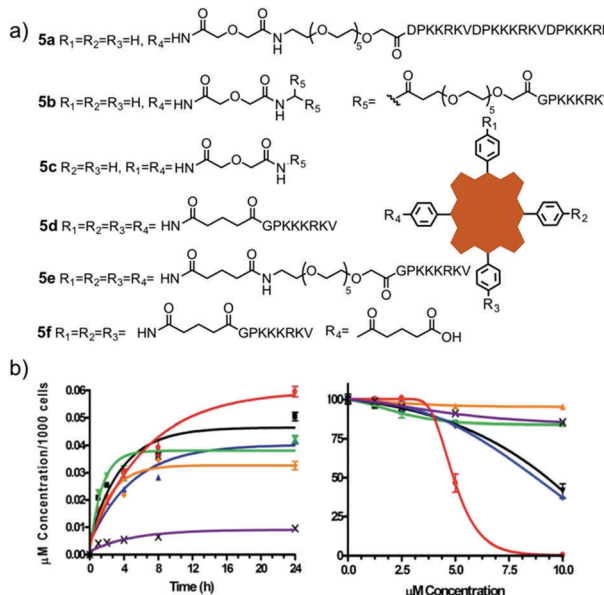


Fig. 6 (a) Structures of multimeric NLS-H<sub>2</sub>Por conjugates studied by Vicente and co-workers. (b) Time-dependent uptake of H<sub>2</sub>Por-NLS conjugates 5b (black), 5a (red), 5c (blue), 5d (orange), 5e (green), and 5f (purple) at 10 μM by HEp2 cells. (c) Phototoxicity of H<sub>2</sub>Por-NLS conjugates 5b (black), 5a (red), 5c (blue), 5d (orange), 5e (green), and 5f (purple) toward HEp2 cells using 0.5 J cm<sup>-2</sup> dose light. Adapted with permission from ref. 92. Copyright 2010 Royal Society of Chemistry.

C-terminal ends of apidaecin, an antimicrobial peptide, following different synthetic strategies, which depend on the PS and the peptide component.<sup>95</sup> Conjugating cationic Por to apidaecin resulted in promoting cellular uptake in Gram-negative bacteria, together with a reduction in the minimum effective dose. Importantly, conjugation did not decrease the capacity of the PS for <sup>1</sup>O<sub>2</sub> generation and fluorescence emission, in contrast to the case for porphycene. Furthermore, the peptide ability to enter into Gram-negative bacteria was lost in the porphycene hybrids.

From a different point of view, Vendrell and co-workers proposed the synthesis of conjugates composed of a fluorogenic, BODIPY-containing tryptophan derivative. The incorporation of this fluorogenic amino acid in short antimicrobial peptides (e.g., 6) did not impair their selectivity for fungal cells, and enabled a rapid and direct imaging of *Aspergillus fumigatus* directly in human pulmonary tissue, using different kinds of fluorescence assays and without any washing steps (Fig. 7).<sup>96–98</sup>

### 3.3. Multiple peptide strategy

The multiple peptide strategy consists of conjugating multiple peptides with different functions to the same molecule or material, in the present case, to a PS.<sup>99</sup> Such an approach allows the enhancement of different properties of the PS system, like the binding to a specific cell type or the cellular uptake, among many others. The use of bifunctional peptides, which contain a minimum sequence for translocation across cellular membranes and a signalling sequence to direct the movement of the molecule from the cytoplasm to a desired organelle, forms an interesting example of this strategy.<sup>100–102</sup> In this direction, Vicente and

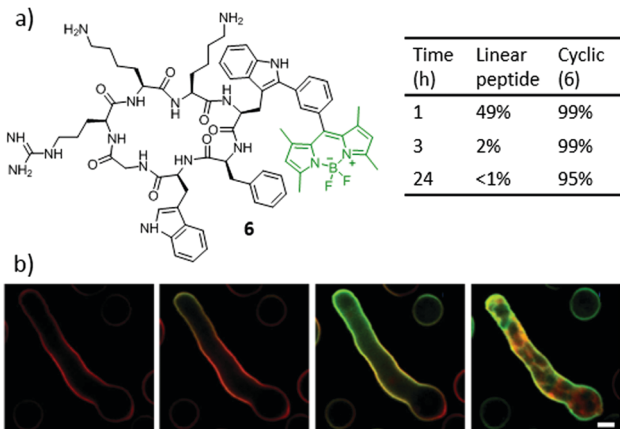


Fig. 7 (a) Structure of the highly stable and fluorogenic BODIPY-peptide biohybrid 6. (b) Time-lapse high-resolution imaging of *A. fumigatus* upon incubation with a cell membrane counterstain (red) and compound 6 (2 μM, green) for 0 min (i), 1 min (ii), 3 min (iii) and 10 min (iv). Scale bar, 2.5 μm. Adapted from ref. 97. Copyright 2016 Nature Publishing Group.

co-workers published a bifunctional peptide-Zn(<sup>II</sup>)Pc conjugate, containing the bipartite NLS nucleoplasmin peptide sequence and a fusogenic peptide sequence that corresponds to the human immunodeficiency virus I transcriptional activator (HIV-1 Tat, 48–60).<sup>49</sup> The presence of a short or long PEG-linker in the conjugates was also explored. The conjugate with the longer linker provoked a higher phototoxicity but, conversely, it presented a lower fluorescence quantum yield.

Alternatively, Engelen *et al.* synthesized a conjugate composed of a Por and two different peptides, CS3 and ES7, which act as thrombin inhibitors.<sup>103</sup> In particular, the authors prepared tetrakis(*p*-[aminomethyl]phenyl) H<sub>2</sub>Por, which carries four amino groups in meso positions, allowing the incorporation of the different peptide fragments through an adequate protection/deprotection strategy. The obtained PS hybrids could be used for sensing and imaging the interaction between different molecules and thrombin. Also with a H<sub>2</sub>Por, Vicente and co-workers synthesized conjugates, which contain cell penetrating peptides (CPP) and NLS peptides, searching for an enhancement of their phototoxic and biological properties,<sup>104</sup> yet no nuclear localization was observed. In the same year, an additional study by the same group explored the photodynamic activity and biodistribution of these types of conjugates (7a–7e), in prostate cancer cells, obtaining good results of phototoxicity and selective subcellular accumulation in the lysosomes and in the endoplasmic reticulum (ER) (Fig. 8).<sup>105</sup> Importantly, both these organelles are normally implicated in the PDT-induced initiation of apoptosis, which explains at least in part the good phototoxicity results observed for these biohybrids.

## 4. PS–protein biohybrids

### 4.1. Hybrids with serum proteins

A very common strategy to administer drugs into the bloodstream is by association with different serum proteins, such as albumin and high and low density lipoproteins, which then act as biological carriers. The association between these proteins



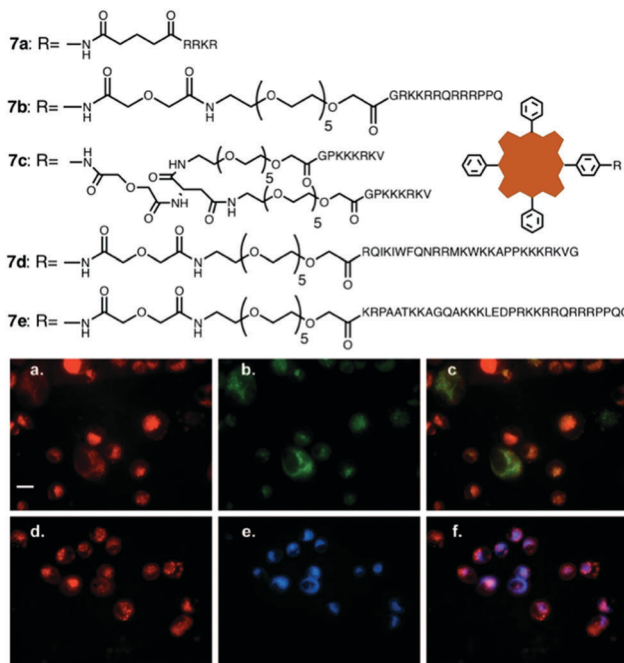


**Fig. 8** Structures of bifunctional NLS/CPP peptide–H<sub>2</sub>Por conjugates **7a–7e** and subcellular localization studies for conjugate **7b**. (a and d) Red fluorescence indicating the location of conjugate **7b**. (b) Green fluorescence indicating the location of lysosomes in cells from (a). (c) Overlay of (a) with (b). (e) Blue fluorescence indicating the location of the ER in cells from (d). (f) Overlay of (d) with (e). The degrees of the orange (c) or purple (f) colours indicate the intensity of conjugate **7b** and organelle co-localization in individual cells. Scale bar, 25  $\mu$ m. Adapted with permission of ref. 105. Copyright 2008 American Chemical Society.

and hydrophobic PS therefore also enhances their photodynamic activity and intracellular accumulation by endocytosis.<sup>100</sup> In this section we review the literature about both covalent and supramolecular combinations of different PS with serum proteins.

**4.1.1. Hybrids with serum albumin.** Out of all serum proteins in the human plasma, human serum albumin (HSA) is the most abundant one. This protein binds many different hydrophobic molecules, thus representing an efficient drug carrier. HSA is actually involved in several cellular processes, including some that are characteristic of cancer.<sup>106</sup> For this reason, PS-albumin conjugates are of much interest for the development of biomedical applications. There are in the literature a lot of publications that explore the fundamental interactions between PS and albumins.<sup>107-114</sup> Such studies, which comprise both physicochemical and biophysical insights, represent an extensive field with the general aim of understanding how natural albumins present in the body can, upon injection of bare PS, become PS carriers and deliver them at the target site. However, as the present review deals with biohybrid materials, herein we will focus on a different strategy, consisting of using synthetic hybrids where the albumin is modified with PS prior to biomedical use, in order to enhance their chemical and biological features.

The first ones to take up this approach were van Lier and co-workers, who synthesized both non-covalent and covalent

Pc-BSA (bovine serum albumin) hybrids in two successive publications. The non-covalent hybrid consisted of Zn(II)Pc-BSA in an 11:1 molar ratio.<sup>115</sup> Two different models of tumour-bearing mice were employed to study the biocompatibility and tumour control capacity of this biohybrid. The same authors later covalently coupled two water-soluble tetrasulphonated Al(III)Pc derivatives to BSA, in a 9:1 molar ratio, *via* a spacer bearing a free carboxylic acid group that can react with the free amines of the BSA protein.<sup>116</sup> Due to the possible aggregation of the Al(III)Pc within the BSA pocket, the activities of these hybrids were not so high.

Supramolecular complexes of BSA or HSA have also been described with Si(iv)Pc compounds bearing cationic substituents at their axial positions.<sup>117–119</sup> In all cases, the photodynamic activities of the hybrids were higher than that of the free Si(iv)Pc. Importantly, PS aggregation in the protein cavity was proven detrimental for the PDT efficacy, as it quenches the PS excited state. Consequently, the most promising results were obtained for a dicationic Si(iv)Pc that was, in contrast to the others, completely water-soluble. Following these studies, other examples of BSA/HSA–Pc conjugates have been described in the literature.<sup>120–123</sup> As an interesting case, a Zn(ii)Pc was linked to a bifunctional protein containing HSA and an amino-terminal fragment of urokinase (ATF).<sup>124</sup> ATF binds to the urokinase receptor, which appears with high expression levels in tumoral cells, and so this conjugate could serve as a dual-mode PDT and imaging agent (Fig. 9a). Li *et al.* described, on the other hand, a covalent hybrid of IR700DX, a commercially available Si(iv)Pc, and HSA bearing tumour targeting RGD peptides, connected through an oligoethylene glycol spacer.<sup>125</sup> Phototoxicity studies in ovarian cancer cells showed that cellular delivery with this conjugate occurred *via* an endocytosis process. Moreover, this multivalent biohybrid resulted in being highly specific towards carcinogenic cells, while cells that did not express  $\alpha_v\beta_3$  integrin were not affected.

Concerning PS other than *Pc*, *Lu et al.* prepared BODIPY-based hierarchical nanostructures by hydrogen bonding with *Mn(II)* complexes, which in turn were bound to HSA by hydrophobic forces.<sup>126</sup> In order to increase the biocompatibility and tumoral selectivity of the resulting particles, they were conjugated to PEG-folic acid derivatives. Under irradiation of red LED light, these nanohybrids were capable of generating  $^1\text{O}_2$  and ROS, and of acting as MR agents for imaging techniques. With chlorin e6, similar theranostic approaches have been considered. *Hu et al.*, for example, reported the synthesis and application of activatable HSA-chlorin e6 assemblies that can be thermally modulated for imaging and PDT action against cancer cells.<sup>127</sup> Chlorin e6 was linked to HSA using hydrophobic interactions and intermolecular disulfide bonds, and the resulting hybrids showed promising features such as tumour selectivity, programmed self-assembly and controllable activation of their theranostic activity. Using a similar approach, chlorin e6, among other PS, has also been encapsulated in protein-based nanospheres consisting of HSA and poly-L-lysine, using the electrostatic assembly strategy.<sup>128</sup> Moreover, the said nanospheres were designed to selectively release chlorin e6 upon a combination of multiple tumour

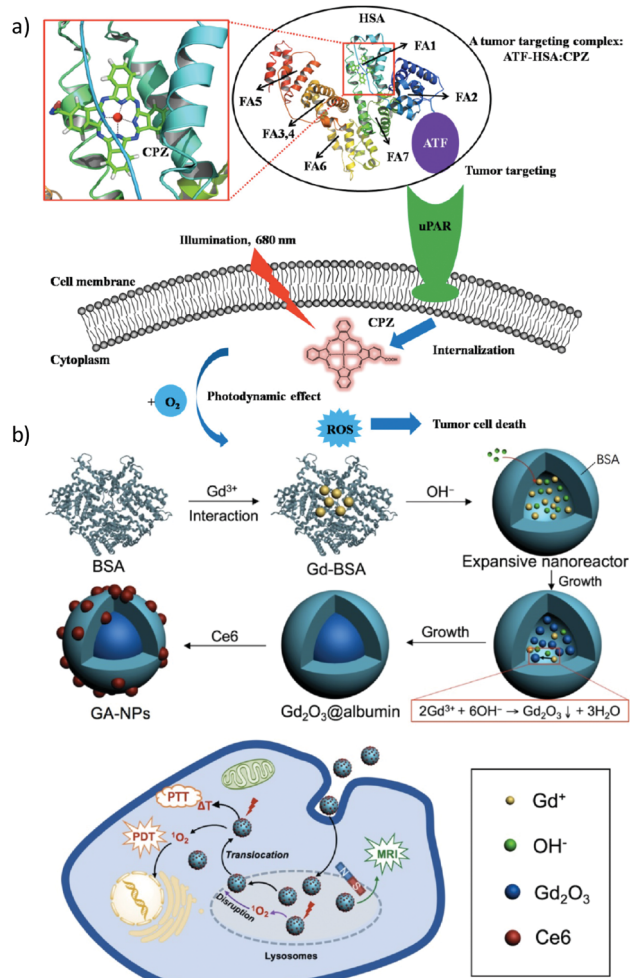


**Fig. 9** Two examples of theranostic systems based on PS-containing HAS biohybrids. (a) Strategy to use a bifunctional recombinant protein (ATF-HSA) loaded with a Zn(II)Pc, for targeting the urokinase receptor (uPAR) and thus treating uPAR-expressing tumour cells upon illumination. The PS is bound at the fatty acid binding site FA1 of HAS. Reproduced with permission from ref. 124. Copyright 2014 Ivspring. (b) Schematic representation of the use of albumin as a nanoreactor for the synthesis of chlorin e6-loaded  $\text{Gd}_2\text{O}_3$ -albumin nanoparticles as agents that enable MRI-guided cancer PDT treatments. Reproduced with permission from ref. 130. Copyright 2017 Ivspring.

related triggers, resulting in highly tumour-responsive PDT treatment. Effectively, the hybrid nanospheres were proven to be nontoxic in the dark and cytotoxic under irradiation in three different cancerous cell lines, including HeLa, B16 and MCF-7.

As a different concept, chlorin e6 has been linked to BSA and, simultaneously, to polypyrrole nanoparticles, to form conjugates with good PDT and photothermal therapy (PTT) efficiencies, without dark toxicity.<sup>129</sup> With Gd(III) labelling, the conjugates could act as imaging agents, thus presenting multiple biological applications. In 2017, Zhou *et al.* described the growth of  $\text{Gd}_2\text{O}_3$  nanocrystals using the hollow cavity of albumin as a nanoreactor, followed by a later carbodiimide-mediated coupling reaction with chlorin e6.<sup>130</sup> These systems were evaluated as magnetic resonance imaging (MRI) agents for tumour localization, PDT and PTT, with good results of cellular toxicity (Fig. 9b).

Finally, nanoparticles composed of pheophorbide *a*, BSA and polyethylene glycosylated folate have been synthesized by Battogtokh and Ko.<sup>131</sup> The use of the pH-responsive cleavable *cis*-aconityl moiety as a spacer between the PS and BSA allowed activating the hybrid fluorescence intracellularly, while the presence of folate gave rise to enhanced results of phototoxicity in cancer cells, compared to conjugates without the folate targeting units. As an interesting example, an Fe(II)Por has been conjugated to BSA, and at the same time, the porphyrinoid was encapsulated in a covalent way into the inner cavity of cyclodextrins (CD) to form complexes that could act as oxygen carriers.<sup>132</sup> This concept of encapsulation of PS into the inner cavity of CD will be further discussed in Section 6.

**4.1.2. Hybrids with lipoproteins.** There are different examples of naturally produced lipoprotein particles, the most common groups being high-density lipoproteins (HDL), low-density lipoproteins (LDL) and very low-density lipoproteins (VLDL), among others. These proteins are able to transport different hydrophobic compounds. The use of LDL, in particular, has been a widespread strategy in recent years for the construction of biohybrid materials. LDL consist of a cholesterol ester core, surrounded by a shell of cholesterol and phospholipids, with a copy of the apolipoprotein B100. The LDL receptor is over-expressed in tumour cells, making these particles a good choice as drug delivery carriers.<sup>133,134</sup> However, most of this research was published in the 90s and the first years of this century, and has been reviewed extensively.<sup>100</sup> Herein we thus only give a general impression about this research line, while for a better inspection of the topic we refer to the reading of such review articles.

In order to link PS drugs to LDL, three main types of methodologies can be employed, which include the PS covalent linkage to the apolipoprotein, the introduction of the drug into the protein core, and its non-covalent adsorption to the surface of the lipoprotein. The most useful method is the last one, which leads to stable conjugates that do not alter the LDL transport properties.<sup>135</sup> As a prominent recent example, Tang *et al.* carried out PDT experiments using lactone-containing fluorinated H<sub>2</sub>Por and Zn(II)Por derivatives **8a–8d**, with conjugated glucose moieties improving the affinity for LDL (Fig. 10).<sup>136</sup> The association with LDL improved cellular uptake *via* an LDL-dependent pathway, which in turn favored a selective localization in the lysosomes.  $\beta$ -Lactonization at the Por macrocycle, on the other hand, increased the intracellular production of ROS, having a positive effect on phototoxicity against HeLa cells, through an apoptotic mechanism.

#### 4.2. PS–antibody biohybrids

The preparation of hybrids between antibodies and PS has led to the development of a completely new field, called photoimmunotherapy (PIT), a term that was first coined in 1983.<sup>14</sup> In PIT, the PS imparts phototoxic properties to the hybrid, while monoclonal antibodies (MAb) act as targeting molecules, directing the PS to the desired cells or tissues. An important aspect in the design of this kind of therapeutic agent is to preserve both the antigenic specificity of the MAb and the



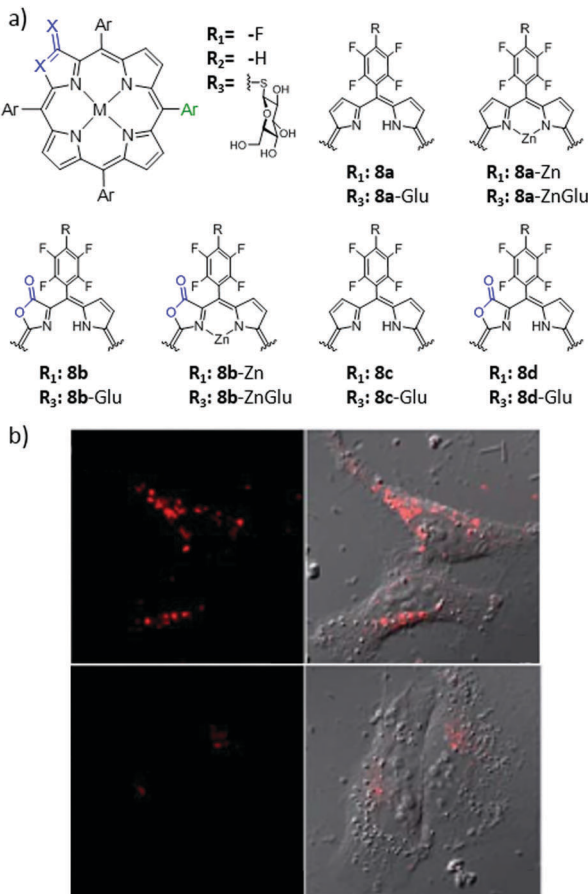


Fig. 10 (a) Chemical structures of Por derivatives **8a–8d**. (b) Confocal images of HeLa cells treated with 2  $\mu\text{M}$  **8b**-Glu, 100  $\mu\text{g mL}^{-1}$  LDL and 0  $\text{mg mL}^{-1}$  heparin (top) or 5  $\text{mg mL}^{-1}$  heparin (bottom). Adapted with permission from ref. 136. Copyright 2014 Royal Society of Chemistry.

intrinsic photophysical properties of the PS in the hybrids. An excellent and extensive review about different conjugation strategies of PS with antibodies has been recently published and should be consulted for getting a deeper insight into this topic.<sup>137</sup> As a consequence, herein we only focus on the most important and most recent examples, classifying them according to the biological receptors that they are aimed to target.

**4.2.1. Targeting of the epidermal growth factor receptor (EGFR).** As a precursor of this strategy, in 2009, a sulphonated Ga(III) corrole derivative (Ga(III)Cor) was linked to a breast cancer-targeted CPP (HerPBK10), with the aim of targeting HER2, thus mimicking the role of anti-HER MAb, while acting as a dual-functioning imaging and therapeutic agent (Fig. 11).<sup>138</sup> The *in vivo* targeted delivery of the protein–corrole complex actually led to tumour cell death, which could be visualized by the intense corrole red fluorescence.

The synthesis of PS–antibody conjugates, in turn, has become of growing interest since Kobayashi and co-workers initiated the field by describing two Si(iv)Pc–MAb conjugates based on the same Si(iv)Pc compound, denoted IR700, with the resulting biohybrids presenting super-enhanced permeability and retention (SUPR) effects, upon activation by near-infrared irradiation.<sup>139</sup> In the

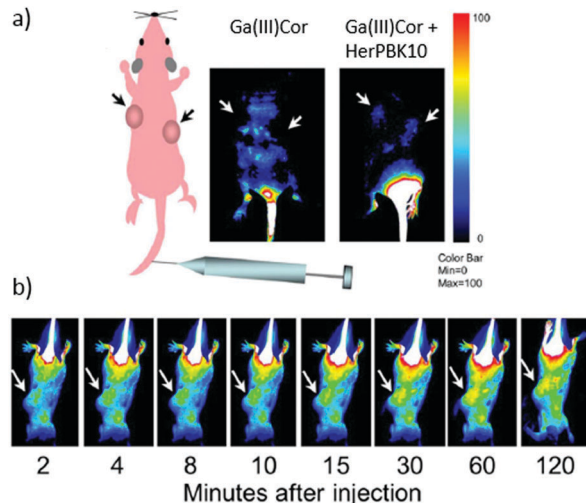


Fig. 11 (a) Detection of Ga(III)Cor–HerPBK10 *in vivo* targeting and intracellular trafficking. Live animal imaging of corrole fluorescence after the IV delivery of either the Ga(III)Cor or targeted complex. The scheme on the left indicates the whole body and tumour orientation of the mice in the fluorescence images. (b) Images capturing the time course of corrole circulation in mice after receiving the Ga(III)Cor–HerPBK10 hybrid. Arrows in both (a) and (b) point to tumours. The Ga(III)Cor fluorescence is indicated by blue-red pseudocolouring, with the fluorescence intensity represented according to the colour bar on the right. Reproduced with permission from ref. 138. Copyright 2009 National Academy of Sciences.

first of a series of *in vivo* studies with IR700–MAb conjugates, the authors made use of two different MAb targeting the EGFR, namely panitumumab (directed against human EGFR 1 (HER-1)) and trastuzumab (directed against human EGFR 2 (HER-2)).<sup>140</sup> The resulting conjugates were denoted Pan-IR700 and Tra-IR700, respectively (Fig. 12). About three IR700 molecules were linked to each Mab in these conjugates, and no MAb aggregation was observed. Cytotoxicity studies revealed that both IR700–MAb conjugates exhibited the exceptional characteristic of being active only when bound to the cell membrane, and not in their free unbound form. Off-target phototoxicity, until now the largest side effect generally encountered in PDT, was in this way reduced or almost completely excluded. This inherent selectivity is of vital importance for real therapeutic applications.

Importantly, since IR700 can be activated by near infrared light of reasonably high wavelengths ( $\lambda_{\text{max}} = 689$  nm), the technique can also be referred to as NIR-PIT. In a subsequent publication by Kobayashi *et al.*, it was demonstrated that repeated administrations of NIR light could actually enhance, even more, the effect of the NIR-PIT.<sup>141</sup> Another desirable feature of PIT using IR700–MAb conjugates is that they emit fluorescence upon activation, so before the PIT the hybrid can be used to monitor the application of light and minimize the exposure of the surrounding tissues. The success of IR700–MAb conjugates has generated a lot of research to understand the mechanism and rates of cell death caused by NIR-PIT. On the other hand, apart from observing cell death, Kobayashi and co-workers have also monitored the acute cytotoxic effects caused by PIT with the use of different techniques such as bioluminescence,<sup>142</sup> fluorescence lifetime imaging<sup>143</sup> and <sup>18</sup>F-FDG PET.<sup>144</sup> Up to now,



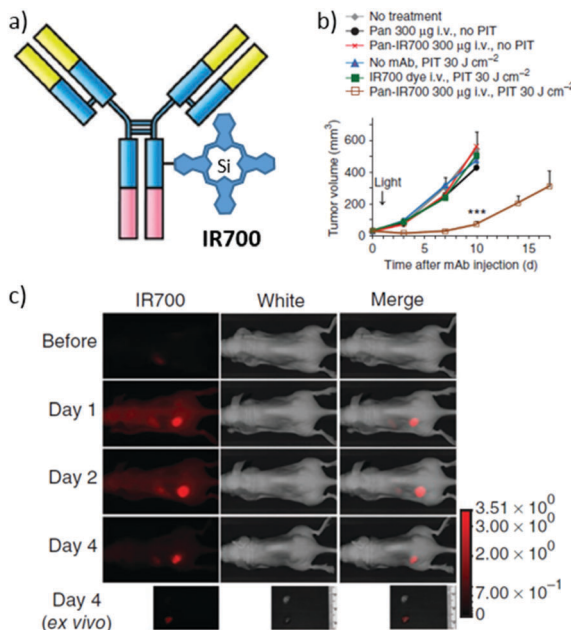


Fig. 12 (a) Schematic representation of IR700-MAb conjugates, designed and developed for use in PIT. (b) Target-specific tumour growth inhibition by Pan-IR700 after PIT in A431 tumours. (c) Biodistribution of Pan-IR700. A431 tumours (from both sides of the dorsum) were selectively visualized with IR700 fluorescence as early as 1 day after injection of 300 µg of Pan-IR700. Adapted with permission from ref. 140. Copyright 2011 Nature Publishing Group.

NIR-PIT with Tra-IR700 as the PS has been successfully tested in preclinical trials for the treatment of peritoneal ovarian cancer<sup>145</sup> and lung metastases.<sup>146,147</sup>

Following this successful work, various examples have appeared in the literature about Por conjugation to EGFR-targeting MAbs. Maruani *et al.* described in 2015 a PS-MAb conjugate composed of trastuzumab and a water-soluble azide-containing H<sub>2</sub>Por.<sup>148</sup> In particular, they chose a disulfide linker to modify the MAb with a dibromopyridinedione-strained alkyne, which was subjected to a copper-free strain-promoted alkyne-azide cycloaddition (SPAAC) reaction with the H<sub>2</sub>Por derivative. The obtained biohybrid showed good results of phototoxicity, and a minimal dark toxicity, in experiments with HER2+ cells. More recently, Oliveira and co-workers synthesized a different H<sub>2</sub>Por-trastuzumab conjugate to target HER2 in gastric cancer,<sup>149</sup> and the PIT results were promising, reducing side effects in cells that do not express HER2. The accumulation of the conjugate in lysosomes could actually be the reason for its higher phototoxicity. As the last example, again using the SPAAC strategy, a water-soluble aza-BODIPY has also been conjugated to trastuzumab.<sup>150</sup> This conjugate showed selectivity for HER2 receptors and has been claimed as a potential candidate for *in vivo* imaging techniques.

**4.2.2. Targeting of the carcinoembryonic antigen (CEA).** CEA belongs to the family of cell surface glycoproteins, and is overexpressed in human colon carcinomas, among others, for which it can be used as a tumour marker.<sup>151</sup> On these bases, in 1996, Pereyre and co-workers described the synthesis of radioactive In(III)Por, and their conjugation to BSA bearing anticarcinoembryonic MAb (anti-CEA).<sup>152</sup> After that, Kuroki and co-workers

published the bioconjugation of a MAb against CEA, F11-39, to a Ga(III)Por-based PS, by converting the PS carboxyl groups into succinimidyl esters.<sup>153</sup> The authors evaluated the cytotoxic effect of the conjugate in combination with sonodynamic therapy (SDT), which uses ultrasound irradiation, against CEA-expressing human gastric cells, obtaining much better results when applying SDT than with just visible light irradiation.

In a different approach, Pellegrin and co-workers described the conjugation of the MAb 37A7, directed against CEA, to tetrasulphonated Al(III)Pc, using the sulpho-NHS activation strategy.<sup>154</sup> *In vitro* and *in vivo* properties like immunoreactivity and photocytotoxicity were tested to understand the potential use of these conjugates in PDT. After that, a second paper was published evaluating the potential role of internalisation of the PS on its photoinduced cytotoxicity.<sup>155</sup> A related study was published in 2005, covalently linking MAb 35A7, which is not internalised upon binding CEA, to H<sub>2</sub>Por, making use of isothiocyanate chemistry. Assays of *in vitro* photoinduced cell inhibition in SKOv3-CEA-1B9 cell lines showed that these conjugates were more effective than the free PS, but even better results were obtained working with conjugates of MAb FSP 77 to the same H<sub>2</sub>Por, which target the extracellular domain of the HER2 receptor, present in this cell line and which is normally internalised.<sup>156</sup> More recently, Vicente and co-workers synthesized two Zn(II)Pc-antiCEA conjugates through carbodiimide-mediated coupling reactions, targeting and labelling human colorectal HT-29 cells with higher efficiency compared to the free Zn(II)Pc.<sup>157</sup> Finally, CEA targeting with MAb was reported by Bouvet and co-workers, who synthesized an anti-CEA-IR700 conjugate that expressed an extensive tumour cell killing in pancreatic cancer in mice.<sup>158</sup>

#### 4.2.3. Targeting of the cluster of differentiation molecules.

In 2005, Boyle and co-workers focussed on the synthesis of a Zn(II)Pc derivative absorbing and emitting in the 700–850 nm range, which can be obtained by a selective choice of its peripheral groups. Furthermore, this PS contained a single amine-reactive isothiocyanate group suitable for conjugation with MAb, which permits employing the obtained conjugates as luminescent probes.<sup>159</sup> To demonstrate this concept, the Zn(II)Pc was conjugated to both the anti-CD146 and the anti-CD104 MAb, which are tumour-associated antigens upregulated in different cancers. Analysis of flow cytometry data showed excellent selectivity of the conjugates for their respective targets, and a very low degree of non-specific binding. The conjugates were also demonstrated to be non-phototoxic at concentrations higher than those generally used for imaging, making them highly suitable for use in bioimaging applications. In a different approach, H<sub>2</sub>Por have been conjugated to BSA/HSA proteins and anti-CD104 Mab, taking advantage of the presence of an *N*-hydroxysuccinimide activated ester group in the Por structure, which reacts with the amino groups from Lys amino acid residues.<sup>160</sup> The phototoxicities of these conjugates were evaluated in the human bladder cancer cell line UM-UC-3, with the bioconjugation to anti-CD104 MAb yielding better results than the conjugates with BSA or HSA.

**4.2.4. Other types of antibodies.** Apart from the PS-MAb biohybrids discussed before, there are a few studies in the



literature that utilized other kinds of MAb for the same purpose. Because the number of examples for each type is limited, and they do not constitute an extensive research line on their own, we include them in a single, common section.

In 1986, Yarmush and co-workers described the synthesis of conjugates between chlorin-e6 and the MAb anti-Leu-1, which targets T-cells.<sup>161</sup> The conjugates were synthesized through coupling of the chlorin to a dextran polymer, which was able to bind the MAb supramolecularly. Phototoxicity studies in HPB-ALL human T-leukemia cells showed an effective production of  ${}^1\text{O}_2$  and a high cellular selectivity. Alonso *et al.*, in turn, synthesized a series of water-soluble H<sub>2</sub>Por derivatives that bear maleimide moieties with different spacers. Such PS were coupled by click reactions of the Por maleimide functionalities with cysteine residues from the SIP(L19) MAb, which targets the tumour neoangiogenesis marker EDB of fibronectin.<sup>162</sup> Phototoxicity was evaluated in LM-fibroblasts, and the best results were obtained with the conjugate that presented the longest and most hydrophilic spacer. Finally, a different example targeted GPC3, which is a cell-surface protein overexpressed in hepatocellular carcinoma (HCC), among others.<sup>163</sup> Based on the knowledge that YP7 is an anti-GPC3 MAb, Kobayashi and co-workers designed an IR700-YP7 conjugate, testing it in GPC3 expressing cells and tumour-bearing mice.<sup>164</sup> The effectiveness of this GPC3-targeted PIT could be increased by co-administering the nanoparticle albumin-bound paclitaxel (nab-paclitaxel), increasing the drug delivery and thus its therapeutic effect.

**4.2.5. Antibody fragments.** All PS-antibody conjugates mentioned above were based on full size MAb. Full size MAb allow getting a higher degree of labelling, because they present a high number of residues with reactive functional groups for conjugation. However, such a high loading of PS molecules sometimes affects the immune-reactivity of the MAb, increasing non-specific binding due to a longer serum half-life and decreasing diffusion in tumours with a poor vascularisation.<sup>137</sup> To overcome these limitations, the use of antibody fragments represents a possible improvement in the area of PIT.

There are some examples in the literature that explore this strategy. Kobayashi and co-workers, for example, made use of anti-prostate specific membrane antigen (PSMA) diabody (Db) and minibody (Mb) components, and compared their effectiveness as PIT agents with that of the full size anti-PSMA MAb (IgG).<sup>165</sup> Upon NIR irradiation in *in vitro* and *in vivo* experiments, PIT with IgG-IR700, Mb-IR700 and Db-IR700 resulted in the death of PSMA-positive cells. From biodistribution data of the different conjugates, however, it became clear that Db-IR700 was characterized by a significantly shorter time interval between injection and tumour uptake. This advantageously enabled the possibility of reducing the time interval between injection and NIR irradiation, pointing out the utility of such an approach.

Boyle and co-workers conjugated MAb fragments to Por derivatives through an elegant strategy that ensures the stability of the hybrids.<sup>166</sup> In particular, they functionalized two water-soluble Zn(II)Por using azide-alkyne cycloaddition reactions. In one case, the azide group was directly substituted onto the Por ring (**9a**), whereas for the other conjugate a short OEG spacer

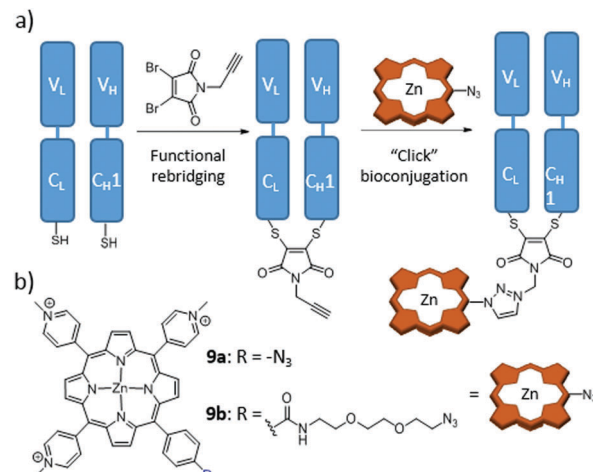


Fig. 13 (a) Scheme of the novel conjugation strategy followed to produce trastuzumab Fab fragments, through functional rebridging and click chemistry with Zn(II)Por. (b) Chemical structures of employed Zn(II)Por **9a** and **9b**. Adapted with permission from ref. 166. Copyright 2014 American Chemical Society.

chain was used (**9b**), in order to study the possible reduction of photodynamic activity by quenching of the PS excited state due to the proximity to the MAb fragment (Fig. 13). For conjugation, the authors used the antigen binding fragment (Fab) from trastuzumab, which was first reduced with tris(2-carboxethyl)-phosphine to break the disulfide bridge, and the resulting thiol-containing fragments (V<sub>L</sub>-C<sub>L</sub>-SH and V<sub>H</sub>-C<sub>H1</sub>-SH) were reacted with a propargyl-containing dibromomaleimide. The last step in their approach was to click this fragment with the azide-Zn(II)Por derivatives **9a** and **9b**. Importantly, no difference in phototoxicity between the two Fab-Zn(II)Por conjugates was found, both of them showing very good selectivity for HER2<sup>+</sup> cells, with no dark toxicity.

#### 4.3. PS-protein cage hybrids

Hollow protein scaffolds such as ferritin and virus-like particles (VLP) have been employed during the last two decades as nanocarriers and nanoreactors, due to their ability to accommodate different kinds of materials, including synthetic polymers and drugs, enzymes, inorganic nanoparticles and organic dyes, inside their inner cavity.<sup>167,168</sup> These protein cage architectures are precise assemblies of protein subunits with a diversity of roles in Nature, from nucleic acid storage and transport in viruses to iron mineralization in ferritins. Importantly, not only the native cages but also analogues obtained by functionalization of their inner and outer surfaces, or of the interstitial protein environment, have led to new hybrid materials for direct application in materials synthesis, drug delivery, and catalysis. Among all these possibilities, the present section will focus on research about the incorporation of PS in different protein cages, which can actually be classified according to their natural origin.

**4.3.1. PS biohybrids based on the cowpea chlorotic mottle virus (CCMV) capsid.** One of the most common protein cages used in nanotechnology is the CCMV capsid. CCMV is a positively charged, single-stranded RNA plant virus composed of 90 coat protein (CP) dimers. In the native state, these CP dimers



self-assemble into a  $T = 3$  icosahedral capsid formed by 12 pentameric and 20 hexameric capsomers, with outer and inner diameters of 28 and 18 nm, respectively.<sup>168,169</sup> The inner cavity can be utilized to host different materials, through its disassembly into CP dimers by changing the pH and ionic strength, followed by reassembly in the presence of the cargo.<sup>170–172</sup> Besides, other protein cage architectures can be obtained (*e.g.*,  $T = 1$  and  $T = 2$  capsids, with outer diameters of 18 and 22 nm, respectively), when the reassembly process occurs at neutral pH and in the presence of polyanionic templates.<sup>173</sup>

de la Escosura, Cornelissen and co-workers were the first to describe the loading of tetrasulphonated Zn( $\text{II}$ )Pc aggregates inside CCMV-based VLP, following two different strategies, which led to obtaining  $T = 3$  and  $T = 1$  VLP.<sup>174</sup> The UV-Vis spectrum of encapsulated Zn( $\text{II}$ )Pc exhibited changes compared to the free Zn( $\text{II}$ )Pc, and the resulting hybrid particles showed their potential as PS carrier systems for PDT. Both kinds of VLP were further studied by Luque *et al.*, through cryo-electron microscopy (cryo-EM) and atomic force microscopy.<sup>175</sup> These studies showed that, in the  $T = 3$  VLP, the Zn( $\text{II}$ )Pc molecules are localized underneath the pores of the protein cage, while  $T = 1$  VLP present in their interior a well-packed Zn( $\text{II}$ )Pc nanosphere of 10 nm diameter, this being the reason for their enhanced mechanical properties (Fig. 14).

Other polyanionic Pc-based systems have been reported as templates for the preparation of CCMV biohybrids. The same group described the inclusion of two Zn( $\text{II}$ )Pc and two Ru( $\text{II}$ )Pc dendritic compounds, functionalized with carboxylate dendrons at their peripheral or axial positions, respectively.<sup>176</sup> Despite the encapsulation of all these dendritic Pcs, the authors demonstrated that those which present 16 negative charges are the most efficient templates for VLP assembly, as they match the number of positively charged residues present in the N-termini of each CP dimer.<sup>170</sup> This result highlights the importance of the template effect in this kind of cooperative self-assembly process. Moreover, UV-Vis spectra of the biohybrids showed no significant changes in the Pcs absorption when encapsulated, ensuring that the photosensitizing properties remain intact when compared to the Pcs in solution, and demonstrating the suitability of these biohybrids as PS agents. In a different approach, the hierarchical self-assembly of a monocationic Zn( $\text{II}$ )Pc in

paramagnetic anionic micelles, which were subsequently encapsulated into CCMV VLP, has led to a promising multimodal imaging and theranostic agent.<sup>177</sup> To this end, the anionic micelles were formed by an amphiphilic Gd<sup>3+</sup> complex. Interestingly, it is the self-assembly of the micelles which triggers the self-assembly of the VLP particles. This elaborate strategy aimed at avoiding undesired aggregation of Zn( $\text{II}$ )Pc molecules within the hybrid ensemble, to preserve their fluorescence and photosensitizing properties. Gd<sup>3+</sup> complexes, in turn, are well-known MRI agents, giving rise to a multimodal imaging biohybrid.

**4.3.2. PS biohybrids based on the use of phages.** A different virus that has been used to construct biohybrids with PS is the MS2 phage. This virus is an icosahedral RNA bacteriophage, with  $T = 3$  architecture.<sup>178</sup> Its structure, as in the case of CCMV, can be assembled and disassembled reversibly, and so different kinds of molecules and materials, including PS, can be incorporated in its capsid.

Cohen and Bergkvist, for example, reported the construction of MS2 biohybrids loaded with *ca.* 80 cationic H<sub>2</sub>Por molecules per capsid, *via* a nucleotide-driven packaging, and decorated on the outer surface with aptamers that act as targeting moieties for human breast cancer cells.<sup>179</sup> As control, capsids that were decorated with non-targeting nucleotide sequences did not show any phototoxic effect. This proves that the linkage of DNA sequences to virus capsids can be extremely useful to direct PS–VLP hybrids to different tumoral tissues. Stephanopoulos *et al.* described, for instance, an MS2 biohybrid decorated with up to 180 H<sub>2</sub>Por **10** units at the capsid's inner surface (Fig. 15).<sup>180</sup> This was achieved by linking the thiol corresponding to Cys87, located in the inner cavity upon assembly, with the maleimide-modified **10** *via* the thiol–maleimide “click” reaction. Furthermore, DNA aptamers targeting protein tyrosine kinase 7 (PTK7) receptors on Jurkat leukaemia T cells were grafted onto the capsid outside. As a consequence, the selectivity shown by these biohybrids, with a ratio of 20 copies of the aptamer per capsid, was very high, and they also presented an excellent PDT activity.

Similarly, the P22 phage, which is another example of a bacteriophage with an icosahedral capsid and, in this case, double-stranded DNA as genomic material,<sup>181</sup> has been used to include porphyrinoid PS in its structure. In particular, Douglas and co-workers encapsulated Mn( $\text{III}$ )Por inside VLP–polymer covalent hybrids, to be used as MRI contrast agents.<sup>182</sup> To this end, a mutant P22 phage was swollen by resuspension of the protein pellet into PBS 100 mM and NaCl 50 mM, pH 7.6, and subjected to polymerization within the capsid. Further modification was achieved through EDC-mediated labelling of the amino-containing polymer with NHS-modified Mn( $\text{III}$ )Por.

**4.3.3. PS biohybrids based on ferritin.** Ferritins constitute a family of iron storage proteins with ubiquitous distribution among most of the life forms, with internal and external diameters of 8 and 12 nm, respectively. Their natural predisposition to mineralize a variety of minerals and metals within the cage empty cavity (*i.e.*, apoferritin (aFt)) and their well-known structural features, such as their stability and the possibility of redesigning the interior, are key values to their wide use in various fields of research, including nanotechnology, biomedicine and materials science.<sup>183</sup>

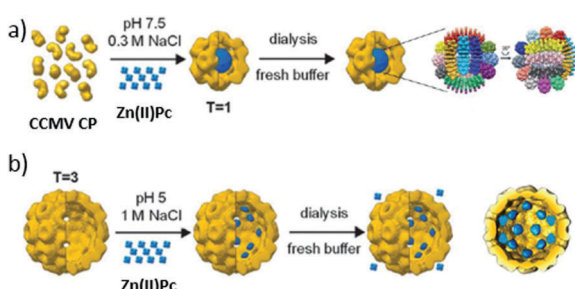


Fig. 14 (a) Self-assembly of 10 nm Zn( $\text{II}$ )Pc nanospheres within  $T = 1$  CCMV VLP (diameter: 20 nm) and their cryo-EM 3D reconstruction. (b) Encapsulation of Zn( $\text{II}$ )Pc inside  $T = 3$  CCMV VLP (diameter: 28 nm) and cryo-EM 3D reconstruction. Reproduced with permission from ref. 175. Copyright 2014 Royal Society of Chemistry.



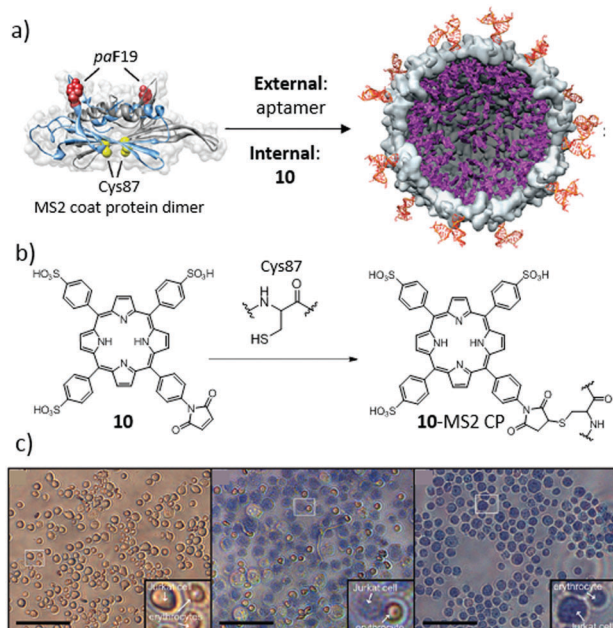


Fig. 15 (a) Construction of a multivalent cell-targeted PDT vehicle using recombinant bacteriophage MS2. (b) Scheme of the inner-wall modification of MS2 CP with H<sub>2</sub>Por **10**. (c) Selective killing of Jurkat T cells in the presence of erythrocytes. (Left) Live control cells. (Middle) Cells exposed to 7.2 nM **10**-MS2 VLP at 0 °C, and then irradiated with 415 nm light for 20 min at room temperature. Only the larger Jurkat cells are dead, as indicated by the trypan blue stain. (Right) Positive control cells exposed to 30% ethanol before staining to induce cell death. Scale bars: 100 μm. Adapted with permission from ref. 180. Copyright 2010 American Chemical Society.

Two examples of Pc–ferritin hybrids have been described so far. First, Zhen *et al.* reported a surface-modified aFt cage that was loaded with hexadecafluoro-Zn(II)Pc, acting as a potent PS with a high  ${}^1\text{O}_2$  quantum yield.<sup>184</sup> The importance of this approach relies on the vehiculization and specific tumour targeting of this highly hydrophobic PS with a high loading ratio. When tested with U87MG subcutaneous tumour models, the biohybrid showed a good tumour inhibition rate and a low toxicity to the skin and other organs, resembling other safe and efficient carriers for PDT.

On the other hand, de la Escosura, Kostiainen and co-workers described the hierarchical organization of aFt into the first photoactive protein crystals (Fig. 16).<sup>185</sup> The co-crystallization could be achieved by the formation of a supramolecular complex between an octacationic Zn(II)Pc (**11**) and a tetraanionic pyrene (**PTSA**), which acted as a molecular glue between the anionic patches of the aFt cage. The obtained ternary face-centered cubic packed cocrystals were efficient  ${}^1\text{O}_2$  producers upon irradiation, thus representing a promising material for PDI applications and diagnostic arrays, among other possible uses.

## 5. PS–nucleic acid biohybrids

Deoxyribonucleic acid (DNA) and ribonucleic acid (RNA) constitute, along with proteins and carbohydrates, one of the essential families of macromolecules for all known forms of life. Both types of nucleic acids are assembled as chains of

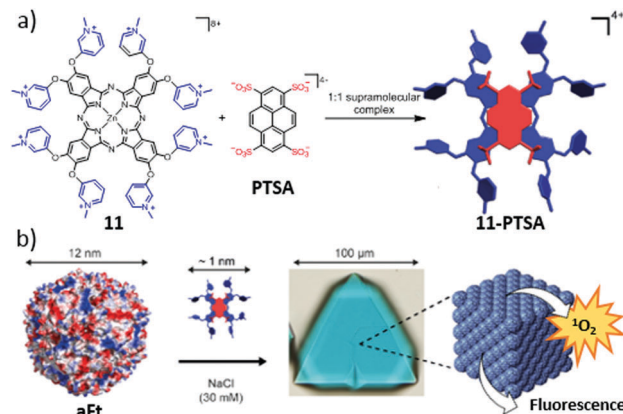


Fig. 16 Scheme of the followed hierarchical strategy toward photoactive biohybrid crystals (**11-PTSA-aFt**). (a) Chemical structures of **11** and **PTSA**, and their self-assembly into the tetracationic **11-PTSA** supramolecular complex. (b) Illustrations of the 12 nm sized **aFt** cage and its further co-crystallization with the **11-PTSA** complex driven by electrostatic interactions. Adapted with permission from ref. 185. Copyright 2016 American Chemical Society.

(ribo)nucleotides, which in turn are composed of a nitrogenous base (nucleobase), a five-carbon sugar (ribose or deoxyribose), and at least one phosphate group. A nucleoside is defined as a nucleotide without the phosphate group, thus consisting of the nucleobase and the 5-carbon sugar. Oligonucleotides, on the other hand, are oligomers of various nucleotides, forming short DNA or RNA molecules. Aiming to take advantage of the informational and biological properties of nucleic acids and their components, PS molecules have been integrated into biohybrid materials with nucleobases, nucleosides, nucleotides or oligonucleotides as biological counterparts. Strictly speaking, nucleobases, nucleosides and nucleotides lack the informational capacity of DNA and RNA, but they can induce interesting self-assembly behaviour in the corresponding PS biohybrids, which in turn has an effect on their properties in biological media. Connecting PS to oligonucleotides with adequate sequences of nucleobases, on the other hand, provides them real potential to address specific biological targets, and thus constitutes a different, more elaborate approach, which will be reviewed in a different section. Regarding the methods of conjugation, a wide variety of them is again available (Fig. 17), the most utilized ones including Sonogashira coupling reactions,<sup>186,187</sup> *O*-alkylation,<sup>188</sup> amide formation,<sup>189,190,197</sup> isothiocyanate chemistry,<sup>193</sup> and axial substitutions.<sup>194,195</sup> For Por, there is a recent review by Stulz describing covalent strategies for their conjugation with DNA,<sup>196</sup> which can be easily extrapolated to the other PS types. Herein, anyhow, we will mainly focus on the biomedical perspective of this research line.

### 5.1. PS biohybrids with nucleobases, nucleosides and nucleotides

Based on their structural similarity, PS-nucleobase, PS-nucleoside and PS-nucleotide conjugates will be discussed together, as they also have common features regarding their properties and functions. Their main interest relies on the fact that they

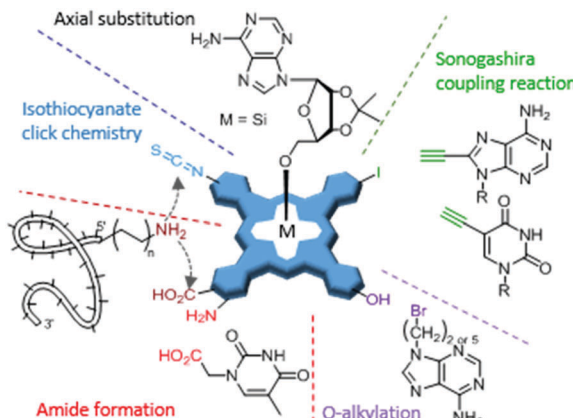


Fig. 17 Scheme of the most important strategies for chemical modification of nucleic acids with PS molecules, illustrated for MPC, but which can be easily extrapolated to Por, chlorin and BODIPY derivatives.

can interact with nucleic acids, or with other molecules containing complementary nucleobases, through hydrogen bonding interactions. The first experiments of this kind date from 1993 for Por<sup>197</sup> and from 2000 for Pc.<sup>188</sup> No biological experiments were carried out for any of these examples, but their base-pairing capacities were examined in different ways.

The first and only Zn(II)Pc-nucleobase biohybrid with a real biomedical application was reported by Liu and co-workers, who developed a Hg<sup>2+</sup> sensor based on Zn(II)Pc-thymine conjugates.<sup>189</sup> Aggregation and subsequent precipitation of the Zn(II)Pc was induced by interaction of its thymine units with Hg<sup>2+</sup>, resulting in a decrease of the PS absorption Q-band, and thus of the concomitant fluorescence emission. Other examples of the use of PS-nucleobase conjugates as sensors have been reported with Por. In particular, Balaz and co-workers studied their dependency on the presence of thymine or adenine, the number of nucleobases, and the Por central metal.<sup>198</sup> Linking adenine instead of thymine produced a decrease in the limit of detection of Hg<sup>2+</sup> in water, while the combination of zinc as the central metal and oligodeoxythymidine as the sensing unit showed the best results toward this mercury cation. Cytosine-substituted Co(II)Por and Zn(II)Por have been used, on the other hand, as nucleotide receptors.<sup>192</sup> Moreover, adenine and thymine have been linked to H<sub>2</sub>Por, in order to study the interaction of the resulting hybrids with nucleic acids and nucleosides.<sup>199</sup> The authors concluded that self-aggregation, due to  $\pi$ - $\pi$  stacking between the PS and nucleobases, has a big influence on the conjugates' binding properties.

In 2013, the first Pc-nucleoside biohybrid with a biomedical application was reported by Huang and co-workers.<sup>195</sup> They synthesized a series of novel Si(IV)Pc that are axially conjugated with uridine and cytidine derivatives, and their photodynamic activities were evaluated as a function of the nucleoside employed. Due to its high cellular uptake and lack of aggregation, the compound containing uridine showed the best PDT results.

Regarding nucleotides, conjugates of BODIPY with adenosine triphosphate and gold nanoparticles have been used as detection systems for adenosine, being able to discriminate between adenosine and their analogues.<sup>200</sup> In a different scenario,

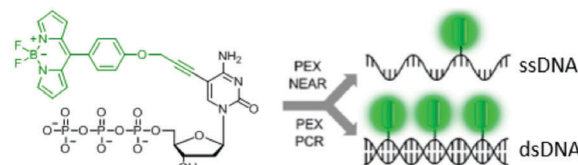


Fig. 18 BODIPY-labelled nucleoside triphosphate analogues suitable for their use in polymerase-based methods such as primer extension (PEX) or polymerase chain reaction (PCR). Reproduced with permission from ref. 186. Copyright 2014 American Chemical Society.

Hocek and co-workers reported in 2014 the synthesis of deoxy-nucleoside triphosphate analogues labelled with a BODIPY unit, through a flexible and short linker.<sup>186</sup> The conjugates were used as nucleotide monomers by polymerases in the synthesis of DNA (Fig. 18). The BODIPY fluorescence was not quenched in the resulting DNA duplexes, thus serving as a labelling method for this biopolymer. Using the same concept, two years later, Dziuba *et al.* described the use a rotational BODIPY-nucleotide hybrid as a sensor of DNA interactions *in vitro* and *in vivo*, further stressing the great potential of such a strategy for labelling genetic material.<sup>187</sup>

## 5.2. PS-oligonucleotide biohybrids

Although there exist a number of articles related to the combination of PS and nucleic acid monomers, as shown in the previous section, the most interesting properties emerge from their combination with biologically active nucleic acids. Indeed, there are different possible uses of PS-oligonucleotide hybrids, which include photocatalytic processes for modification of DNA, the development of DNA-based fluorescence diagnostic systems, light-induced gene transfer, and G-quadruplex recognition. These applications are discussed separately in the following subsections.

**5.2.1. Photocatalytic oxidative modification of DNA.** The modification of DNA using PS through various strategies has been reported in the literature. In 1996, Hélène and co-workers described conjugates of two different chlorin derivatives with oligodeoxynucleotide components, through carboxylic or aldehyde groups linked to the 3'-activated phosphate of the terminal nucleotides.<sup>201</sup> Under red light irradiation, the conjugates were able to produce damage to specific sequences of DNA. One year after, Li *et al.* reported the solid-phase synthesis of H<sub>2</sub>Por-oligonucleotide conjugates for the same purpose.<sup>202</sup> Fedorova and co-workers published a series of MPC (M = Zn(II), Al(III), Co(II)) conjugated with oligonucleotides that direct the Pc to the selected complementary sequence on the DNA target.<sup>190</sup> The Zn(II)Pc and Al(III)Pc conjugates were able to produce <sup>1</sup>O<sub>2</sub>, while in the case of Co(II)Pc DNA oxidation was promoted by molecular oxygen and the production of ROS species. On these bases, these systems could be very useful in genetic regulation and in the treatment of cancer.

A very promising research line relates to photoinduced DNA interstrand cross-linking, induced in furan-modified genetic material by a PS irradiated with light of adequate wavelength.<sup>203</sup> The production of <sup>1</sup>O<sub>2</sub> close to the furan moieties leads to their rupture, generating reactive intermediate species that result in



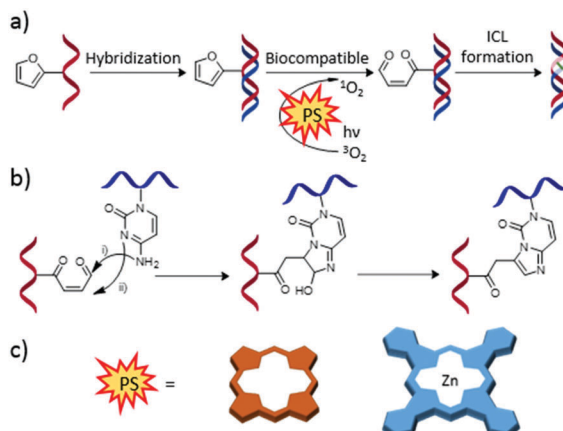


Fig. 19 (a) General scheme of the interstrand cross-link (ICL) formation of furan-modified DNA strands triggered by photooxidation. (b) Detailed ICL mechanism. (c) Schematic representation of the different PS employed for this strategy. Adapted with permission from ref. 203. Copyright 2012 American Chemical Society.

DNA interstrand cross-linking (Fig. 19). This approach leads to covalently linked DNA duplexes with high stability, employed in biosensing.<sup>204</sup> Torres and co-workers explored in detail this methodology, working with both Pc- and Por-based PS.<sup>205</sup>

**5.2.2. DNA-based fluorescence diagnostic systems.** DNA-based fluorescence diagnostic systems are very useful at the time of monitoring different biological activities, including those of enzymes,<sup>206</sup> antibodies and other proteins.<sup>207</sup> There are indeed very good reviews in the literature about the use of PS fluorescence for bioimaging.<sup>9,208</sup> Therefore, herein we only focus on the main examples involving the combination of PS with an oligonucleotide, which are not many at all. The first PS–oligonucleotide conjugates proposed for use in diagnostic systems were reported by Hammer *et al.*,<sup>193</sup> based on the covalent linkage of various Zn(II)Pc compounds to the M13 primer through isothiocyanate chemistry. However, the authors of this work did not test any real application. A more important contribution to the field was then made by Nesterova *et al.*, who published the Zn(II)Pc–oligonucleotide conjugates (**12a** and **12b**) for PCR fluorescence assays.<sup>191</sup> The conjugates showed water solubility and non-altered fluorescence emission, compared to the free PS, which allowed utilizing them as primers for PCR amplifications, and which could be detected and monitored by near-IR fluorescence (Fig. 20).

**5.2.3. Light-induced gene transfer.** The delivery of DNA inside cells can be light-induced (PCI), requiring the presence of a PS that is able to destabilize the endosomal membrane. Since the control of gene transfection in the body is a core issue in gene therapy, this technique is of great interest in that field. Kataoka and co-workers assessed *in vivo* DNA delivery in 2005 with the design of a ternary complex composed of a core containing DNA packed with a cationic NLS peptide, enveloped in an anionic dendritic Zn(II)Pc.<sup>209</sup> The complex exhibited a reduced photocytotoxicity and an important enhancement in the transgene expression *in vitro*. This transgene expression was shown to be highly selective in animal experiments, occurring

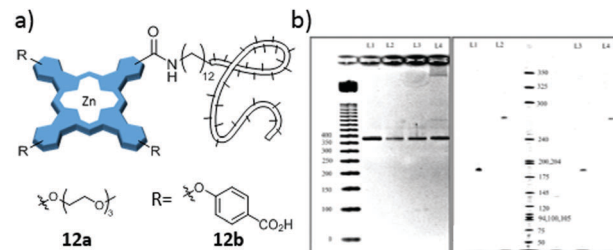


Fig. 20 (a) Scheme of Zn(II)Pc derivatives **12a** and **12b** as labelling agents in oligonucleotide PCR. (b) Images of agarose (left) and polyacrylamide (right) gels after electrophoresis of PCR products. Detection was accomplished using UV absorption at 254 nm after staining the gel with ethidium bromide (left) or near-IR fluorescence at 700 nm (right). Adapted with permission from ref. 191. Copyright 2007 American Chemical Society.

only at the irradiated site (Fig. 21). Some years after, in 2013, the same group published another study with the same dendritic Zn(II)Pc, but in this case working with micelles forming a multifunctional nanocarrier platform.<sup>210</sup> In a different,

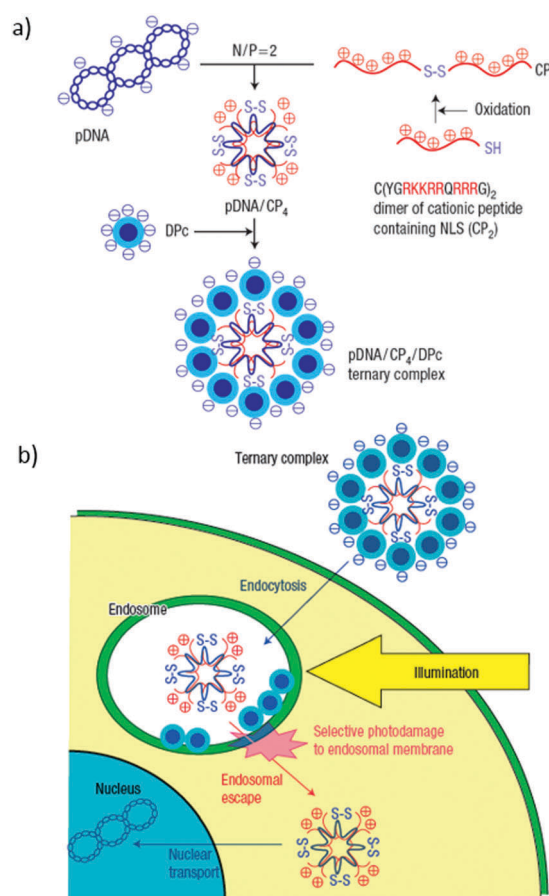


Fig. 21 (a) Schematic representation of a plasmid DNA (pDNA)/quadruplicated cationic peptide (CP<sub>4</sub>)/dendritic Zn(II)Pc (DPC) ternary complex preparation. (b) Scheme showing the itinerary of this ternary complex for transgene expression. The design of the ternary complex shows effective control over the initial steps (*i.e.* internalization by endocytosis and photodamage to the endosomal membrane to release the polyplex to the cytoplasm) in PCI-mediated gene delivery. Reproduced with permission from ref. 209. Copyright 2005 Nature Publishing Group.

covalent approach, chlorin e6 has been used for the transfection of directly linked oligonucleotides by PCI, avoiding in this way that the major fraction of the internalized oligonucleotides got trapped in endosomes or lysosomes, which is usually the main limit for their therapeutic potential.<sup>211</sup>

**5.2.4. G-Quadruplex recognition.** Among the countless nucleic acid combinations present in Nature, guanine-rich sequences have attracted great attention in recent decades. G-Quadruplex structures involving G-quartets linked by loop oligonucleotides have shown critical regulatory roles like DNA replication, transcription and translation, among others.<sup>212,213</sup>

The literature about G-quadruplex biohybrids with Por and Pc has been recently reviewed in a few review articles and, therefore, it will not be fully covered herein.<sup>214–216</sup> There are only two additional remarkable examples. The first one is by Zhang *et al.*, who reported an extensive study where one BODIPY derivative was selected among 5000 candidates to specifically bind to parallel quadruplets, increasing its fluorescence quantum yield ( $\Phi_F$ ) from 0.014 to 0.28 when intercalated in such structure.<sup>217</sup> Kim and Kim also developed a BODIPY-labelled G-rich sequence (5'-BOD<sup>+</sup>UGGGTT-3'), employed as a 3'-overhang of telomeric DNA, based on the formation of (3 + 1) intermolecular G-quadruplexes.<sup>218</sup>

## 6. PS–carbohydrate biohybrids

The conjugation of PS to carbohydrates, including mono- and disaccharides, oligosaccharides (*e.g.*, cyclodextrins) and polysaccharides (*e.g.*, cellulose, chitosan and dextran), is arguably the most extensively explored strategy in order to obtain biocompatible photoactive materials. Carbohydrates improve the aqueous solubility of PS and allow cellular recognition *via* specific carbohydrate–protein interactions on cell surfaces,<sup>219,220</sup> thus being able to provide specificity toward certain tumours.<sup>221</sup> Compared to peptides, proteins and nucleic acids, there is not a clear correlation between the type carbohydrate employed and the biohybrid application, yet the combination of these biomolecules with PS is normally directed to use in PDT, PDI and theranostics. In any case, the structure of this section will be better based on the distinction between, on the one hand, mono-, di- and oligosaccharides, which are molecularly well-defined; and, on the other hand, polysaccharides, with very different structural, nanoscopic and biological properties.

### 6.1. Biohybrids of PS with mono-, di- and oligosaccharides

Glycosylation of PS with mono- and disaccharides has been performed extensively, and it was recently addressed in an excellent and in-depth review by Drain and co-workers.<sup>222</sup> The following paragraphs will therefore focus only on cyclodextrins (CD), as a particularly useful class of oligosaccharides. CD are cyclic oligosaccharides composed of repetitive units of  $\alpha$ -D-glucopyranose. Depending on the number of constituting monomers, CD can be divided into  $\alpha$ -CD (6 monomeric units),  $\beta$ -CD (7) and  $\gamma$ -CD (8). Different hydrophobic molecules can be encapsulated in the cavity of CD depending on their size.<sup>223</sup> Furthermore, the

chemical and biological properties of guest molecules can be modulated by encapsulation in this cages, while CD can be used as nanocarriers in aqueous media.

The chemical modification of CD can be achieved in a covalent or in a supramolecular way. A large variety of studies have been published regarding the non-covalent association between CD and PS, but most of them did not have a biomedical interest. Some examples of this supramolecular approach include: the construction of supramolecular assemblies composed of permethyl- $\beta$ -CD, modified with perylene bisimides and Zn(II)Por through the establishment of hydrophobic interactions,<sup>224</sup> the study of photoinduced electron transfer in complexes formed by a H<sub>2</sub>Por and a  $\beta$ -CD containing viologen moieties,<sup>225</sup> the inclusion of two different tetrasulphonated H<sub>2</sub>Por and Zn(II)Por compounds into the inner cavity of BODIPY- $\beta$ -CD conjugates, for the study of photo-induced processes,<sup>226</sup> the complexation of inorganic anions in aqueous medium by an Fe(III)Por associated with  $\beta$ -CD,<sup>227</sup> and the encapsulation of H<sub>2</sub>Por within  $\beta$ -CD dimers,<sup>228</sup> among others. A different approximation is the construction of supramolecular structures from covalent conjugates between CD and PS, including the formation of water-soluble nanospheres<sup>229</sup> or nanowires.<sup>230</sup> The literature in this field is anyhow very extensive and it falls out of the scope of the present review. Consequently, only the relevant cases concerning biological applications will be discussed in the rest of this section.

Although PS could be encapsulated in the inner cavity of CD, the presence of hydroxyl groups in the structures of CD derivatives provides the most useful anchor to perform the covalent grafting of both kinds of molecules. In the case of Pc, for example, a  $\beta$ -CD was covalently grafted onto 4-nitrophthalonitrile, through an *ipso* substitution reaction, followed by crossed statistical condensation with different phthalonitriles, yielding asymmetrically substituted Zn(II)Pc hybrids for the first time.<sup>231</sup> Following a different strategy, through axial substitution, symmetrically and asymmetrically substituted Si(IV)Pc (**13a**–**13d**) bearing one or two  $\beta$ -CD moieties have been published for testing their photodynamic activity against HT29 human colon adenocarcinoma and HepG2 human hepatocarcinoma cells (Fig. 22).<sup>232</sup> Besides Si(IV)Pc, a H<sub>2</sub>Por-based conjugate has also been used for testing the photodynamic activity

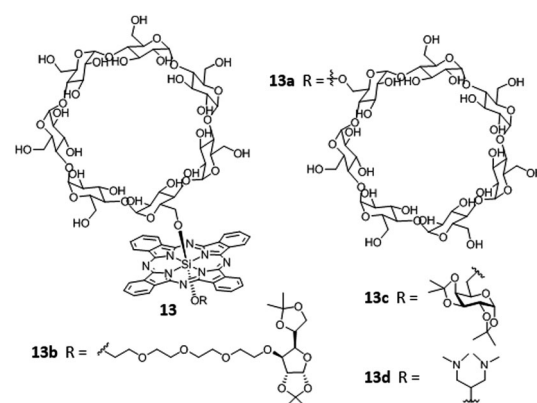


Fig. 22 Structures of asymmetrically substituted Si(IV)Pc- $\beta$ -CD derivatives (**13a**–**13d**).



against HT29 human colon adenocarcinoma cells, with similar results.<sup>233</sup>

In 2014, Tomé and co-workers evaluated the effect that the CD macrocycle size has on phototoxicity, specifically against UM-UC-3 human bladder cancer cells, by studying three Zn(II)Pc derivatives connected to  $\alpha$ -CD,  $\beta$ -CD or  $\gamma$ -CD.<sup>234</sup> More recently, a supramolecular Si(IV)Pc- $\beta$ -CD hybrid was successfully applied to the photoinactivation of antibiotic resistant bacteria.<sup>235</sup> The biohybrid preparation consisted of decorating  $\beta$ -CD vesicles with a Si(IV)Pc carrying an axial adamantyl moiety, allowing the incorporation in the vesicles *via* host-guest inclusion. As a second axial substituent, a pyridinium moiety was employed to provide good solubility to the Si(IV)Pc in aqueous media. Both axial substituents also contributed to avoid H-type aggregation in water, yet, according to UV-Vis data, J-type aggregation was still present, decreasing the fluorescence and  $^1\text{O}_2$  production of the Si(IV)Pc. Importantly, after complexation with the  $\beta$ -CD-vesicles, reduced aggregation and an enhancement of those properties could be observed in the conjugates.

Concerning other porphyrinoids, in 2006 Král and co-workers synthesized conjugates through covalent linkage of a fluorinated H<sub>2</sub>Por with one or two  $\beta$ -CDs, and their PDT activity was tested in different lines of cancer cells.<sup>236</sup> *In vitro*, the H<sub>2</sub>Por-( $\beta$ -CD)<sub>1</sub> complex showed a more lipophilic character, resulting in a more efficient cellular uptake compared to H<sub>2</sub>Por-( $\beta$ -CD)<sub>2</sub>. Nevertheless, experiments *in vivo* showed that the latter conjugate provoked a more effective photodynamic effect. The authors suggested that the reason for this could be the possible association of H<sub>2</sub>Por-( $\beta$ -CD)<sub>2</sub> with albumin or other serum proteins, allowing a faster transport to tumour tissues, compared to H<sub>2</sub>Por-( $\beta$ -CD)<sub>1</sub>, which would associate with HDL due its more hydrophobic character. A few years later, a new article by the same group described four conjugates of H<sub>2</sub>Por and CD, with different combinations and types of CD as substituents (Fig. 23).<sup>237</sup> The resulting hybrids were interesting agents not only for PDT but also for chemotherapy, due to the ability of these CD moieties to include different anticancer drugs in the inner cavity.

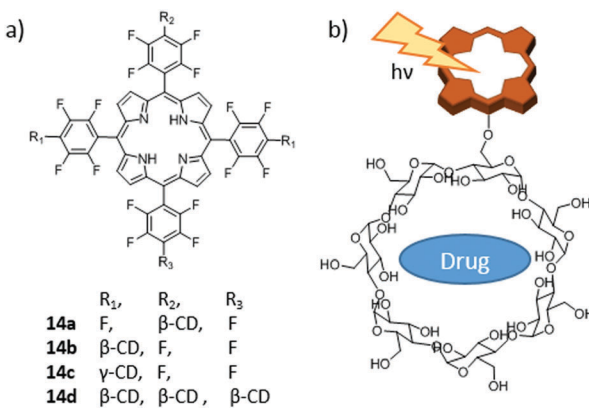


Fig. 23 (a) Structures of  $\beta$ -( $\gamma$ )-CD-H<sub>2</sub>Por conjugates (14a–14d). (b) Schematic representation of the dual activity of the conjugates, where the CD unit can host in the inner cavity cytostatic drugs, while H<sub>2</sub>Por acts as a phototoxic agent. Adapted with permission from ref. 237. Copyright 2010 American Chemical Society.

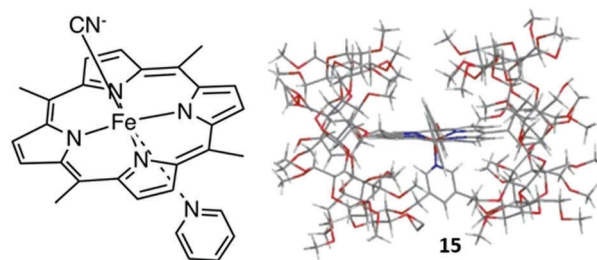


Fig. 24 Structure of the  $\beta$ -CD-Fe(III)Por complex (15), which mimics haemoglobin/myoglobin and functions as an antidote for cyanide poisoning. Adapted with permission from ref. 243. Copyright 2013 Wiley.

Fluorinated chlorins, in turn, have also been linked to  $\beta$ -CD,<sup>238</sup> yielding conjugates with high water solubility and a good photo-induced production of  $^1\text{O}_2$ .

Liu and co-workers reported the synthesis of Por-CD conjugates through a different method, that is, by a Huisgen cycloaddition click reaction between a triple bond-containing Zn(II)Por and an azide-bearing  $\beta$ -CD.<sup>239</sup> PDT experiments were not performed with these conjugates, but the authors proposed further research to evaluate their potential use as nanocontainers for drug delivery. More recently,  $\beta$ -CD-derivatives have been linked to H<sub>2</sub>Por and Zn(II)Por, and the resulting hybrids studied as possible modulators of the aggregation of the amyloid beta (A $\beta$ ) peptide, whose aggregates are involved in Alzheimer's disease. These complexes were able to block the cytotoxic effect of A $\beta$ <sub>42</sub> oligomers in human neuroblastoma cell lines.<sup>240</sup> Corrole derivatives have been linked to CD macrocycles too. In particular, 5,10,15-tris(pentafluorophenyl)corrole (TPFC) has been linked to one or two units of  $\beta$ -CD (namely,  $\beta$ -CD1 and  $\beta$ -CD2), and PDT experiments were carried out in HeLa cells. Both conjugates showed the ability to produce  $^1\text{O}_2$ , but still TPFC was the most efficient  $^1\text{O}_2$  generator in this series of compounds.<sup>241</sup>

Finally, concerning the supramolecular approach, intracellular delivery of an anionic tetrasulphonated H<sub>2</sub>Por has been achieved through its encapsulation into the inner cavity of octaarginine- $\beta$ -CD derivatives.<sup>242</sup> Another example is the work published by Kano and co-workers, relative to complex 15, composed of a  $\beta$ -CD-dimer and an Fe(III)Por (Fig. 24). This complex is a mimic of haemoglobin/myoglobin, with a hydrophobic region created around the iron center that allows it to act as an antidote for cyanide poisoning.<sup>243</sup>

## 6.2. Biohybrids of PS with polysaccharides

**6.2.1. PS-cellulose hybrids.** Cellulose is the most abundant biopolymer in the biosphere, and it has been processed industrially for more than 150 years. In the last few decades, nanotechnology has enabled the development of new high-end cellulose derivatives. Rod-shaped cellulose nanocrystals (CNC), for example, are attracting much attention due to their excellent mechanical properties, high aspect ratio and surface area, colloidal stability, biocompatibility and cheap processing as a well-defined nanomaterial.<sup>244</sup> In this respect, CNC are also subjectable to be combined with PS, as shown in the next paragraphs, with the resulting biohybrids benefiting from the properties of both components in the area of biomedicine.



Pc have been incorporated onto CNC mainly by supramolecular means, in two different examples that make use of electrostatic interactions. In the first case, CNC bearing primary alcohol groups were treated with (2,3-epoxypropyl)trimethylammonium chloride, in order to obtain cationic groups on the CNC surface, onto which negatively charged tetrasulphonated Zn(II)Pc was bound by a synergy of electrostatic interactions and hydrogen bonding.<sup>245</sup> The resulting biohybrid was used as a selective catalyst for the oxidation of alcohols and alkyl arenes. In the second case, de la Escosura and co-workers developed a method for the non-covalent immobilization of octacationic Zn(II)Pc (**16a** and **16b**) derivatives onto the negative surface of sulphated CNC.<sup>246</sup> These biohybrids presented a strong PDI effect against *S. aureus*, *E. coli* and *C. albicans*. Importantly, the hybrids actually outperformed the free Zn(II)Pc and all published related nanosystems that bear the PS covalently attached to the cellulose surface (Fig. 25), highlighting the utility and advantages of this new approach.

Regarding covalent hybrids, Chauhan and Yan performed the synthesis of conjugates between CNC and BODIPY derivatives, through sulphonamide linkages.<sup>247</sup> The PS in this case was a sulphonated BODIPY, covalently attached to CNC that were previously modified to contain amino groups on their surface. The resulting biohybrids were able to produce  $^1\text{O}_2$  upon irradiation, but biological experiments were not carried out.  $^1\text{O}_2$ -Producing hybrids composed of nanocrystalline cellulose and H<sub>2</sub>Por or Zn(II)Por were also developed by Carofiglio and co-workers, through amide bond formation between an amino group of

the Por component and carboxylic acid groups from the CNC.<sup>248</sup> Following a different strategy, Krausz and co-workers grafted an acetylenic Zn(II)Por into cotton, *via* click chemistry.<sup>249</sup> The obtained hybrid material showed good PDI activity against *E. coli* and *S. aureus*. In 2011, the same approach was used by Ghiladi and co-workers.<sup>250</sup> The Zn(II)Por was functionalized with a propargyl chain, and cellulose was modified with azide groups. In this case, their PDI efficiency was tested against *Mycobacterium smegmatis*, *S. aureus* and *E. coli*, obtaining the best results against *M. smegmatis* and *S. aureus*. One year later, this study was extended to get a better understanding of the mechanisms of photoinactivation, and PDI activity was evaluated against other microorganisms such as *P. aeruginosa*.<sup>251</sup>

**6.2.2. PS-chitosan hybrids.** Chitosan is a linear polysaccharide composed of randomly distributed  $\beta$ -(1  $\rightarrow$  4)-linked D-glucosamine and N-acetyl-D-glucosamine. This polymer is made by deacetylation of chitin, treating it with an alkaline medium, like sodium hydroxide. Chitosan is easily modified in a physical or chemical way, through covalent grafting or enzymatic modification. Interestingly, the high biocompatibility, biodegradability and permeability of chitosan, among others, render this biomaterial ideal for manufacturing nanostructures, microspheres and hydrogels with biomedical potential.<sup>252</sup> Chitosan therefore represents a promising scaffold to incorporate PS of different natures.

Másson and co-workers published the synthesis of four nanoconjugates composed of chitosan and amphiphilic chlorins bearing an amino or a carboxyl group. To this end, they used different strategies and linkers, and experiments in tumour-bearing mice showed good PDT results.<sup>253</sup> Another synthetic strategy involved the conjugation of chlorin e6 to iodinated chitosan.<sup>254</sup> Apart from the generation of  $^1\text{O}_2$  and the use of these conjugates for PDT, they could be utilized as imaging agents, given that NIR fluorescence signals from the cytoplasm were detected after incubation with HeLa cells. Photosensitizing nanoparticles made through the linkage of glycol chitosan to pheophorbide *a* were also proposed.<sup>255</sup>

**6.2.3. PS-dextran hybrids.** Dextran is composed of a linear chain of  $\alpha$ -1,6-linked D-glucopyranose residues, with  $\alpha$ -1,2-,  $\alpha$ -1,3- and  $\alpha$ -1,4-linked side chains in low percentages. The straightforward chemical modification of this biopolymer, due to the presence of hydroxyl groups in its structure, and its good properties for the development of nanomaterials, as in the case of chitosan, make dextran a good PS carrier.<sup>256</sup> Sortino and co-workers reported, for example, a supramolecular hydrogel built out of four components that included a polymer of  $\beta$ -CD, dextran, a Zn(II)Pc and a nitric oxide photodonor.<sup>257</sup> The generation of  $^1\text{O}_2$  and nitric oxide by this complex was achieved after irradiation with visible light, and so this formulation could be used in PDT and PDI experiments. Dextran has been linked to chlorin e6 too, by modifying the polymer with a cystamine group, which could then be used to react with the carboxylic acid group of the chlorin through amide bond formation.<sup>258</sup> The fluorescence of the resulting nanoparticles was higher than that of chlorin e6 by itself. In experiments with HCT116 human colon cancer cells, the hybrid also showed a higher cellular uptake, ROS generation and phototoxicity. Importantly, this highly efficient performance of the biohybrid could also be confirmed *in vivo*.

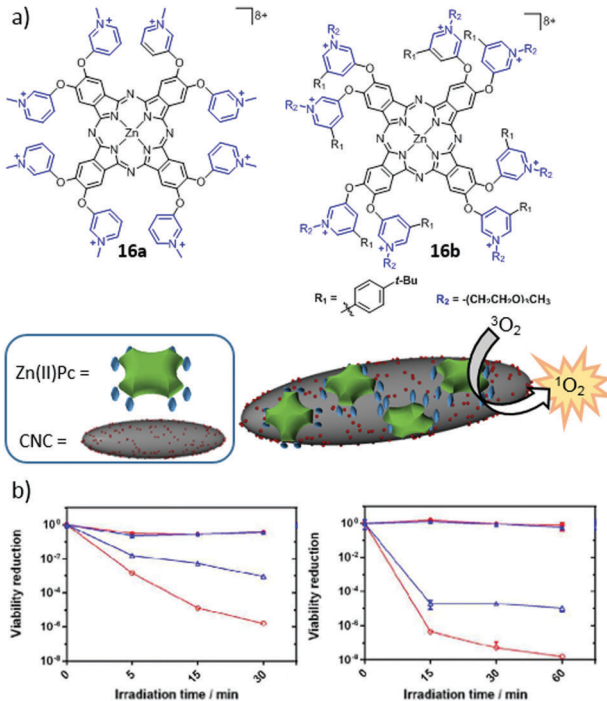


Fig. 25 (a) Chemical structures of **16a** and **16b**, as well as a schematic representation of the supramolecular functionalization of CNCs. (b) Photo-inactivation of *S. aureus* (left) and *E. coli* (right) upon red light irradiation (620–645 nm; 18 mW cm<sup>-2</sup>). The results are shown in blue for Zn(II)Pc **16a** and red for complex **16a**–CNC. Reproduced with permission from ref. 246. Copyright 2017 Wiley.



From a different perspective, the binding of dextran to Mn(III)Por was carried out to test if linking the PS to dextran could improve its properties as an MRI contrast agent.<sup>259</sup> In this way, the specific targeting of HepG2 cancer cells could be facilitated when using this conjugate. Working also with Por, Sol and co-workers reported in 2015 the synthesis of iron oxide nanoparticles covered with dextran.<sup>260</sup> Through the incorporation of azide moieties onto these particles, the authors were able to attach different hydrosoluble Zn(II)Por derivatives, bearing a propargyl group, through click chemistry reactions. They tested the phototoxicity of these systems in human keratinocyte cells, evaluating the effect of the number of charges in the Por structure. The obtained results revealed that both cationic and neutral nanoparticles were promising PS.

## 7. PS–liposome biohybrids

Liposomes are phospholipidic bilayer vesicles that present an aqueous lumen within. The amphiphilic nature of phospholipids results in their self-organization in aqueous solution, with the polar head pointing toward the solvent and the aliphatic chains forming the core of the bilayer shell. This distribution makes them ideal delivery agents, due to the possibility of accommodating both hydrophilic and hydrophobic drugs in their inner cavity or inserted in the hydrophobic bilayer, respectively (Fig. 26a and b). This duality has been intensively employed in medical research and clinical applications since the early 1970s.<sup>261</sup> Also lipid composition, size and charge have actually been extensively studied in the literature, with the aim of enhancing the drug delivery performance, including properties such as cellular uptake, circulation time and passive recognition.<sup>262–264</sup>

The employment of liposomes for the encapsulation and vehiculization of PS presents additional advantages.<sup>265</sup> There is,

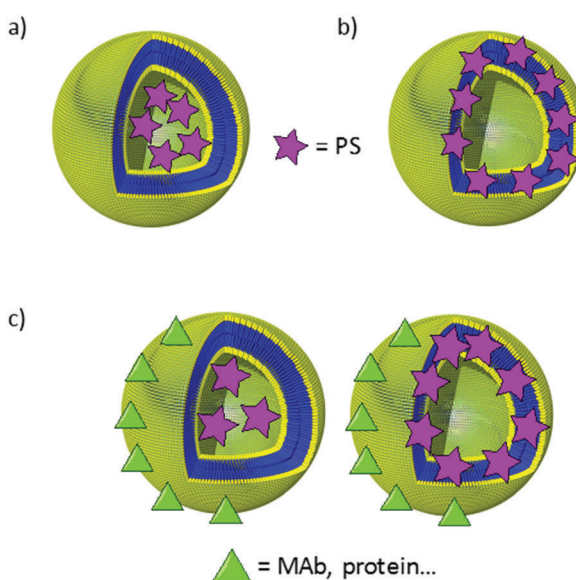


Fig. 26 Schematic representation of (a) hydrophilic PS encapsulated in the inner cavity of a liposome, (b) hydrophobic PS inserted in the membrane of a liposome, and (c) liposome formulation of two different active components, including targeting units at the periphery.

for example, no need to incorporate hydrophilic substituents in the PS, due to the intrinsic lipophilic nature of the liposome membrane.<sup>266</sup> Moreover, the non-aggregated state of most PS in membrane media allows maintaining intact their intrinsic capacity for ROS generation, and their fluorescence, both *in vitro* and *in vivo*.<sup>267</sup> Some liposomes also possess the ability to deliver PS in a controlled manner into the plasma membrane of cells, resulting in an enhancement of phototoxicity,<sup>268</sup> among other interesting features. For all these reasons, many studies have been focused on exploring different aspects of the behaviour of these carrier systems, as the involved mechanism in cell death,<sup>269,270</sup> or the determination of the most favourable lipidic composition for their performance.<sup>271–273</sup>

Several groups have reported on PS–liposome hybrid systems for different biomedical purposes, like imaging techniques,<sup>274</sup> and PDT or PDI treatments of different cancerous cell lines or tumours,<sup>275–281</sup> leishmaniasis,<sup>282,283</sup> *Candida albicans*,<sup>284</sup> or human chronic periodontitis,<sup>285</sup> among others. More interestingly, liposomes that enable the formulation of more than one active component have recently attracted much attention, as they can be employed as suitable platforms to render more complex third-generation PS (Fig. 26). In particular, liposomes containing PS have been combined with antibodies, other proteins or peptides in ternary biohybrids that enhance the biological selectivity and increase the PS cell penetration capacity. This is currently the most interesting approach regarding the use of liposomes for PS vehiculization, and so we will focus on it, leaving out the traditional strategies for liposome formulation of PS, which have been reviewed recently.<sup>265,286,287</sup> Besides antibodies, proteins and peptides, other types of materials have been incorporated into ternary liposome–PS systems but, due to their synthetic nature, fall out of the scope of the present review.

### 7.1. PS–liposome–antibody biohybrids

Taking advantage of the outstanding biological selectivity conferred by MAb, discussed earlier in this review, a few examples of ternary hybrids consisting of PS-containing liposomes formulated together with MAb have been described.

Early in 1989, Morgan *et al.* described the first example of PC compounds (*i.e.*, a series of mono-, di-, tri- and tetrasulphonated Al(III)PC) encapsulated in liposomes, which were further coupled to the 791T/36 antibody.<sup>288</sup> The PDT effect of these liposomes was evaluated in two different cell lines: osteosarcoma 791T and colorectal carcinoma C170, as well in a control line bearing no antigen (DW-BCL). Phototoxicity was observed against both types of cells, and parameters such as the PS concentration, the time of light exposure and the amount of cell antigens were decisive in the obtained results. The same liposomal system was later coupled to the polyclonal sheep anti-mouse-Ig antibody and was employed to destroy target populations of cells in bone marrow.<sup>289</sup>

Years later, Broekgaarden *et al.* described liposomes with a bilayer made up of Zn(II)PC molecules, functionally decorated with single-domain antibodies directed against the EGFR, with the objective of improving the delivery and selectivity of the



PDT effect of this Zn(II)Pc compound.<sup>290</sup> *In vitro* studies with EGFR-positive human epidermoid carcinoma (A431) cells and EGFR-negative 3T3 2.2 murine fibroblasts effectively demonstrated a selective PS incorporation by EGFR overexpressing cells, as determined by fluorescence spectroscopy and confocal laser scanning microscopy. Further exposure to red light resulted in a good phototoxicity, revealing increased PDT efficacy as compared to non-targeted liposomes, due to a higher and more selective cell uptake combined with a redistribution of the Zn(II)Pc molecules from the liposomes into different intracellular localizations, thus maximizing the PDT effect.

With Por derivatives, Hasan and co-workers designed another ternary liposome-based biohybrid that is able to target epithelial ovarian cancer cells.<sup>291</sup> This conjugate was composed of 5,10,15,20-tetrakis(benzo[*b*]thiophene)-H<sub>2</sub>Por and the MAb Cetuximab, which were associated in preformed plain liposomes. The optical properties and the quantum yield efficiency of the PS in the PICAL conjugate were more stable than for the free PS. Ovar-5 and CAMA-1 cell lines were used to study the affinity of the conjugate to the EGFR, and the PS uptake was higher when the amount of MAb was increased. The conjugate also showed higher PDT efficacy than the PS by itself.

## 7.2. PS-liposome–protein biohybrids

Ngweniform *et al.* reported the co-assembly of Zn(II)Pc-liposome hybrids with flagellar filaments, a type of protein nanotube protruding from the surfaces of some bacteria.<sup>292</sup> The Zn(II)Pc was entrapped in the lipid bilayer of cationic liposomes, and the flagella acquired a negatively charged surface by displaying an anionic polypeptide on it. Consequently, a ternary biohybrid arose from the assembly of the liposomes and the flagella through electrostatic interactions. After the formation of these complexes, an increase in the fluorescence intensity of the Zn(II)Pc was observed, probably due to a reduction in its vibrational motion. Following a similar strategy, Zn(II)Pc-loaded cationic liposomes have been co-assembled with the M13 phage, a rod-like virus known to be able to carry drugs and penetrate the blood–brain barrier without inducing toxicity or obvious immune responses in human beings (Fig. 28).<sup>293</sup> As in the previous example, the formation of the ternary complex resulted in an increase in the fluorescence intensity of the Zn(II)Pc in the lipid bilayer. A preliminary study indicated that the phage-liposome complex could be internalized in breast cancer cells, making the phage-liposome-PS biohybrid a promising PDT agent.

Likewise, the conjugation of tetrasulphonated Al(III)Pc liposomes with human transferrin was evaluated in HeLa cells.<sup>294</sup> Transferrin receptor levels are overexpressed in various cancers, and so transferrin-decorated liposomes could be good candidates for the delivery of PS in cancer therapy. The phototoxicity of the hybrid was actually much higher than that of the free Al(III)Pc, and the non-targeted Al(III)Pc-liposome system showed poorer phototoxicity results. Based on such positive behaviour, a complementary study was published in 2004 employing the same approach for the PDT treatment of rat bladder carcinoma cells.<sup>295</sup>

## 7.3. PS-liposome–peptide biohybrids

Apart from the above mentioned proteins, shorter peptide sequences have also been used in the decoration of liposomes to target specific tissues. Oku and co-workers, for example, published a study in which benzoporphyrin derivative monoacid ring A (BPD-MA) has been internalized in PEG-modified liposomes, decorated with Ala-Pro-Arg-Pro-Gly (APRPG), a pentapeptide that is specific for angiogenic endothelial cells.<sup>296</sup> The resulting complexes showed good results of phototoxicity after irradiation in tumoral cells.

The most interesting example regarding the combination of peptides with liposomes for the delivery of PS, however, was published by Lovell and co-workers in 2015. In their study, a Por derivative containing a phospholipid (17-Co) was ensembled together with dioleoylphosphatidylcholine (DOPC) to form a bilayer of 100 nm diameter liposomes (Fig. 27a).<sup>297</sup> Interestingly, the presence of Co(II) chelated into the macrocycle allowed the binding of peptides and proteins that carry a polyhistidine tag (his-tag), endowing systems with very promising potential as drug delivery systems. As proof-of-concept, the authors employed his-tag RGD-targeting polypeptide-decorated liposomes, loaded with sulphorhodamine B in their inner cavity. Biodistribution assays visualising the cargo release demonstrated the specific targeting of tumoral tissues in mice (Fig. 27b).

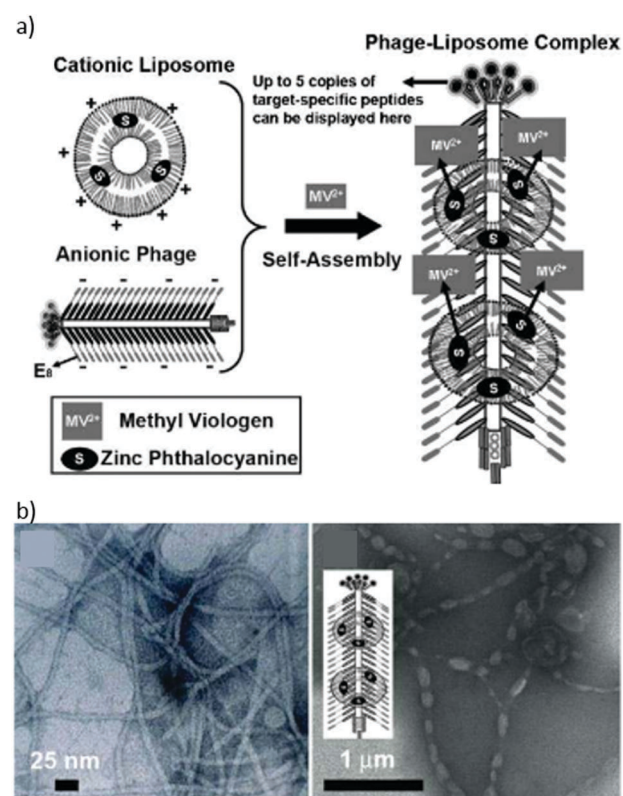


Fig. 27 (a) Schematic representation of the self-assembly of cationic Zn(II)Pc-entrapped liposomes on the anionic genetically engineered phage to form a rod-like phage–liposome complex. Structures not to scale. (b) TEM images of stained engineered phages before (left) and after complexation with Zn(II)Pc-loaded liposomes (right). Reproduced with permission from ref. 293. Copyright 2009 Wiley.



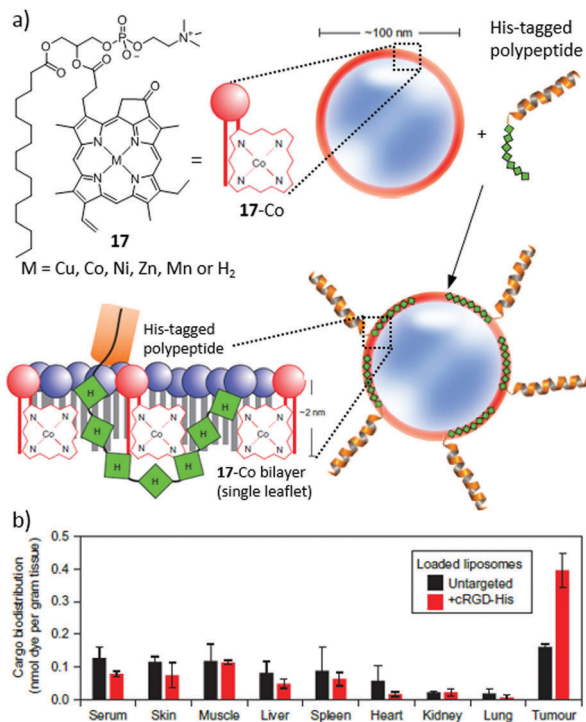


Fig. 28 (a) Chemical structure of compound **17**, and the liposome assembling strategy. (b) Biodistribution of sulphorhodamine B delivered by untargeted (black) and RGD-containing liposomes (red) 45 minutes after intravenous injection into nude mice bearing subcutaneous U87 tumours. Adapted with permission from ref. 297. Copyright 2015 Nature Publishing Group.

## 8. Other types of photosensitizing biohybrid materials

### 8.1. Biohybrids of PS and steroid hormones

Steroids that act as hormones are also called steroid hormones. As they are lipid soluble, they can pass easily through the cell membrane and bind to steroid hormone receptors, bringing about changes within the cell.<sup>298</sup> Their linkage to PS is therefore of interest for biomedical applications,<sup>299</sup> as we illustrate with a few examples in the next paragraphs, focusing only on the most representative cases of steroid hormones.

Cholesterol, for example, is a steroid hormone which is essential for cell growth, as it is a key component of the plasmatic and intracellular cell membranes.<sup>300</sup> For this reason, easily proliferating cancer cells are prone to take up more cholesterol than healthy ones. Conjugating cholesterol to PS could therefore result in biohybrids with increased cell uptake and photodynamic efficiency. In 1994, Segalla *et al.* described the synthesis of a Ge(iv)Pc conjugate with two units of cholesterol axially ligated, which was then incorporated into liposomes for delivery, showing a high phototoxic effect in mice bearing an MS-2 fibrosarcoma.<sup>301</sup> A different grafting strategy was developed by Maree *et al.*, who prepared a Zn(ii)Pc substituted with eight cholesterol moieties at the periphery of the macrocycle.<sup>302</sup> Unfortunately, the resulting biohybrids showed a high tendency for aggregation and no biological evaluation was performed. Other kinds of PS that

have been linked to cholesterol are pyropheophorbide<sup>303</sup> and chlorin e6,<sup>304</sup> but in these cases the phototoxic effect of the conjugates was not evaluated in biological media.

Estradiol and estrone, on the other hand, are two of several natural oestrogens, the primary female sex hormones. Breast cancer cells are known to overexpress estrone and estradiol receptors.<sup>305</sup> Therefore, the design of PS-estradiol and PS-estrone biohybrids constitutes a promising strategy to target breast cancer. van Lier *et al.* explored this strategy by synthesizing Zn(ii)Pc-estradiol conjugates, employing the palladium-catalysed Sonogashira reaction to couple estradiol to a monoiodo-Zn(ii)Pc *via* a 17 $\alpha$ -ethynyl group.<sup>306</sup> They also prepared Zn(ii)Pc-estrogen conjugates through spacers with an aliphatic or aromatic nature, and trisulphonated Zn(ii)Pc-estradiol conjugates, enabling a comparison of their biological activities. The best phototoxic effects were obtained with the sulphonated derivatives, whereas the use of a spacer did not show any remarkable influence.

### 8.2. PS-folic acid biohybrids

Folic acid (FA) is an essential vitamin with an important role in different metabolic pathways, such as the biosynthesis of nucleotides, and so it takes part in the proliferation of cells. Its receptor, the folate receptor (FR), appears in an upregulated way in cancer cells of ovary and kidney cancers, among others. Consequently, the main advantages of the use of this molecule for carrying attached drugs to cancer cells include the high selectivity, combined with the achievement of high binding affinity, low immunogenicity and good biocompatibility.<sup>307</sup> These advantages have also been used in a number of cases for the conjugation to PS with applications in biomedicine.

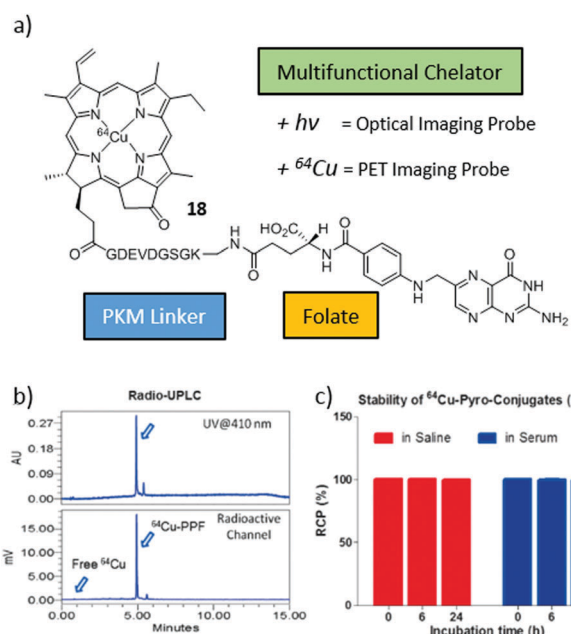


Fig. 29 (a) Chemical structure of compound **18**. (b) Ultrafast protein liquid chromatography (UPLC) of compound **18**, detecting its elution time by UV absorption and radioactivity. (c) *In vitro* stability of **18** in saline or serum (10% FBS) solution. Reproduced with permission from ref. 310. Copyright 2011 Iryspring Publishing Group.

Herein we review a few of these cases, in order to illustrate the potential of this strategy.

In 2008, Gravier *et al.* synthesized a conjugate composed of a chlorin and FA, with an OEG motif as the spacer through an EDC-mediated coupling reaction.<sup>308</sup> The aim was to study the PDT activity in KB tumours. Only the  $\gamma$ -folate conjugate was used for *in vivo* experiments, and it was found that both cell uptake and tumour destruction increased with conjugation of the PS to FA. Pyropheophorbide a, in turn, has also been linked to FA through a pharmacokinetics modifying (PKM) peptide chain prepared by Zheng and co-workers.<sup>309</sup> A few years later, a continuation of this work was carried out, in order to incorporate  $^{64}\text{Cu}$  in pyropheophorbide a (**18**), to convert the conjugate into a PET imaging agent (Fig. 29).<sup>310</sup> Finally, graphene oxide has been loaded with FA and different anticancer drugs, as a nanocarrier platform to target human breast cancer cells.<sup>311</sup> With chlorin e6, bound to the nanoplatform through hydrophobic and  $\pi$ – $\pi$  stacking non-covalent interactions, the system showed good solubility properties and a low cytotoxicity in experiments with MGC803 cells, suggesting it as a possible candidate for PDT.<sup>312</sup>

## 9. Summary and conclusions

In sum, the field of biohybrid materials has been merging in the last few decades with that of PS, enabling the implementation of a number of biomedical technologies with enormous future impact. In a way, photosensitizing biohybrid materials represent a new generation of PS systems, with improved features regarding their behaviour in biological media. Importantly, the wide variety of biomolecular structures available in Nature makes this approach really versatile, allowing tuning the kind of biohybrid depending on the aimed application or the target tissue. There are also many methods available in the literature for the linkage, either covalent or supramolecular, of synthetic PS to biomolecules and their assemblies. The field is therefore now equipped with a complete toolbox of building blocks and methodologies, which ensures a fruitful growth in the coming decades, through an explosion of possible combinations of PS molecules and biomolecules, presumably leading to novel PS uses. In this respect, some new promising applications that are just starting to be explored for light-induced nanomedicine include the use of PS in phototherapy,<sup>62</sup> biophotonics,<sup>313</sup> and photoacoustic and thermal theranostics.<sup>314</sup> On these bases, and by further developing photoactive biohybrids, scientists from disciplines at the crossroads between chemistry, biology, nanomedicine and materials science are taking major steps towards an efficient biomedical management of light.

## Conflicts of interest

There are no conflicts to declare.

## Acknowledgements

The work carried out to write this review article has received funding from the People Program (Marie Curie Actions) of the

European Union's Seventh Framework Program FP7-PEOPLE-2012-ITN under REA grant agreement no. GA 316975. This work was supported by the EU (CosmoPHOS-nano, FP7-NMP-2012-6, 310337-2), Spanish MINECO (CTQ2017-85393-P (TT), CTQ-2014-53673-P and CTQ-2017-89539-P (AdLE), PCIN-2017-042/EuroNanoMed2017-191, TEMPEAT (TT)), and the Comunidad Autonoma de Madrid (FOTOCARBON, S2013/MIT-2841). IMDEA Nanociencia acknowledges support from the 'Severo Ochoa' Programme for Centres of Excellence in R&D (MINECO, Grant SEV-2016-0686).

## References

- 1 E.-K. Lim, T. Kim, S. Paik, S. Haam, Y. M. Huh and K. Lee, *Chem. Rev.*, 2015, **115**, 327.
- 2 H. Chen, W. Zhang, G. Zhu, J. Xie and X. Chen, *Nat. Rev. Mater.*, 2017, **2**, 17024.
- 3 F. Caruso, T. Hyeon and V. M. Rotello, *Chem. Soc. Rev.*, 2012, **41**, 2537.
- 4 G. Chen, I. Roy, C. Yang and P. N. Prasad, *Chem. Rev.*, 2016, **116**, 2826.
- 5 X. Ai, J. Mu and B. Xing, *Theranostics*, 2016, **6**, 2439.
- 6 N. R. Finsen, *Phototherapy*, Edward Arnold, London, 1901.
- 7 O. Raab, *Z. Biol.*, 1900, **39**, 524.
- 8 R. Ackroyd, C. Kelty, N. Brown and M. Reed, *Photochem. Photobiol.*, 2001, **74**, 656.
- 9 J. F. Lovell, T. W. B. Liu, J. Chen and G. Zheng, *Chem. Rev.*, 2010, **110**, 2839.
- 10 F. Dumoulin, *Photosensitizers in Medicine, Environment and Security*, Springer, New York, 2012.
- 11 M. H. Abdel-Kader, *Photodynamic Therapy – From Theory to Application*, Springer, 2014.
- 12 S. Nonell and C. Flors, *Singlet Oxygen: Applications in Biosciences and Nanosciences*, RSC Publishing, 2016.
- 13 M. Wainwright, T. Maisch, S. Nonell, K. Plaetzer, A. Almeida, G. P. Tegos and M. R. Hamblin, *Lancet Infect. Dis.*, 2017, **17**, e49.
- 14 D. Mew, C. K. Wat, G. H. N. Towers and J. G. Levy, *J. Immunol.*, 1983, **130**, 1473.
- 15 K. Berg, A. Weyergang, L. Prasmickaite, A. Bonsted, A. Høgset, M. T. Strand, E. Wagner and P. K. Selbo, *Methods Mol. Biol.*, 2010, **635**, 133.
- 16 A. Høgset, L. Prasmickaite, T. E. Tjelle and K. Berg, *Hum. Gene Ther.*, 2000, **11**, 869.
- 17 I. Johnson, *Optical Imaging Cancer*, Springer, New York, NY, 2010, pp. 59–77.
- 18 M. Ethirajan, Y. Chen, P. Joshi and R. K. Pandey, *Chem. Soc. Rev.*, 2011, **40**, 340.
- 19 M. R. Detty, S. L. Gibson and S. J. Wagner, *J. Med. Chem.*, 2004, **47**, 3897.
- 20 A. E. O'Connor, W. M. Gallagher and A. T. Byrne, *Photochem. Photobiol.*, 2009, **85**, 1053.
- 21 J. G. Moser, *Photodynamic Tumor Therapy: 2nd and 3rd Generation Photosensitizers*, Harwood Academic Publishers, Amsterdam, 1998.



22 K. M. Kadish, K. M. Smith and R. Guilard, *Handbook of Porphyrin Science*, World Scientific, Singapore, 2016.

23 V. V. Roznyatovskiy, C.-H. Lee and J. L. Sessler, *Chem. Soc. Rev.*, 2013, **42**, 1921.

24 H. Lu and N. Kobayashi, *Chem. Rev.*, 2016, **116**, 6184.

25 T. Basova, A. Hassan, M. Durmus, A. G. Gürek and V. Ahsen, *Coord. Chem. Rev.*, 2016, **310**, 131.

26 J. F. B. Barata, M. G. P. M. S. Neves, M. A. F. Faustino, A. C. Tomé and J. A. S. Cavaleiro, *Chem. Rev.*, 2017, **117**, 3192.

27 A. Kamkaew, S. H. Lim, H. B. Lee, L. V. Kiew, L. Y. Chung and K. Burgess, *Chem. Soc. Rev.*, 2013, **42**, 77.

28 C. G. Claessens, D. González-Rodríguez, M. S. Rodríguez-Morgade, A. Medina and T. Torres, *Chem. Rev.*, 2014, **114**, 2192.

29 J. L. Sessler, Z. Gross and H. Furuta, *Chem. Rev.*, 2017, **117**, 2201.

30 C. Preihs, J. F. Arambula, D. Magda, H. Jeong, D. Yoo, J. Cheon, Z. H. Siddik and J. L. Sessler, *Inorg. Chem.*, 2013, **52**, 12184.

31 N. Stephanopoulos and M. B. Francis, *Nat. Chem. Biol.*, 2011, **7**, 876.

32 N. Sewald and H.-D. Jaakubke, *Application of Peptides and Proteins*, Wiley-VCH Verlag GmbH & Co. KGaA, Darmstadt, 2009.

33 H.-Y. Liu, J.-W. Huang, X. Tian, X.-D. Jiao, G.-T. Luo and L.-N. Ji, *Chem. Commun.*, 1997, 1575.

34 E. Biron and N. Voyer, *Chem. Commun.*, 2005, 4652.

35 K. Liu, H. Zhang, R. Xing, Q. Zou and X. Yan, *ACS Nano*, 2017, **11**, 12840.

36 K. Karikis, E. Georgilis, G. Charalambidis, A. Petrou, O. Vakuliuk, T. Chatziioannou, I. Raptaki, S. Tsovoli, I. Papakyriacou, A. Mitraki, D. T. Gryko and A. G. Coutsolelos, *Chem. – Eur. J.*, 2016, **22**, 11245.

37 Z.-W. Gu, J. D. Spikes, P. Kopečková and J. Kopeček, *Collect. Czech. Chem. Commun.*, 1993, **58**, 2321.

38 U. Drechsler, M. Pfaff and M. Hanack, *Eur. J. Org. Chem.*, 1999, 3441.

39 S. L. Haywood-Small, D. I. Vernon, J. Griffiths, J. Schofield and S. B. Brown, *Biochem. Biophys. Res. Commun.*, 2006, **339**, 569.

40 X. He, J. Li, S. An and C. Jiang, *Ther. Delivery*, 2013, **4**, 1499.

41 A. Wang, L. Gui, S. Lu, L. Zhou, J. Zhou and S. Wei, *Dyes Pigm.*, 2016, **126**, 239.

42 A. K. Paul, S. C. Karunakaran, J. Joseph and D. Ramaiah, *Photochem. Photobiol.*, 2015, **91**, 1348.

43 S. Meng, Z. Xu, G. Hong, L. Zhao, Z. Zhao, J. Guo, H. Ji and T. Liu, *Eur. J. Med. Chem.*, 2015, **92**, 35.

44 Y. Yuan, Z.-Q. Liu, H. Jin, S. Sun, T.-J. Liu, X. Wang, H.-J. Fan, S.-K. Hou and H. Ding, *PLoS One*, 2017, **12**, e0176529.

45 V. V. Serra, A. Zamarrón, M. A. F. Faustino, M. C. Iglesias-dela Cruz, A. Blázquez, J. M. M. Rodrigues, M. G. P. M. S. Neves, J. A. S. Cavaleiro, A. Juarranz and F. Sanz-Rodríguez, *Bioorg. Med. Chem.*, 2010, **18**, 6170.

46 Z. Meng, B. Yu, G. Han, M. Liu, B. Shan, G. Dong, Z. Miao, N. Jia, Z. Tan, B. Li, W. Zhang, H. Zhu, C. Sheng and J. Yao, *J. Med. Chem.*, 2016, **59**, 4999.

47 R. G. W. Jinadasa, X. Hu, M. G. H. Vicente and K. M. Smith, *J. Med. Chem.*, 2011, **54**, 7464.

48 F. Giuntini, C. M. A. Alonso and R. W. Boyle, *Photochem. Photobiol. Sci.*, 2011, **10**, 759.

49 M. Sibrian-Vázquez, J. Ortiz, I. V. Nesterova, F. Fernández-Lázaro, A. Sastre-Santos, S. A. Soper and M. G. H. Vicente, *Bioconjugate Chem.*, 2007, **18**, 410.

50 P. Xu, J. Chen, Z. Chen, S. Zhou, P. Hu, X. Chen and M. Huang, *PLoS One*, 2012, **7**, e37051.

51 F. Li, Q. Liu, Z. Liang, J. Wang, M. Pang, W. Huang, W. Wu and Z. Hong, *Org. Biomol. Chem.*, 2016, **14**, 3409.

52 B. G. Ongarora, K. R. Fontenot, X. Hu, I. Sehgal, S. D. Satyanarayana-Jois and M. G. H. Vicente, *J. Med. Chem.*, 2012, **55**, 3725.

53 M.-R. Ke, S.-L. Yeung, W.-P. Fong, D. K. P. Ng and P.-C. Lo, *Chem. – Eur. J.*, 2012, **18**, 4225.

54 C. Dubuc, R. Langlois, F. Bénard, N. Cauchon, K. Klarskov, P. Tone and J. E. van Lier, *Bioorg. Med. Chem. Lett.*, 2008, **18**, 2424.

55 H. Ali, S. Ait-Mohand, S. Gosselin, J. E. van Lier and B. Guérin, *J. Org. Chem.*, 2011, **76**, 1887.

56 E. Ranyuk, N. Cauchon, K. Klarskov, B. Guérin and J. E. Van Lier, *J. Med. Chem.*, 2013, **56**, 1520.

57 M.-R. Ke, D. K. P. Ng and P.-C. Lo, *Chem. – Asian J.*, 2014, **9**, 554.

58 R. Dondi, E. Yaghini, K. M. Tewari, L. Wang, F. Giuntini, M. Loizidou, A. J. MacRobert and I. M. Eggleston, *Org. Biomol. Chem.*, 2016, **14**, 11488.

59 N. Umezawa, N. Matsumoto, S. Iwama, N. Kato and T. Higuchi, *Bioorg. Med. Chem.*, 2010, **18**, 6340.

60 N. Zhao, T. M. Williams, Z. Zhou, F. R. Fronczek, M. Sibrian-Vázquez, S. D. Jois and M. G. H. Vicente, *Bioconjugate Chem.*, 2017, **28**, 1566.

61 R. Garifullin, T. S. Erkal, S. Tekin, B. Ortaç, A. G. Gürek, V. Ahsen, H. G. Yaglioglu, A. Elmali and M. O. Guler, *J. Mater. Chem.*, 2012, **22**, 2553.

62 Q. Zou, M. Abbas, L. Zhao, S. Li, G. Shen and X. Yan, *J. Am. Chem. Soc.*, 2017, **139**, 1921.

63 A. J. van Hell, M. M. Fretz, D. J. Crommelin, W. E. Hennink and E. Mastrobattista, *J. Controlled Release*, 2010, **141**, 347.

64 Q. Zou, K. Liu, M. Abbas and X. Yan, *Adv. Mater.*, 2016, **28**, 1031.

65 H. C. Fry, J. M. Garcia, M. J. Medina, U. M. Ricoy, D. J. Gosztola, M. P. Nikiforov, L. C. Palmer and S. I. Stupp, *J. Am. Chem. Soc.*, 2012, **134**, 14646.

66 A. M. Master, Y. Qi, N. L. Oleinick and A. S. Gupta, *Nanomedicine*, 2012, **8**, 655.

67 G. Charalambidis, E. Georgilis, M. K. Panda, C. E. Anson, A. K. Powell, S. Doyle, D. Moss, T. Jochum, P. N. Horton, S. J. Coles, M. Linares, D. Beljonne, J. V. Naubron, J. Conradt, H. Kalt, A. Mitraki, A. G. Coutsolelos and T. S. Balaban, *Nat. Commun.*, 2016, **7**, 12657.

68 L. Ciu, Q. Lin, C. S. Jin, W. Jiang, H. Huang, L. Ding, N. Muhanna, J. C. Irish, F. Wang, J. Chen and G. Zheng, *ACS Nano*, 2015, **9**, 4484.

69 K. Liu, R. Xing, Q. Zou, G. Ma, H. Möhwald and X. Yan, *Angew. Chem., Int. Ed.*, 2016, **55**, 3036.

70 M. Abbas, R. Xing, N. Zhang, Q. Zou and X. Yan, *ACS Biomater. Sci. Eng.*, 2018, **4**, 2046.



71 H. Sun, S. Li, W. Qi, R. Xing, Q. Zou and X. Yan, *Colloids Surf, A*, 2018, **538**, 795.

72 S. Li, R. Xing, R. Chang, Q. Zou and X. Yan, *Curr. Opin. Colloid Interface Sci.*, 2018, **35**, 17.

73 M. Abbas, Q. Zou, S. Li and X. Yan, *Adv. Mater.*, 2017, **29**, 1605021.

74 C. Yewale, D. Baradaria, I. Vhora, S. Patil and A. Misra, *Biomaterials*, 2013, **34**, 8690.

75 S. Song, D. Liu, J. Peng, H. Deng, Y. Guo, L. X. Xu, A. D. Miller and Y. Xu, *FASEB J.*, 2009, **23**, 1396.

76 Z. Li, R. Zhao, X. Wu, Y. Sun, M. Yao, J. Li, Y. Xu and J. Gu, *FASEB J.*, 2005, **19**, 1978.

77 K. R. Fontenot, B. G. Ongarora, L. E. LeBlanc, Z. Zhou, S. D. Jois and M. G. H. Vicente, *J. Porphyrins Phthalocyanines*, 2016, **20**, 352.

78 S. Banappagari, A. McCall, K. Fontenot, M. G. H. Vicente, A. Gujar and S. Satyanarayananjois, *Eur. J. Med. Chem.*, 2013, **65**, 60.

79 D. B. Cornelio, R. Roesler and G. Schwartsmann, *Ann. Oncol.*, 2007, **18**, 1457.

80 J. Zhang, G. Niu, L. Lang, F. Li, X. Fan, X. Yan, S. Yao, W. Yan, L. Huo, L. Chen, Z. Li, Z. Zhu and X. Chen, *J. Nucl. Med.*, 2017, **58**, 228.

81 G. Mion, C. Mari, T. Da Ros, R. Rubbiani, G. Gasser and T. Gianferrara, *ChemistrySelect*, 2017, **2**, 190.

82 B. Brizet, V. Goncalves, C. Bernhard, P. D. Harvey, F. Denat and C. Goze, *Chem. – Eur. J.*, 2014, **20**, 12933.

83 P. C. Brooks, R. A. Clark and D. A. Cheresh, *Science*, 1994, **264**, 569.

84 R. Haubner, H. J. Wester, U. Reuning, R. Senekowitsch-Schmidtke, B. Diefenbach, H. Kessler, G. Stocklin and M. Schwaiger, *J. Nucl. Med.*, 1999, **40**, 1061.

85 V. Chaleix, V. Sol, Y. M. Huang, M. Guilloton, R. Granet, J. C. Blais and P. Krausz, *Eur. J. Org. Chem.*, 2003, 1486.

86 C. Frochot, B. Di Stasio, R. Vanderesse, M. Belgy, M. Dodeller, F. Guillemin, M. Viriot and M. Barberi-Heyob, *Bioorg. Chem.*, 2007, **35**, 205.

87 C. L. Conway, I. Walker, A. Bell, D. J. H. Roberts, S. B. Brown and D. I. Vernon, *Photochem. Photobiol. Sci.*, 2008, **7**, 290.

88 L. W. T. Cheung and A. S. T. Wong, *FEBS J.*, 2008, **275**, 5479.

89 S. Rahimipour, N. Ben-Aroya, K. Ziv, A. Chen, M. Fridkin and Y. Koch, *J. Med. Chem.*, 2003, **46**, 3965.

90 A. Lange, R. E. Mills, C. J. Lange, M. Stewart, S. E. Devine and A. H. Corbett, *J. Biol. Chem.*, 2007, **282**, 5101.

91 S. K. Bisland, D. Singh and J. Gariépy, *Bioconjugate Chem.*, 1999, **10**, 982.

92 M. Sibrian-Vazquez, T. J. Jensen and M. G. H. Vicente, *Org. Biomol. Chem.*, 2010, **8**, 1160.

93 P. Dozso, M. Koo, S. Berger, T. M. Forte and S. B. Kahl, *J. Med. Chem.*, 2005, **48**, 357.

94 P. Verwilst, C. C. David, V. Leen, J. Hofkens, P. A. M. de Witte and W. M. De Borggraeve, *Bioorg. Med. Chem. Lett.*, 2013, **23**, 3204.

95 R. Dosselli, C. Tampieri, R. Ruiz-González, S. De Munari, X. Ragàs, D. Sanchez-García, M. Agut, S. Nonell, E. Reddi and M. Gobbo, *J. Med. Chem.*, 2013, **56**, 1052.

96 L. Mendive-Tapia, R. Subiros-Funosas, C. Zhao, F. Albericio, N. D. Read, R. Lavilla and M. Vendrell, *Nat. Protoc.*, 2017, **12**, 1588.

97 L. Mendive-Tapia, C. Zhao, A. R. Akram, S. Preciado, F. Albericio, M. Lee, A. Serrels, N. Kielland, N. D. Read, R. Lavilla and M. Vendrell, *Nat. Commun.*, 2016, **7**, 10940.

98 R. Subiros-Funosas, L. Mendive-Tapia, J. Sot, J. D. Pound, N. Barth, Y. Varela, F. M. Goñi, M. Paterson, C. D. Gregory, F. Albericio, I. Dransfield, R. Lavilla and M. Vendrell, *Chem. Commun.*, 2017, **53**, 945.

99 W. Tang and M. L. Becker, *Chem. Soc. Rev.*, 2014, **43**, 7013.

100 W. M. Sharman, J. E. van Lier and C. M. Allen, *Adv. Drug Delivery Rev.*, 2004, **56**, 53.

101 D. Derossi, A. Joliot, G. Chassaigne and A. Prochiantz, *J. Biol. Chem.*, 1994, **269**, 10444.

102 J. B. Rothbard, T. C. Jessop, R. S. Lewis, B. A. Murray and P. A. Wender, *J. Am. Chem. Soc.*, 2004, **126**, 9506.

103 M. Engelen, A. Lombardi, R. Vitale, L. Lista, O. Maglio, V. Pavone and F. Nastri, *Biotechnol. Appl. Biochem.*, 2015, **62**, 383.

104 M. Sibrian-Vazquez, T. J. Jensen and M. G. H. Vicente, *J. Med. Chem.*, 2008, **51**, 2915.

105 I. Sehgal, M. Sibrian-Vazquez and M. G. H. Vicente, *J. Med. Chem.*, 2008, **51**, 6014.

106 G. Fanali, A. di Masi, V. Trezza, M. Marino, M. Fasano and P. Ascenzi, *Mol. Aspects Med.*, 2012, **33**, 209.

107 H. R. Jiménez and M. Arbona, *J. Coord. Chem.*, 2018, **71**, 890.

108 J. Matsumoto, Y. Kai, H. Yokoi, S. Okazaki and M. Yasuda, *J. Photochem. Photobiol. B*, 2016, **161**, 279.

109 V. A. Ol'shevskaya, R. G. Nikitina, A. N. Savchenko, M. V. Malshakova, A. M. Vinogradov, G. V. Golovina, D. V. Belykh, A. V. Kutchin, M. A. Kaplan, V. N. Kalinin, V. A. Kuzmin and A. A. Shtil, *Bioorg. Med. Chem.*, 2009, **17**, 1297.

110 O. Rinco, J. Brenton, A. Douglas, A. Maxwell, M. Henderson, K. Indrelie, J. Wessels and J. Widin, *J. Photochem. Photobiol. A*, 2009, **208**, 91.

111 S. A. G. Lambrechts, M. C. G. Aalders, F. D. Verbraak, J. W. M. Lagerberg, J. B. Dankert and J. J. Schuitmaker, *J. Photochem. Photobiol. B*, 2005, **79**, 51.

112 P. Sarbadhikary and A. Dube, *Photochem. Photobiol. Sci.*, 2017, **16**, 1762.

113 Y. Zhang and H. Gorner, *Dyes Pigm.*, 2009, **83**, 174.

114 S. Patel and A. Datta, *J. Phys. Chem. B*, 2007, **111**, 10557.

115 C. Larroque, A. Pelegrin and J. E. van Lier, *Br. J. Cancer*, 1996, **74**, 1886.

116 N. Brasseur, R. Langlois, C. La Madeleine, R. Ouellet and J. E. van Lier, *Photochem. Photobiol.*, 1999, **69**, 345.

117 J.-D. Huang, W.-P. Fong, E. Y. M. Chan, M. T. M. Choi, W.-K. Chan, M.-C. Chan and D. K. P. Ng, *Tetrahedron Lett.*, 2003, **44**, 8029.

118 X.-J. Jiang, J.-D. Huang, Y.-J. Zhu, F.-X. Tang, D. K. P. Ng and J.-C. Sun, *Bioorg. Med. Chem. Lett.*, 2006, **16**, 2450.

119 J.-D. Huang, P.-C. Lo, Y.-M. Chen, J. C. Lai, W.-P. Fong and D. K. P. Ng, *J. Inorg. Biochem.*, 2006, **100**, 946.

120 D. Xu, Y. Ke, X. Jiang, Y. Cai, Y. Peng and Y. Li, *Br. J. Neurosurg.*, 2010, **24**, 660.



121 D. Xu, X. Chen, K. Chen, Y. Peng, Y. Li, Y. Ke and D. Gan, *J. Biomater. Appl.*, 2014, **29**, 378.

122 E. P. O. Silva, E. D. Santos, C. S. Gonçalves, M. A. G. Cardoso, C. P. Soares and M. Beltrame, *Laser Phys.*, 2016, **26**, 105601.

123 A. M. Garcia, H. de Alwis Weerasekera, S. P. Pitre, B. McNeill, E. Lissi, A. M. Edwards and E. I. Alarcon, *J. Photochem. Photobiol., B*, 2016, **163**, 385.

124 R. Li, K. Zheng, P. Hu, Z. Chen, S. Zhou, J. Chen, C. Yuan, S. Chen, W. Zheng, E. Ma, F. Zhang, J. Xue, X. Chen and M. Huang, *Theranostics*, 2014, **4**, 642.

125 F. Li, Y. Zhao, C. Mao, Y. Kong and X. Ming, *Mol. Pharmaceutics*, 2017, **14**, 2793.

126 W.-L. Lu, Y.-Q. Lan, K.-J. Xiao, Q.-M. Xu, L.-L. Qu, Q.-Y. Chen, T. Huang, J. Gao and Y. Zhao, *J. Mater. Chem. B*, 2017, **5**, 1275.

127 D. Hu, Z. Sheng, G. Gao, F. Siu, C. Liu, Q. Wan, P. Gong, H. Zheng, Y. Ma and L. Cai, *Biomaterials*, 2016, **93**, 10.

128 N. Zhang, F. Zhao, Q. Zou, Y. Li, G. Ma and X. Yan, *Small*, 2016, **12**, 5936.

129 X. Song, C. Liang, H. Gong, Q. Chen, C. Wang and Z. Liu, *Small*, 2015, **11**, 3932.

130 L. Zhou, T. Yang, J. Wang, Q. Wang, X. Lv, H. Ke, Z. Guo, J. Shen, Y. Wang, C. Xing and H. Chen, *Theranostics*, 2017, **7**, 764.

131 G. Battogtokh and Y. T. Ko, *J. Mater. Chem. B*, 2015, **3**, 9349.

132 K. Kitagishi, H. Kawasaki and K. Kano, *Chem. – Asian J.*, 2015, **10**, 1768.

133 N. Gueddari, G. Favre, H. Hachem, E. Marek, F. Le Gaillard and G. Soula, *Biochimie*, 1993, **75**, 811.

134 D. A. Bricarello, J. T. Smilowitz, A. M. Zivkovic, J. B. German and A. N. Parikh, *ACS Nano*, 2011, **5**, 42.

135 J. M. Shaw, *Lipoproteins as carriers of pharmacological agents*, Dekker, 1991.

136 J. Tang, J.-J. Chen, J. Jing, J.-Z. Chen, H. Lv, Y. Yu, P. Xu and J.-L. Zhang, *Chem. Sci.*, 2014, **5**, 558.

137 P. M. R. Pereira, B. Korsak, B. Sarmento, R. J. Schneider, R. Fernandes and J. P. C. Tomé, *Org. Biomol. Chem.*, 2015, **13**, 2518.

138 H. Agadjanian, J. Ma, A. Rentsendorj, V. Valluripalli, J. Y. Hwang, A. Mahammed, D. L. Farkas, H. B. Gray, Z. Gross and L. K. Medina-Kauwe, *Proc. Natl. Acad. Sci. U. S. A.*, 2009, **106**, 6105.

139 H. Kobayashi and P. L. Choyke, *Nanoscale*, 2016, **8**, 12504.

140 M. Mitsunaga, M. Ogawa, N. Kosaka, L. T. Rosenblum, P. L. Choyke and H. Kobayashi, *Nat. Med.*, 2011, **17**, 1685.

141 M. Mitsunaga, T. Nakajima, K. Sano, P. L. Choyke and H. Kobayashi, *Bioconjugate Chem.*, 2012, **23**, 604.

142 M. Mitsunaga, T. Nakajima, K. Sano, G. Kramer-Marek, P. L. Choyke and H. Kobayashi, *BMC Cancer*, 2012, **12**, 345.

143 M. Mitsunaga, T. Nakajima, K. Sano, P. L. Choyke and H. Kobayashi, *Cancer Res.*, 2012, **72**, 4622.

144 K. Sano, M. Mitsunaga, T. Nakajima, P. L. Choyke and H. Kobayashi, *J. Nucl. Med.*, 2013, **54**, 770.

145 K. Sato, H. Hanaoka, R. Watanabe, T. Nakajima, P. L. Choyke and H. Kobayashi, *Mol. Cancer Ther.*, 2015, **14**, 141.

146 K. Sato, T. Nagaya, M. Mitsunaga, P. L. Choyke and H. Kobayashi, *Cancer Lett.*, 2015, **365**, 112.

147 K. Sato, T. Nagaya, P. L. Choyke and H. Kobayashi, *Theranostics*, 2015, **5**, 698.

148 A. Maruani, H. Savoie, F. Bryden, S. Caddick, R. Boyle and V. Chudasama, *Chem. Commun.*, 2015, **51**, 15304.

149 B. Korsak, G. M. Almeida, S. Rocha, C. Pereira, N. Mendes, H. Osório, P. M. R. Pereira, J. M. M. Rodrigues, R. J. Schneider, B. Sarmento, J. P. C. Tomé and C. Oliveira, *Int. J. Cancer*, 2017, **141**, 1478.

150 M. H. Y. Cheng, A. Maruani, H. Savoie, V. Chudasama and R. W. Boyle, *Org. Biomol. Chem.*, 2018, **16**, 1144.

151 S. Benchimol, A. Fuks, S. Jothy, N. Beauchemin, K. Shiota and C. P. Stanners, *Cell*, 1989, **57**, 327.

152 C. H. Bedel-Cloutour, L. Mauclaire, A. Saux and M. Pereyre, *Bioconjugate Chem.*, 1996, **7**, 617.

153 H. Abe, M. Kuroki, K. Tachibana, T. Li, A. Awasthi, A. Ueno, H. Matsumoto, T. Imakiire, Y. Yamauchi, H. Yamada, A. Ariyoshi and M. Kuroki, *Anticancer Res.*, 2002, **22**, 1575.

154 M. Carcenac, C. Larroque, R. Langlois, J. E. van Lier, J. C. Artus and A. Pèlegrin, *Photochem. Photobiol.*, 1999, **70**, 930.

155 M. Carcenac, M. Dorvillius, V. Garambois, F. Glaussel, C. Larroque, R. Langlois, N. E. Hynes, J. E. van Lier and A. Pèlegrin, *Br. J. Cancer*, 2001, **85**, 1787.

156 R. Hudson, M. Carcenac, K. Smith, L. Madden, O. J. Clarke, A. Pèlegrin, J. Greenman and R. W. Boyle, *Br. J. Cancer*, 2005, **92**, 1442.

157 I. Sehgal, H. Li, B. Ongarora, D. Devillier and M. G. H. Vicente, *J. Porphyrins Phthalocyanines*, 2013, **17**, 150.

158 A. A. Maawy, Y. Hiroshima, Y. Zhang, R. Heim, L. Makings, M. Garcia-Guzman, G. A. Luiken, H. Kobayashi, R. M. Hoffman and M. Bouvet, *PLoS One*, 2015, **10**, e0121989.

159 W. Duan, K. Smith, H. Savoie, J. Greenman and R. W. Boyle, *Org. Biomol. Chem.*, 2005, **3**, 2384.

160 P. M. R. Pereira, J. J. Carvalho, S. Silva, J. A. S. Cavaleiro, R. J. Schneider, R. Fernandes and J. P. C. Tomé, *Org. Biomol. Chem.*, 2014, **12**, 1804.

161 A. R. Oseroff, D. Ohuoha, T. Hasan, J. C. Bommer and M. L. Yarmush, *Proc. Natl. Acad. Sci. U. S. A.*, 1986, **83**, 8744.

162 C. M. A. Alonso, A. Palumbo, A. J. Bullous, F. Pretto, D. Neri and R. W. Boyle, *Bioconjugate Chem.*, 2010, **21**, 302.

163 M. Ho and H. Kim, *Eur. J. Cancer*, 2011, **47**, 333.

164 H. Hanaoka, T. Nakajima, K. Sato, R. Watanabe, Y. Phung, W. Gao, T. Harada, I. Kim, C. H. Paik, P. L. Choyke, M. Ho and H. Kobayashi, *Nanomedicine*, 2015, **10**, 1139.

165 R. Watanabe, H. Hanaoka, K. Sato, T. Nagaya, T. Harada, M. Mitsunaga, I. Kim, C. H. Paik, A. M. Wu, P. L. Choyke and H. Kobayashi, *J. Nucl. Med.*, 2015, **56**, 140.

166 F. Bryden, A. Maruani, H. Savoie, V. Chudasama, M. E. B. Smith, S. Caddick and R. W. Boyle, *Bioconjugate Chem.*, 2014, **25**, 611.

167 M. Uchida, M. T. Klem, M. Allen, P. Suci, M. Flenniken, E. Gillitzer, Z. Varpness, L. O. Liepold, M. Young and T. Douglas, *Adv. Mater.*, 2007, **19**, 1025.

168 A. de la Escosura, R. J. M. Nolte and J. J. L. M. Cornelissen, *J. Mater. Chem.*, 2009, **19**, 2274.

169 R. F. Garmann, M. Comas-Garcia, C. M. Knobler and W. M. Gelbart, *Acc. Chem. Res.*, 2016, **49**, 48.



170 J. A. Speir, S. Munshi, G. Wang, T. S. Baker and J. E. Johnson, *Structure*, 1995, **3**, 63.

171 J. E. Johnson and J. A. Speir, *J. Mol. Biol.*, 1997, **269**, 665.

172 R. M. Putri, J. J. L. M. Cornelissen and M. S. T. Koay, *ChemPhysChem*, 2015, **16**, 911.

173 J. Tang, J. M. Johnson, K. A. Dryden, M. J. Young, A. Zlotnick and J. E. Johnson, *J. Struct. Biol.*, 2006, **154**, 59.

174 M. Brasch, A. De La Escosura, Y. Ma, C. Utrecht, A. J. R. Heck, T. Torres and J. J. L. M. Cornelissen, *J. Am. Chem. Soc.*, 2011, **133**, 6878.

175 D. Luque, A. De La Escosura, J. Snijder, M. Brasch, R. J. Burnley, M. S. T. Koay, J. L. Carrascosa, G. J. L. Wuite, W. H. Roos, A. J. R. Heck, J. J. L. M. Cornelissen, T. Torres and J. R. Castón, *Chem. Sci.*, 2014, **5**, 575.

176 F. Setaro, M. Brasch, U. Hahn, M. S. T. Koay, J. J. L. M. Cornelissen, A. de la Escosura and T. Torres, *Nano Lett.*, 2015, **15**, 1245.

177 J. G. Millán, M. Brasch, E. Anaya-Plaza, A. De La Escosura, A. H. Velders, D. N. Reinhoudt, T. Torres, M. S. T. Koay and J. J. L. M. Cornelissen, *J. Inorg. Biochem.*, 2014, **136**, 140.

178 Y. Fu and J. Li, *Virus Res.*, 2016, **211**, 9.

179 B. A. Cohen and M. Bergkvist, *J. Photochem. Photobiol. B*, 2013, **121**, 67.

180 N. Stephanopoulos, G. J. Tong, S. C. Hsiao and M. B. Francis, *ACS Nano*, 2010, **4**, 6014.

181 J. Chang, P. Weigle, J. King, W. Chiu and W. Jiang, *Structure*, 2006, **14**, 1073.

182 S. Qazi, M. Uchida, R. J. Usselman, R. Shearer, E. Edwards and T. Douglas, *J. Biol. Inorg. Chem.*, 2014, **19**, 237.

183 G. Jutz, P. Van Rijn, B. Santos Miranda and A. Böker, *Chem. Rev.*, 2015, **115**, 1653.

184 Z. Zhen, W. Tang, C. Guo, H. Chen, X. Lin, G. Liu, B. Fei, X. Chen, B. Xu and J. Xie, *ACS Nano*, 2013, **7**, 6988.

185 J. Mikkilä, E. Anaya-Plaza, V. Liljestrom, J. Ruiz-Castan, T. Torres, A. de la Escosura and M. A. Kostiainen, *ACS Nano*, 2016, **10**, 1565.

186 D. Dziuba, R. Pohl and M. Hocek, *Bioconjugate Chem.*, 2014, **25**, 1984.

187 D. Dziuba, P. Jurkiewicz, M. Cebecauer, M. Hof and M. Hocek, *Angew. Chem.*, 2016, **128**, 182.

188 X.-Y. Li and D. K. P. Ng, *Tetrahedron Lett.*, 2001, **42**, 305.

189 X. Liu, C. Qi, T. Bing, X. Cheng and D. Shangguan, *Anal. Chem.*, 2009, **81**, 3699.

190 A. A. Chernonosov, V. V. Koval, D. G. Knorre, A. A. Chernenko, V. M. Derkacheva, E. A. Lukyanets and O. S. Fedorova, *Bioinorg. Chem. Appl.*, 2006, **2006**, 63703.

191 I. V. Nesterova, V. T. Verdree, S. Pakhomov, K. L. Strickler, M. W. Allen, R. P. Hammer and S. A. Soper, *Bioconjugate Chem.*, 2007, **18**, 2159.

192 V. Král, T. V. Shishkanova, J. L. Sessler and C. T. Brown, *Org. Biomol. Chem.*, 2004, **2**, 1169.

193 R. P. Hammer, C. V. Owens, S. H. Hwang, C. M. Sayes and S. A. Soper, *Bioconjugate Chem.*, 2002, **13**, 1244.

194 B. Y. Zheng, X. M. Shen, D. M. Zhao, Y. Bin Cai, M. R. Ke and J. D. Huang, *J. Photochem. Photobiol. B*, 2016, **159**, 196.

195 X.-M. Shen, B.-Y. Zheng, X.-R. Huang, L. Wang and J.-D. Huang, *Dalton Trans.*, 2013, **42**, 10398.

196 E. Stulz, *Acc. Chem. Res.*, 2017, **50**, 823.

197 C. Casas, C. J. Lacey and B. Meunier, *Bioconjugate Chem.*, 1993, **4**, 366.

198 J. K. Choi, G. Sargsyan, A. M. Olive and M. Balaz, *Chem. – Eur. J.*, 2013, **19**, 2515.

199 V. Malinovski, L. Tumir, I. Piantanida, M. Zinic and H. Schenider, *Eur. J. Org. Chem.*, 2002, 3785.

200 S.-Y. Hung, Y.-C. Shih and W.-L. Tseng, *Anal. Chim. Acta*, 2015, **857**, 64.

201 A. S. Boutorine, D. Brault, M. Takasugi, O. Delgado and C. Hélène, *J. Am. Chem. Soc.*, 1996, **118**, 9469.

202 H. Li, O. S. Fedorova, W. R. Trumble, T. R. Fletcher and L. Czuchajowski, *Bioconjugate Chem.*, 1997, **8**, 49.

203 M. Op de Beeck and A. Madder, *J. Am. Chem. Soc.*, 2012, **134**, 10737.

204 C. V. Montes, H. Memczak, E. Gyssels, T. Torres, A. Madder and R. J. Schneider, *Langmuir*, 2017, **33**, 1197.

205 E. M. Llamas, J. P. C. Tome, J. M. M. Rodrigues, T. Torres and A. Madder, *Org. Biomol. Chem.*, 2017, **15**, 5402.

206 N. Dai and E. T. Kool, *Chem. Soc. Rev.*, 2011, **40**, 5756.

207 S. Ranallo, M. Rossetti, K. W. Plaxco, A. Vallée-Bélisle and F. Ricci, *Angew. Chem., Int. Ed.*, 2015, **54**, 13214.

208 M. N. Stojanovic, D. Stefanovic and S. Rudchenko, *Acc. Chem. Res.*, 2014, **47**, 1845.

209 N. Nishiyama, A. Iriyama, W.-D. Jang, K. Miyata, K. Itaka, Y. Inoue, H. Takahashi, Y. Yanagi, Y. Tamaki, H. Koyama and K. Kataoka, *Nat. Mater.*, 2005, **4**, 934.

210 T. Nomoto, S. Fukushima, M. Kumagai, K. Machitani, A. Arnida, Y. Matsumoto, M. Oba, K. Miyata, K. Osada, N. Nishiyama and K. Kataoka, *Nat. Commun.*, 2014, **5**, 3545.

211 A. Yuan, B. Laing, Y. Hu and X. Ming, *Chem. Commun.*, 2015, **51**, 6678.

212 C. K. Kwok and C. J. Merrick, *Trends Biotechnol.*, 2017, **35**, 997.

213 M. Sauer and K. Paeschke, *Biochem. Soc. Trans.*, 2017, **45**, 1173.

214 G. Pratviel, *Coord. Chem. Rev.*, 2016, **308**, 460.

215 H. Yaku, T. Fujimoto, T. Murashima, D. Miyoshi and N. Sugimoto, *Chem. Commun.*, 2012, **48**, 6203.

216 H. Yaku, T. Murashima, D. Miyoshi and N. Sugimoto, *Molecules*, 2012, **17**, 10586.

217 L. Zhang, J. C. Er, K. K. Ghosh, W. J. Chung, J. Yoo, W. Xu, W. Zhao, A. T. Phan and Y.-T. Chang, *Sci. Rep.*, 2014, **4**, 3776.

218 K. T. Kim and B. H. Kim, *Chem. Commun.*, 2013, **49**, 1717.

219 P. Maillard, S. Gaspard, J. L. Guerquin-Kern and M. Momenteau, *J. Am. Chem. Soc.*, 1989, **111**, 9125.

220 G. Fülling, D. Schröder and B. Franck, *Angew. Chem., Int. Ed. Engl.*, 1989, **28**, 1519.

221 R. A. Dwek, *Chem. Rev.*, 1996, **96**, 683.

222 S. Singh, A. Aggarwal, N. V. S. D. K. Bhupathiraju, G. Arianna, K. Tiwari and C. M. Drain, *Chem. Rev.*, 2015, **115**, 10261.

223 G. Crini, *Chem. Rev.*, 2014, **114**, 10940.

224 K.-R. Wang, D.-S. Guo, B.-P. Jiang and Y. Liu, *Chem. Commun.*, 2012, **48**, 3644.



225 W. Deng, T. Onji, H. Yamaguchi, N. Ikeda and A. Harada, *Chem. Commun.*, 2006, 4212.

226 W.-J. Shi, R. Menting, E. A. Ermilov, P.-C. Lo, B. Röder and D. K. P. Ng, *Chem. Commun.*, 2013, **49**, 5277.

227 K. Kano, H. Kitagishi, S. Tamura and A. Yamada, *J. Am. Chem. Soc.*, 2004, **126**, 15202.

228 F. Venema, A. E. Rowan and R. J. M. Nolte, *J. Am. Chem. Soc.*, 1996, **118**, 257.

229 H. Zhang, B. Zhang, M. Zhu, S. M. Grayson, R. Schmehl and J. Jayawickramarajah, *Chem. Commun.*, 2014, **50**, 4853.

230 M. Fathalla, A. Neuberger, S.-C. Li, R. Schmehl, U. Diebold and J. Jayawickramarajah, *J. Am. Chem. Soc.*, 2010, **132**, 9966.

231 A. O. Ribeiro, J. P. C. Tomé, M. G. P. M. S. Neves, A. C. Tomé, J. A. S. Cavaleiro, O. A. Serra and T. Torres, *Tetrahedron Lett.*, 2006, **47**, 6129.

232 J. T. F. Lau, P.-C. Lo, Y.-M. Tsang, W.-P. Fong and D. K. P. Ng, *Chem. Commun.*, 2011, **47**, 9657.

233 X. Leng, C.-F. Choi, P.-C. Lo and D. K. P. Ng, *Org. Lett.*, 2007, **9**, 231.

234 L. M. O. Lourenço, P. M. R. Pereira, E. Maciel, M. Válega, F. M. J. Domingues, M. R. M. Domingues, M. G. P. M. S. Neves, J. A. S. Cavaleiro, R. Fernandes and J. P. C. Tomé, *Chem. Commun.*, 2014, **50**, 8363.

235 A. Galstyan, U. Kauscher, D. Block, B. J. Ravoo and C. A. Strassert, *ACS Appl. Mater. Interfaces*, 2016, **8**, 12631.

236 J. Králová, A. Synytsya, P. Poučková, M. Koc, M. Dvorak and V. Král, *Photochem. Photobiol.*, 2006, **82**, 432.

237 J. Králová, Z. Kejík, T. Bříza, P. Poučková, A. Král, P. Martásek and V. Král, *J. Med. Chem.*, 2010, **53**, 128.

238 J. N. Silva, A. M. G. Silva, J. P. Tomé, A. O. Ribeiro, M. R. M. Domingues, J. A. S. Cavaleiro, A. M. S. Silva, M. G. P. M. S. Neves, A. C. Tomé, O. A. Serra, F. Bosca, P. Filipe, R. Santus and P. Morlière, *Photochem. Photobiol. Sci.*, 2008, **7**, 834.

239 J. Zhao, H.-Y. Zhang, H.-L. Sun and Y. Liu, *Chem. – Eur. J.*, 2015, **21**, 4457.

240 V. Oliveri, S. Zimbone, M. L. Giuffrida, F. Bellia, M. F. Tomasello and G. Vecchio, *Chem. – Eur. J.*, 2018, **24**, 6349.

241 J. F. B. Barata, A. Zamarrón, M. G. P. M. S. Neves, M. A. F. Faustino, A. C. Tomé, J. A. S. Cavaleiro, B. Röder, Á. Juarranz and F. Sanz-Rodríguez, *Eur. J. Med. Chem.*, 2015, **92**, 135.

242 H. Kitagishi, F. Chai, S. Negi, Y. Sugiura and K. Kano, *Chem. Commun.*, 2015, **51**, 2421.

243 K. Watanabe, H. Kitagishi and K. Kano, *Angew. Chem., Int. Ed.*, 2013, **52**, 6894.

244 R. J. Moon, A. Martini, J. Nairn, J. Simonsen and J. Youngblood, *Chem. Soc. Rev.*, 2011, **40**, 3941.

245 P. Chauhan and N. Yan, *RSC Adv.*, 2015, **5**, 37517.

246 E. Anaya-Plaza, E. van de Winckel, J. Mikkilä, J.-M. Malho, O. Ikkala, O. Gulías, R. Bresolí-Obach, M. Agut, S. Nonell, T. Torres, M. A. Kostiainen and A. de la Escosura, *Chem. – Eur. J.*, 2017, **23**, 4320.

247 P. Chauhan and N. Yan, *RSC Adv.*, 2016, **6**, 32070.

248 P. Chauhan, C. Hadad, A. Sartorelli, M. Zarattini, A. Herreros-López, M. Mba, M. Maggini, M. Prato and T. Carofiglio, *Chem. Commun.*, 2013, **49**, 8525.

249 C. Ringot, V. Sol, R. Granet and P. Krausz, *Mater. Lett.*, 2009, **63**, 1889.

250 E. Feese, H. Sadeghifar, H. S. Gracz, D. S. Argyropoulos and R. A. Ghiladi, *Biomacromolecules*, 2011, **12**, 3528.

251 B. L. Carpenter, E. Feese, H. Sadeghifar, D. S. Argyropoulos and R. A. Ghiladi, *Photochem. Photobiol.*, 2012, **88**, 527.

252 S. K. Shukla, A. K. Mishra, O. A. Arotiba and B. B. Mamba, *Int. J. Biol. Macromol.*, 2013, **59**, 46.

253 V. S. Gaware, M. Håkerud, A. Juzeniene, A. Høgset, K. Berg and M. Másson, *Biomacromolecules*, 2017, **18**, 1108.

254 C.-K. Lim, J. Shin, I. C. Kwon, S. Y. Jeong and S. Kim, *Bioconjugate Chem.*, 2012, **23**, 1022.

255 I.-H. Oh, H. S. Min, L. Li, T. H. Tran, Y.-K. Lee, I. C. Kwon, K. Choi, K. Kim and K. M. Huh, *Biomaterials*, 2013, **34**, 6454.

256 G. Sun and J. J. Mao, *Nanomedicine*, 2012, **7**, 1771.

257 A. Fraix, R. Gref and S. Sortino, *J. Mater. Chem. B*, 2014, **2**, 3443.

258 C. W. Chu, J. H. Ryu, Y.-I. Jeong, T. W. Kwak, H. L. Lee, H. Y. Kim, G. M. Son, H. W. Kim and D. H. Kang, *J. Nanomater.*, 2016, **2016**, 4075803.

259 Z. Zhang, R. He, K. Yan, Q.-N. Guo, Y.-G. Lu, X.-X. Wang, H. Lei and Z.-Y. Li, *Bioorg. Med. Chem. Lett.*, 2009, **19**, 6675.

260 J.-P. Mbakidi, F. Brégier, T.-S. Ouk, R. Granet, S. Alves, E. Rivière, S. Chevreux, G. Lemercier and V. Sol, *Chem-PlusChem*, 2015, **80**, 1416.

261 G. Sessa and G. Weissmann, *J. Biol. Chem.*, 1970, **245**, 3295.

262 V. P. Torchilin, *Nat. Rev. Drug Discovery*, 2005, **4**, 145.

263 A. Samad, Y. Sultana and M. Aqil, *Curr. Drug Delivery*, 2007, **4**, 297.

264 B. S. Pattni, V. V. Chupin and V. P. Torchilin, *Chem. Rev.*, 2015, **115**, 10938.

265 P. Skupin-Mrugalska, J. Piskorz, T. Goslinski, J. Mielcarek, K. Konopka and N. Düzungeş, *Drug Discovery Today*, 2013, **18**, 776.

266 N. C. L. Zeballos, M. C. G. Vior, J. Awruch and L. E. Dicelio, *J. Photochem. Photobiol. A*, 2012, **235**, 7.

267 M. A. Garcia, E. Alarcon, M. Muñoz, J. C. Scaiano, A. M. Edwards and E. Lissi, *Photochem. Photobiol. Sci.*, 2011, **10**, 507.

268 J. Kim, O. A. Santos and J.-H. Park, *J. Controlled Release*, 2014, **191**, 98.

269 J. Soriano, A. Villanueva, J. C. Stockert and M. Cañete, *Int. J. Mol. Sci.*, 2014, **15**, 22772.

270 G. Nam, S. Rangasamy, H. Ju, A. A. S. Samson and J. M. Song, *J. Photochem. Photobiol. B*, 2017, **166**, 116.

271 K. A. Carter, D. Luo, A. Razi, J. Geng, S. Shao, J. Ortega and J. F. Lovell, *Theranostics*, 2016, **6**, 2329.

272 K. Krumova, S. Friedland and G. Cosa, *J. Am. Chem. Soc.*, 2012, **134**, 10102.

273 J. Massiot, A. Makky, F. Di Meo, D. Chapron, P. Trouillas and V. Rosilio, *Phys. Chem. Chem. Phys.*, 2017, **19**, 11460.

274 H.-J. Lv, X.-T. Zhang, S. Wang and G.-W. Xing, *Analyst*, 2017, **142**, 603.

275 M. C. Mijan, J. P. F. Longo, L. N. Duarte de Melo, A. R. Simioni, A. C. Tedesco and R. B. Azevedo, *J. Nanomed. Nanotechnol.*, 2014, **5**, 218.

276 M. Broekgaarden, A. I. P. M. de Kroon, T. M. van Gulik and M. Heger, *Curr. Med. Chem.*, 2014, **21**, 377.



277 P. Castagnos, M. P. Siqueira-Moura, P. L. Goto, E. Perez, S. Franceschi, I. Rico-Lattes, A. C. Tedesco and M. Blanzat, *RSC Adv.*, 2014, **4**, 39372.

278 L. Feng, L. Cheng, Z. Dong, D. Tao, T. E. Barnhart, W. Cai, M. Chen and Z. Liu, *ACS Nano*, 2017, **11**, 927.

279 L. Feng, D. Tao, Z. Dong, Q. Chen, Y. Chao, Z. Liu and M. Chen, *Biomaterials*, 2017, **127**, 13.

280 S. Tachikawa, M. E. El-Zaria, R. Inomata, S. Sato and H. Nakamura, *Bioorg. Med. Chem.*, 2014, **22**, 4745.

281 F. Zhou, B. Feng, T. Wang, D. Wang, Q. Meng, J. Zeng, Z. Zhang, S. Wang, H. Yu and Y. Li, *Adv. Funct. Mater.*, 2017, **27**, 1606530.

282 A. P. Perez, A. Casasco, P. Schilrreff, M. V. D. Tesoriero, L. Duempelmann, M. J. Altube, L. Higa, M. J. Morilla, P. Petray and E. L. Romero, *Int. J. Nanomed.*, 2014, **9**, 3335.

283 D. M. Gardner, V. M. Taylor, D. L. Cedeño, S. Padhee, S. M. Robledo, M. A. Jones, T. D. Lash and I. D. Vélez, *Photochem. Photobiol.*, 2010, **86**, 645.

284 Y.-T. Yang, H.-F. Chien, P.-H. Chang, Y.-C. Chen, M. Jay, T. Tsai and C.-T. Chen, *Lasers Surg. Med.*, 2013, **45**, 175.

285 S. Séguier, S. L. S. Souza, A. C. V. Sverzut, A. R. Simioni, F. L. Primo, A. Bodineau, V. M. A. Correa, B. Coulomb and A. T. Tedesco, *J. Photochem. Photobiol. B*, 2010, **101**, 348.

286 A. S. L. Derycke and P. A. M. de Witte, *Adv. Drug Delivery Rev.*, 2004, **56**, 17.

287 C. S. Jin and G. Zheng, *Lasers Surg. Med.*, 2011, **43**, 734.

288 J. Morgan, A. G. Gray and E. R. Huehns, *Br. J. Cancer*, 1989, **59**, 366.

289 J. Morgan, A. MacRobert, A. G. Gray and E. R. Huehns, *Br. J. Cancer*, 1992, **65**, 58.

290 M. Broekgaarden, R. van Vugt, S. Oliveira, R. C. Roovers, P. M. P. van Bergen En Henegouwen, R. J. Pieters, T. M. van Gulik, E. Breukink and M. Heger, *Nanoscale*, 2016, **8**, 6490.

291 Y. Mir, S. A. Elrington and T. Hasan, *Nanomedicine*, 2013, **9**, 1114.

292 P. Ngweniform, D. Li and C. Mao, *Soft Matter*, 2009, **5**, 954.

293 P. Ngweniform, G. Abbineni, B. Cao and C. Mao, *Small*, 2009, **5**, 1963.

294 A. Gijsens, A. Derycke, L. Missiaen, D. De Vos, J. Huwyler, A. Eberle and P. de Witte, *Int. J. Cancer*, 2002, **101**, 78.

295 A. S. L. Derycke, A. Kamuhabwa, A. Gijsens, T. Roskams, D. De Vos, A. Kasran, J. Huwyler, L. Missiaen and P. A. M. de Witte, *J. Natl. Cancer Inst.*, 2004, **96**, 1620.

296 K. Ichikawa, T. Hikita, N. Maeda, S. Yonezawa, Y. Takeuchi, T. Asai, Y. Namba and N. Oku, *Biochim. Biophys. Acta*, 2005, **1669**, 69.

297 S. Shao, J. Geng, H. A. Yi, S. Gogia, S. Neelamegham, A. Jacobs and J. F. Lovell, *Nat. Chem.*, 2015, **7**, 438.

298 H. C. Chen and R. V. Farese, *Curr. Biol.*, 1999, **9**, 478.

299 S. Osati, H. Ali, B. Guérin and J. E. van Lier, *J. Porphyrins Phthalocyanines*, 2017, **21**, 701.

300 E. Ikonen, *Nat. Rev. Mol. Cell Biol.*, 2008, **9**, 125.

301 A. Segalla, C. Milanesi, G. Jori, H.-G. Capraro, U. Isele and K. Schieweck, *Br. J. Cancer*, 1994, **69**, 817.

302 S. E. Maree and T. Nyokong, *J. Porphyrins Phthalocyanines*, 2001, **5**, 782.

303 G. Zheng, H. Li, M. Zhang, S. Lund-Katz, B. Chance and J. D. Glickson, *Bioconjugate Chem.*, 2002, **13**, 392.

304 I. A. Nikolaeva, A. Yu. Misharin, G. V. Ponomarev, V. P. Timofeev and Y. V. Tkachev, *Bioorg. Med. Chem. Lett.*, 2010, **20**, 2872.

305 H. Samavat and M. S. Kurzer, *Cancer Lett.*, 2015, **356**, 231.

306 E. H. Khan, H. Ali, H. Tian, J. Rousseau, G. Tessier, M. Shafiullah and J. E. van Lier, *Bioorg. Med. Chem. Lett.*, 2003, **13**, 1287.

307 Y. Lu and P. S. Low, *Adv. Drug Delivery Rev.*, 2012, **64**, 342.

308 J. Gravier, R. Schneider, C. Frochot, T. Bastogne, F. Schmitt, J. Didelon, F. Guillemin and M. Barberi-Heyob, *J. Med. Chem.*, 2008, **51**, 3867.

309 K. Stefflova, H. Li, J. Chen and G. Zheng, *Bioconjugate Chem.*, 2007, **18**, 379.

310 J. Shi, T. W. B. Liu, J. Chen, D. Green, D. Jaffray, B. C. Wilson, F. Wang and G. Zheng, *Theranostics*, 2011, **1**, 363.

311 L. Zhang, J. Xia, Q. Zhao, L. Liu and Z. Zhang, *Small*, 2010, **6**, 537.

312 P. Huang, C. Xu, J. Lin, C. Wang, X. Wang, C. Zhang, X. Zhou, S. Guo and D. Cui, *Theranostics*, 2011, **1**, 240.

313 X. Li, C.-Y. Kim, S. Lee, D. Lee, H.-M. Chung, G. Kim, S.-H. Heo, C. Kim, K.-S. Hong and J. Yoon, *J. Am. Chem. Soc.*, 2017, **139**, 10880.

314 Q. Jia, J. Ge, W. Liu, X. Zheng, M. Wang, H. Zhang and P. Wang, *ACS Appl. Mater. Interfaces*, 2017, **9**, 21124.

